The Regulatory Role of Syntaxin 1 N-terminal Conformation in Vesicle Priming and Exocytosis

Dissertation
zur Erlangung des Doktorgrades
der Mathematisch-Naturwissenschaftlichen Fakultäten
der Georg-August-Universität zu Göttingen

Vorgelegt von
Jong-Cheol Rah
aus Seoul, Korea

Göttingen
2004

D 7

Referent: Prof. Dr. Erwin Neher

Korreferent: Prof. Dr. Dietrich Gradmann

Tag der mündlichen Prüfung: 3 November 2004

CONTENTS

Index of figures and tables

Abbreviations

AMPA	Alpha-amino-3-hydroxy-5-methyl-4-isoxazole propionic acid
ATP	Adenosine triphosphate
BSA	Bovine serum albumin
BTC1	Botulinum toxin C1
C. elegans	*Caenorhabditis elegans*
ConA	Concanavalin A
DAG	Diacyl glycerol
DMEM	Dulbecco's Modified Eagle Medium
DNA	Deoxyribonucleic acid
dNTP	Deoxyribonucleoside triphosphat
D-AP5	D-2-amino-5-phosphonopentanoic acid
Drosophila	*Drosophila melanogaster*
EDTA	Ethylenediaminetetraacetic acid
EPSC	Excitatory Postsynaptic Current
EtBr	Ethidium Bromide
FBS	Fetal Bovine Saline
FUDR	2'-deoxy-5-fluorouridine
GTP	Guanine triphosphate
HBSS	Hanks balanced salt solution
HEPES	N-2-Hydroxyethylpiperazine-N'-2-ethanesulfonic acid
HZ	Heterozygote
IPSC	Inhibitory Postsynaptic Current
KA	kainate
KO	Knockout
mEPSC	Miniatur EPSC
mOsm	Miliosmolar
Munc	Mammalian Homolog of unc
NBA	Neurobasal-A-Medium
NBQX	6-nitro-7-sulfamobenzo quinoxaline-2,3-dione
NMDA	N-methyl-D-aspartate
NSF	N-ethylmaleimide-sensitive fusion protein
PAGE	Polyacrylamide gel electrophoresis
PCR	Polymerase chain reaction
PDBU	β-phorbol ester dibutyrate
Pvr	Vesicular release probability

RIM	Rab3 interacting molecule
RRP	readily releasable pool
SDS	Sodium dodecyl sulfate
SEM	Standard Error of the Mean
SNAP	Soluble NSF attachment proteins
SNAP-25	Synaptosomal associated protein of 25 kDa
SNARE	Soluble N-ethylmaleimide-sensitive fusion-attachment protein receptors
STP	Short-Term Plasticity
Stx	Syntaxin
$Stx1B_{of}$	Double mutant mice expressing constitutively open conformation of syntaxin 1b and syntaxin 1a null
Taq	Thermophilus aquaticus
TBE	Tris-Borate-EDTA
TE	Tris-EDTA
TEA	Tetraethyl ammonium
TS	Tris-Sodium Chloride buffer
t-SNARE	Target membrane SNAREs
TTX	Tetrodotoxin
Unc	Uncoordinated Movement Mutant
VAChT	Vesicular acethyl choline transporter
VAMP	Vesicular-associated membrane protein)
VGluT	Vesicular glutamate transporter
VMAT	Vesicular Monoamine transporter
v-SNARE	Vesicular membrane SNAREs
WT	Wild type
β-PE	β-phorbol ester

1. Abstract

ABSTRACT

During vesicle priming at the central synapse, Syntaxin 1, together with SNAP25 and Synaptobrevin, assemble into the synaptic SNARE complex. The formation of SNARE complex is thought to provide the energy needed that enables vesicle exocytosis during Ca^{2+} triggering step at the presynapse. Among the SNARE proteins, Syntaxin 1 is thought to play a special role in regulating the rate of SNARE assembly by adopting two conformations; a closed autoinhibitory conformation in which core complex domain is hindered by N-terminal Habc domain, and an open conformation in which the SNARE motif of syntaxin is open and ready to interact with the other SNAREs.

In the present study we examined the role of the conformational switch of syntaxin 1 by analyzing synaptic properties of genetically modified mice expressing a mutation that leaves syntaxin 1 in a constitutively open conformation. In cultured hippocampal neurons, the mutation led to a significant increase in the rate of vesicle priming, supporting the hypothesis that syntaxin 1 regulates vesicle priming during the SNARE complex assembly process. Surprisingly, we also found that the mutation led to an increase in synaptic release probability, suggesting that the conformation of syntaxin 1 also regulates vesicle fusion by reducing the energy barrier of vesicle fusion to the plasma membrane. Our data support the idea that the SNARE complex member syntaxin 1 and its individual conformations are crucial regulators of the efficacy and short-term plasticity of synaptic transmission.

2. Introduction

1. INTRODUCTION

"*Cogito, ergo sum* (I think therefore I am)", René Descartes said in 1637, however, his question, "how does thinking stuff keep company with material stuff?" still remains unanswered. How do molecules, which are basically permutations and combinations of atomic moieties, synchronize, in perfect harmony, to create the orchestra of life: actions and reactions, thoughts, emotions, language, learning and memory? If one embarks on the journey to trace the origin of these highly sophisticated functions of the brain that creates the mind, the neuron is unquestionably the final destination.

Neurons are the basic units of nervous system. There are trillions of neurons in human brain and each of these neurons makes upto 1000 connections through their processes with one another. Therefore, neurons are the fundamental building blocks of the network of which the nervous system is composed. A neuron is designed to detect and integrate incoming information to transmit the reacting activity along its process to other neurons in the network so as to maintain a constant ebb and flow of information.

2.1 *Basic Function of a Neuron and a Synapse*

Neurons are strongly compartmentalized and polarized cells. With a few exceptions, a neuron has three major functional and morphological domains: cell body, dendrite and axon. The **cell body** contains genetic materials and the cytoplasmic organelles like other cells. **Dendrites** extend from cell body and ramify so as to increase the area of contact with other neurons. These two specialized compartments of the neuron, the cell body and dendrites are the major domains that receive inputs from other neurons. The **axon** extends, in most cases, much further from the cell body than the dendritic arbor does. Many of the axons are surrounded by an insulating myelin sheath, which facilitates rapid impulse conduction. The axon is responsible for transmitting neural information to other cells. The terminal region

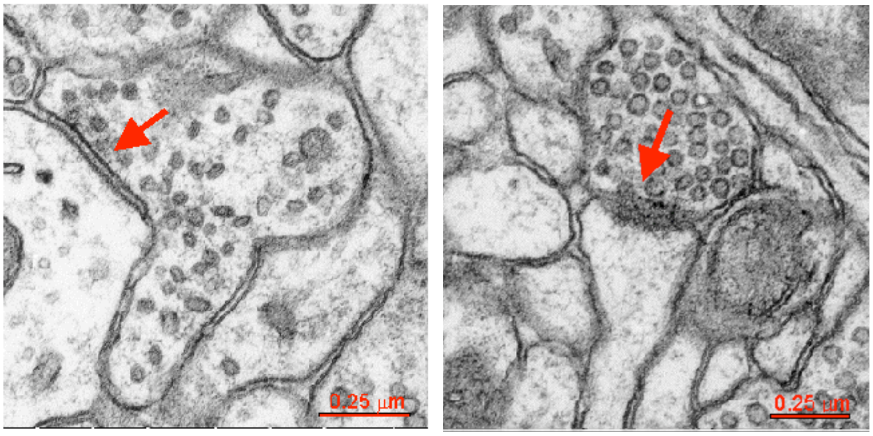

[Figure1] Representative symmetric (presumably inhibitory; left) and asymmetric synapses (presumably excitatory; right). Arrow points to the synapse from the presynaptic side. Adopted from http://synapses.mcg.edu/anatomy/

of the axon, where contacts with other cells are made is called **presynaptic terminal** and is part of a specialized morphological structure called the **synapse**.

Information is encoded in a neuron by electrical impulses. Synapses serve as the junction of this information flow from one cell to the next, directly in the form of electrical signals (e.g. bidirectional electrical synapses) or transformed as chemical signals via the release of neurotransmitter (e.g. unidirectional excitatory and inhibitory synapses based on the type of transmitter released). These chemical synapses can be morphologically and functionally distinguished: the asymmetric synapses usually carrying excitatory inputs and symmetric synapses carrying inhibitory inputs leading to depolarization and hyperpolarization of the postsynaptic neuron, respectively (figure 1).

Most excitable cells have a resting potential in the range of –60 mV to –90 mV, while equilibrium potentials of the four major ions namely Na^+, K^+, Ca^{2+} and Cl^- of around +50 mV, -70 mV, +130 mV and –70 mV, respectively along with their asymmetric distributions across the membrane lead to an electrochemical gradient. Thus, in their resting state, cells maintain a constant driving force, in the form of potential difference, for flow of each ion. This resting state of potential difference across the membrane is called polarized state and is maintained primarily by sodium-potassium ATPase, which actively transport three Na^+ ions out of the cell in

exchange of two K^+ ions, thereby establishing a default negative resting membrane potential.

When the neuron receives a large enough stimulus, the sodium conductance increases transiently, due to voltage-dependent gating of Na^+ channels. These changes in Na^+ conductance drive the membrane potential toward the Na^+ equilibrium potential which depolarizes the membrane, and is followed by an increase in K^+ conductance that later drives the membrane potential back to its resting potential. At this point the action potential propagates along axons by longitudinal spread of current and finally reaches the point of functional contact, the synapse.

When an action potential invades the axon's presynaptic terminal, depolarization activates voltage-gated Ca^{2+} channels (mainly P/Q- and N-type). Ca^{2+} ions move inward and trigger the synaptic vesicles to fuse with presynaptic plasma membrane so as to release their neurotransmitter contents into the synaptic cleft. Released neurotransmitters, then, diffuse and subsequently bind to specific receptors at the postsynapse to evoke excitatory or inhibitory postsynaptic potentials (EPSP/ IPSP). Majority of inter-neuronal communication relies on the use of this chemical transmission. Through this process, an action potential in the presynaptic terminal propagates to neighboring cell in a few milliseconds.

2.2 *Structure of Synapse*

To achieve efficient synaptic transmission, exocytosis of neurotransmitter is restricted to specialized structures known as '**active zones**' in the presynaptic terminal, which targets directly upon specialized '**post synaptic density**'.

2.2.1 Active Zones

One of the structural studies using electron microscope tomography at a model synapse, the frog neuromuscular junction elegantly showed the arrangement and associations of structural components of compact organelle into an active zone. This study showed that it is approximately 1–2 μm long, 75 nm wide and typically extends 50–75 nm from the presynaptic membrane into the cytoplasm. The three main components of this structure are known as beams, ribs and pegs. The ribs extend orthogonally into the ridge's long axis and form approximately 7–12 connections to docked vesicles located on each flank of the ridge (Harlow et al., 2001; Rosenmund et al., 2003). This might help to dock the vesicles and tether the channels for efficient Ca^{2+} supply, which is essential for fast turn on and off of exocytosis. Because intracellular Ca^{2+} concentration ($[Ca^{2+}]_i$) is maintained in very low (about 100 nM) in comparison to external high extracellular Ca^{2+} concentration ($[Ca^{2+}]_{ex}$: millimolar), Ca^{2+} channel opening causes large changes in $[Ca^{2+}]_i$. Proximity of vesicles from the Ca^{2+} channels have an influence on the probability as well as speed of release, one factor determining these two parameters being the Ca^{2+}

cooperativity. For the vesicles located far away from the Ca^{2+} channels would sense apparent changes in presynaptic Ca^{2+}concentration to a smaller extent and since release probability is proportional to the fourth power of the Ca^{2+} concentration (Yoshihara and Littleton, 2002) so accordingly, these distant vesicles will have much lower release probability as well as a longer lasting time course of release compared to their proximal counterparts.

Some proteins are exclusively present at the active zone. Bassoon has been reported to be involved in the tethering of vesicles based on the studies on mice lacking Bassoon, which lead to free floating clustered ribbon in retinal neuron (Dick et al., 2003). Munc13 and RIM are known to have a critical role in the priming process but not in the docking or recruiting of vesicles (Augustin et al., 1999; Koushika et al., 2001a). α-liprins bind to receptor tyrosine kinase and regulates the differentiation of synaptic terminal (Serra-Pages et al., 1998; Zhen and Jin, 1999). CAST (cytometrix at the active zone (CAZ) - associated structural protein) is known to form a protein network with other CAZ associated proteins including RIM, Munc13s and Bassoon at the active zone (Ohtsuka et al., 2002) and Piccolo is another CAZ-associated protein but their physiological function remains not clear (Meyer and Rosenmund, unpublished). How these active zone proteins, CAST and Piccolo contribute to the coordination of presynaptic signal remains unknown.

2.2.2 Postsynaptic Density

The structure known as the postsynaptic density (PSD) is located at the opposite side of the active zone across the synaptic cleft. It is here, where specific sets of molecules including each glutamate receptor and other PSD associated proteins are located. In addition to glutamate receptors, this postsynaptic specialization of neurons, is marked by the presence of scaffolding proteins, like PSD-95 and organization of other membrane proteins such as adhesion molecules, receptor tyrosine kinases, and ion channels.

2.2.3 Glutamate Receptors

Glutamate receptors can be divided into two categories, ionotropic and metabotropic. Ionotropic receptors are classified into AMPA (alpha-amino-3-hydroxy-5-methyl-4-isoxazole propionic acid) receptor subclass, NMDA (N-methyl-D-aspartate) receptor subclass, and KA (kainate) receptor subclass. Metabotropic receptors, consists of 3 classes (class I through class III) and 8 genes (mGluR1 through mGluR8), and they are metabotropic because they are linked by G-proteins to cytoplasmic enzymes and further classified depending on the signal transduction pathway.

The predominant receptor class for fast excitatory synaptic transmission by glutamate is the AMPA receptor. These are widely spread throughout the central nervous system, and require coassembly of 4 subunits (GluR1 through GluR4).

NBQX (6-nitro-7-sulfamobenzo quinoxaline-2,3-dione) and 2,3-benzodiazepine are known to specifically block these receptors. Subunits of the GluR5 through GluR7 have been found to coassemble with KA receptor subunit KA1 or KA2 to form the KA receptor. KA receptors have relatively low binding affinity to glutamate but only two pharmacological drugs, concanavalin A (ConA) and cycothiazide, can distinguish KA receptors from AMPA receptors. These non-NMDA receptors gate cation ions with relatively low conductance (<<20 pS) that are permeable to both Na^+ and K^+ but usually not permeable to Ca^{2+}.

NMDA receptors are very tightly regulated. Since they have two distinguished agonist site for glutamate and glycine and their voltage-dependent blocking by extracellular Mg^{2+}. Mg^{2+} tightly binds to NMDA channel at the resting potential and is expelled from the channel by depolarization. Thus, the activation of NMDA channel requires glutamate, glycine and depolarization of the cell. The receptor controls cation channels of high conductance (50 pC) that is permeable to Ca^{2+} as well as Na^+ and K^+. D-2-amino-5-phosphonopentanoic acid (D-AP5) is the competitive antagonist of NMDA receptor, and MK-801 can selectively block activated NMDA receptors (for further reading, see (Kandel et al., 2000; Siegel et al., 1999))

2.3 *Vesicle Cycle and Pool Dynamics*

The synaptic cleft is too wide to be traversed by current; instead, neurotransmitters stored in synaptic vesicles are secreted to induce postsynaptic excitation. Synaptic vesicles are actively filled with neurotransmitters by 4 different specialized transporter proteins: a monoamine transporter for all biogenic amines (called VMAT), for GABA and glycine, for acetylcholine (called VAChT), and for glutamate (called VGluT). These transporters are basically vacuolar proton pumps, which cause an electrochemical gradient across the synaptic vesicular membrane. This electrochemical gradient across the membrane is energetically coupled to transport of neurotransmitter into the vesicles. The vesicles once filled with transmitters are, then, moved to the active zone of the presynaptic terminal, but exact mechanism is not yet understood (See part 2.5).

Once vesicles arrive at the active zone, vesicles become attach to the plasma membrane. This attachment process is called, '**docking**' (see part 2.5). Then, docked vesicles undergo an ATP-dependent pre-fusion reaction called '**priming**' (see part 2.6) to bring vesicles to a fusion competent state. Vesicle priming is considered to be equivalent to the assembly of the release apparatus that catalyzes the fusion of the vesicle with the plasma membrane when Ca^{2+} influx initiates release. When an action potential arrives at the presynaptic terminal, Ca^{2+} triggers the completion of fusion. This process requires the binding of multiple Ca^{2+} ions to synaptic Ca^{2+} binding sites including synaptotagmin, but it occurs in a very rapid manner.

After exocytosis, synaptic vesicles are rapidly retrieved by endocytosis, most likely via clathrin coated pits. These endocytosed vesicles then get rid of the coats, and are recycled to the interior of the synaptic nerve terminal. Some of the empty vesicles are either refilled immediately with neurotransmitter or may pass through an endoplasmic reticulum while others may be replaced by a rapid endocytosis process called 'kiss and run' (for review (Südhof and Scheller, 2001)).

Readily releasable vesicles cover only a small fraction of the total vesicle population. The pool constitutes those vesicles that are primed and immediately available for release, defined as the **readily releasable pool** (RRP). In synapses of cultured hippocampal neurons, the RRP comprises only five to nine synaptic vesicles per each synapse (Murthy and Stevens, 1999). However, when release is triggered, usually only a single vesicle of the RRP fuses per synapse, although all of the vesicles in the RRP appear to be ready for fusion. The low release probability of each individual vesicle probably restricts exocytosis to a single vesicle. The overall synaptic release probability is the sum of the individual vesicular release probabilities. Consistently, the number of vesicles in the RRP appears to be a major determinant of the synaptic release probability (Dobrunz and Stevens, 1997).

When synapses are stimulated extensively, the RRP will be depleted quickly, and new population of vesicles will replenish the RRP. The population of vesicles

contributing to this replenishment is known as '**reserved pool**', which in the hippocampal neuron is estimated to be around 17-20 vesicles (Murthy and Stevens, 1999). These two pools, RRP and reserved pool can be stained with FM1-43 when synapses are stimulated extensively and these are named as the '**recycling pool**'.

Rather surprisingly, the hippocampal synapses were reported to have about 200 synaptic vesicles in a morphological study (Schikorski and Stevens, 1997), thus majority vesicles are reluctant to fuse under normal conditions. This fraction of the entire vesicular population is referred to as the **'resting pool'** (for review (Südhof, 2000))

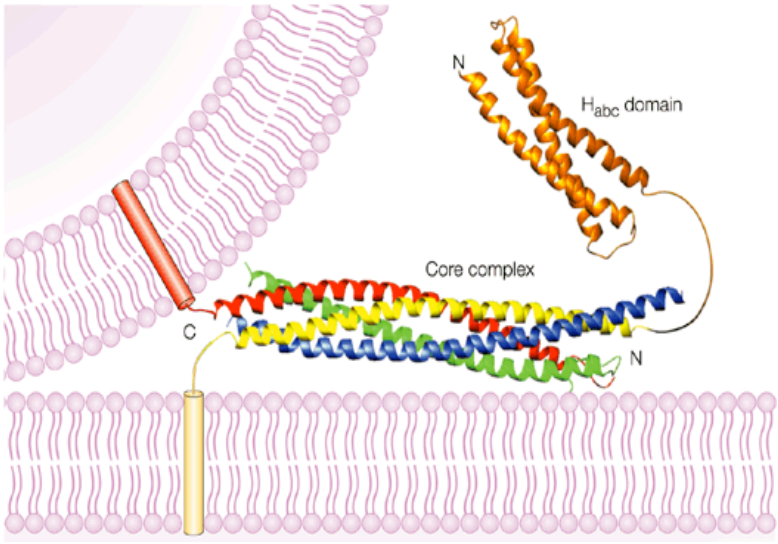

[Figure 2] Model of the neuronal SNAREs assembled into the core complex. The ribbon diagrams represent the crystal structure of the core complex The Habc domain is shown in orange and the SNARE (SNAP receptor) motifs are colored as follows: synaptobrevin, red; syntaxin 1, yellow; SNAP25, blue; SNAP25 carboxyl terminus, green. The cylinders represent the transmembrane regions of synaptobrevin and syntaxin 1, which are inserted into the synaptic vesicle and plasma membranes, respectively. The curved lines represent short sequences that connect the SNARE motifs and the transmembrane regions, as well as the linker region between the Habc domain and the SNARE motif of syntaxin 1. Adopted from (Rizo and Südhof, 2002)

2.4 *Release machinery*

How exactly do fundamental processes like vesicle targeting to the active zones and fusion events occur, are still largely left to be elucidated. However, there is compelling evidence to support the hypothesis that the SNARE (soluble N-ethylmaleimide-sensitive fusion-attachment protein receptors) complexes drive membrane fusion.

The current hypothesis poses that the selective docking of a vesicle with the appropriate target membrane is mediated by the formation of a complex between the vesicle membrane protein (v-SNARE: synaptobrevin or VAMP) and corresponding target membrane proteins (t-SNAREs: syntaxin and SNAP-25 (synaptosomal-associated protein of 25 kDa)). These proteins zipper up from their N-termini towards the C-termini so as to form a stable trans-SNARE complex, thereby, overcoming counteracting electrostatic forces and leading to the close apposition of opposing vesicle and target lipid bilayers [figrue2]. (for review see Fasshauer, 2003 or Jahn et al., 2003).

SNARE motifs, a moderately conserved stretch of 60 to 70 amino acids, at C-terminal domain of syntaxin 1, the cytoplasmic domain of synaptobrevin and N- and C-terminal domains of SNAP-25 assemble spontaneously into an extraordinarily stable complex of four-helix bundles. It has been reported that at the

center of the SNARE complex, there are conserved Leucine-zipper-like layers embedded with ionic layers consisting of three glutamine and one arginine residues contributed from each SNARE motif alpha-helix (Sutton et al., 1998).

Several lines of evidence utilizing SNARE protein-targeted clostidial neurotoxins and genetically modified organisms have shown that the SNARE complex is absolutely necessary for efficient membrane fusion [Table 1]. Furthermore, *in vitro* reconstitution experiments have shown that SNAREs are the minimally sufficient fusion machinery, by demonstrating that SNAREs reconstituted in separate artificial lipid bilayer vesicles lead to spontaneous fusion under physiological condition (Weber et al., 1998).

However, although all of the mutations or truncations in SNARE proteins have led to complete ablation of action-potential induced evoked responses, spontaneous release was still observed in some cases, such as SNAP-25 null mice and synaptobrevin knock out mice (Schoch et al., 2001; Washbourne et al., 2002), Table 1. These findings suggest that perhaps SNARE complex is not necessary for all kinds of neurotransmitter release, or that spontaneous neurotransmitter release uses a different mechanism other than the SNARE complex formation. Another explanation is that the observed releases in theses null mouse lines might be originated from the isoforms of eliminated proteins. For example, in the case of study with SNAP-25 knock-out mouse, SNAP-23 may compensate the lack of

SNAP-25. In fact, western blot analysis in the lack of SNAP-25 in this study showed comparably increased expression of SNAP-23 in both heterozygotes and knock-out mice, even though it has not been discussed in detail (Washbourne et al., 2002). In case of synaptobrevin-2 knockout study, however, synaptobrevin 1 and cellubrevin were examined and considered carefully as a potential substitute for the protein. Furthermore, in this case, 10% of RRP remained. Thus, it is less likely that the release is purely the outcome of compensation, because the compensation under detection limit of western blotting does not sufficiently explain the remaining 10% of RRP (Schoch et al., 2001). A more realistic explanation is that the fusion reaction can still happen without SNARE complex, but SNARE complex is needed because it critically catalyzes an increase in the rate of membrane priming and fusion (Schoch et al., 2001).

In vivo, the SNARE proteins are not the only proteins involved in neurotransmitter release but numerous proteins, which do not function as fusion factors, are reported to mediate or facilitate fusion events. These proteins include NSF (N-ethylmaleimide-sensitive fusion protein), SNAP (soluble NSF attachment proteins). NSF is the ATPase chaperone which disassemble the stable SNARE complex in conjunction with the soluble NSF attachment proteins (SNAPs) as cofactors (Otto et al., 1997). Proteins such as synaptotagmin 1 and complexins are reported to be crucial mediator for Ca^{2+} mediated exocytosis. Munc13s and Munc 18 are known as key regulator for conformation of syntaxin 1 (see part 2.6).

[Table 1] Previous studies on SNARE proteins

Synapto-brevin	Tetanus toxin	Abolished evoked, but not spontaneous synaptic vesicle release	Normal development	(Sweeney et al., 1995)
	C. elegans	Impaired cholinergic transmission; aldicarb resistance	Die after embryogenesis	(Nonet et al., 1998)
	Drosophila	Abolished evoked, and 75% reduced spontaneous, synaptic vesicle release	Lethal; paralysis; normal morphology	(Deitcher et al., 1998)
	Mice	Abolished evoked, and 85% reduced spontaneous, synaptic vesicle release; 90% reduced RRP	Lethal; die immediately after birth	(Schoch et al., 2001)
SNAP-25	Botulinum toxin A/ E	Abolished SNAP-25, overcome by increased Ca^{2+}; decreased Ca^{2+} sensitivity to release		(Binz et al., 1994)
	Antisense oligoneucleotide	Inhibited axonal growth, synaptogenesis		(Osen-Sand et al., 1993; Osen-Sand et al., 1996)
	Botulinum toxin A	Reduced neurite outgrowth		(Morihara et al., 1999)
	Drosophila –temperature sensitive	Reduced SNAP-25 reduced evoked; normal miniature vesicular release		(Rao et al., 2001)
	Mice	Abolished EPSC; still have mEPSC with bigger amplitude	Embryonic lethal	(Washbourne et al., 2002)
Syntaxin	Botulinum toxin C1	Blocked neurotransmitterelease		(Blasi et al., 1993)
	Syntaxin fragment/ Anti-syntaxin antibody	Depression in Ca^{2+}-dependent transmission		(Bennett et al., 1993)
	Drosophila	Complete failure in evoked, very rare spontaneous transmitter release	Abnormal development (cuticle/ gut/ yolk digestion)	(Broadie et al., 1995; Schulze et al., 1995)

2.5 *Docking: Rab3 proteins*

Little is known about how the neurotransmitter vesicles get to have initial contact with plasma membrane (docking). Rab proteins, which are a family of Ras-related small GTPases are proposed to play the main role in membrane docking. When bound to membranes, Rab proteins operate as molecular switches that are active in the GTP-bound form and inactive in the GDP-bound form. The likely function of active Rab3 is the recruitment of a variety of proteins such as rabphilin, RIM (rab3 interacting molecule), etc. that bridge the membranes of the active zone. However, recent studies by Schlüter et al. showed that quadruple knock-out of Rab3A, B, C, D led to 30% decrease in evoked responses due to reduced release probability without significant changes in spontaneous or sucrose-evoked release (Schluter et al., 2004). This finding suggests that Rab3s are essential for Ca^{2+} triggered neurotransmitter release but unlikely for vesicular docking.

Recently, the possible role of Munc18 in vesicle docking is suggested, based on the finding of defects in vesicle docking in null mutant *C.elegans* and mouse chromaffin cells (Voets et al., 2001; Weimer et al., 2003b).

2.6 *Priming: Munc18-1, Munc13 and RIM*

SNARE proteins are not always ready to form, since syntaxin 1 exhibits a closed conformation. Release of syntaxin 1 into an open conformation is believed to be required to allow form the SNARE complex (Dulubova et al., 1999; Munson and Hughson, 2002). Syntaxin contains N-terminal Habc domain, linker domain, SNARE motif and C-terminal transmembrane domain. The N-terminal Habc

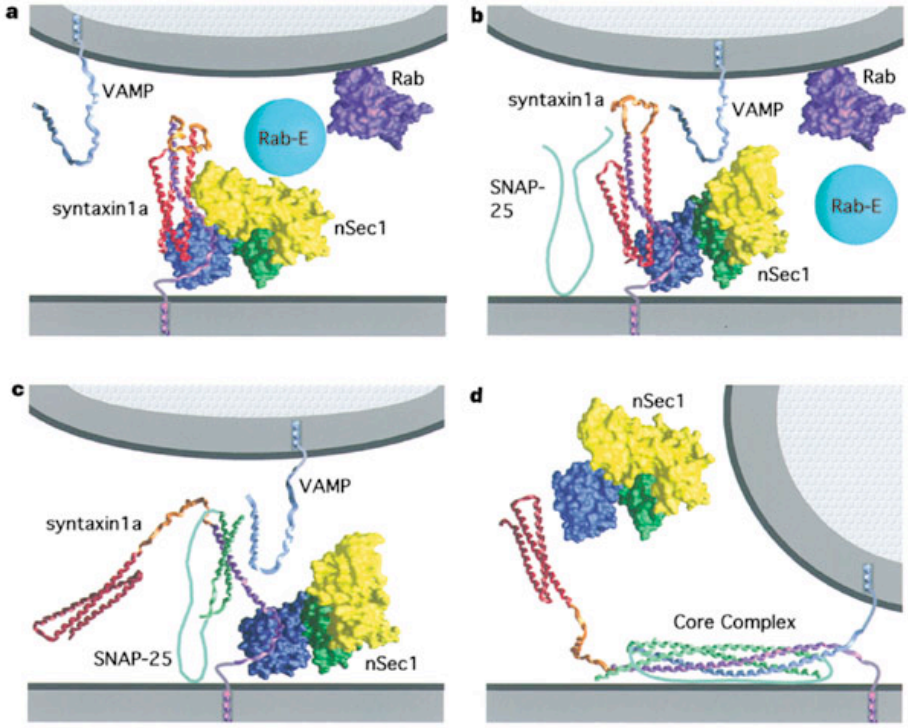

[Figure 3] Model for the role of Munc 18-1(nSec1 in figure) in membrane fusion. **a,** nSec1 bound to closed conformation of syntaxin 1a. Possibly through a Rab or Rab effector protein (not appeared in this figure). **b**, Munc13-1 and RIM induces a conformational change in nSec1 and causes the loss of contacts with syntaxin 1a. Exposed residues of H3a interact with SNAP-25, initiating the formation of the core complex. **c**, The syntaxin Habc domain moves away from the H3 region of syntaxin 1a. The SNAP-25 helices propagate towards the C-terminus, and VAMP begins to bind to the helical H3a region. **d**, The nucleated VAMP–SNAP-25–syntaxin 1a helices assemble rapidly and complete the long straight helical bundle structure (SNARE complex). Formation of SNARE might then promote membrane fusion. Adopted with modification from (Misura et al., 2000)

domain is essential for the binding to its interacting partners including Munc13, Munc 18, and N-type Ca^{2+} channel (Bennett et al., 1992; Betz et al., 1997; Hata et al., 1993), and reversibly folds back upon the SNARE motif (Dulubova et al., 1999; Fernandez et al., 1998). NMR studies on Habc domain showed three long alpha-helices in a twisted left-handed up-down bundles (Fernandez et al., 1998). The linker domain of syntaxin 1 is known to be highly flexible and plays a crucial role in determining a conformation of syntaxin mainly based on the finding that double point mutation of the linker domain (L165, E166) led to fixed open-conformation of syntaxin (Dulubova et al., 1999; Margittai et al., 2003a).

The closed conformation of syntaxin 1 is believed to be stabilized by Munc18-1. Single-molecule fluorescence resonance energy transfer study on the conformation of free syntaxin showed dynamic equilibrium between closed and open conformation with 0.8 ms of relaxation time, explaining the requirement of regulatory proteins to arrest in one conformational state (Margittai et al., 2003b). Munc18-1 is a hydrophilic, 60-70 kDa polypeptide that was first discovered in *C. elegans* for an uncoordinated phenotype named Unc-18 (Brenner, 1974) and rediscovered in yeast as sec1 as a gene involved in the yeast secretory pathway (Novick et al., 1980). It is generally believed that the role of Munc 18 is to bind to the closed conformation of syntaxin and compete with SNARE complex formation. These consensus based on the finding that the binding of syntaxin to other SNARE partners preclude their interaction with Munc 18 and that Munc 18 binds selectively

to closed form of syntaxin 1 (Dulubova et al., 1999; Yang et al., 2000). This hypothesis is supported by the findings in *Drosophila*, that syntaxin mutations that eliminate ROP (Munc-18 orthologue in *Drosophila*) binding display increased neurotransmitter release, suggesting that ROP negatively regulates neurosecretion through its interaction with syntaxin (Wu et al., 1999).

Unexpectedly, the lack of Munc18-1 led to complete failure of neurotransmitter release in mammalian system (Verhage et al., 2000). Furthermore, overexpression of Munc 18 in chromaffin cells induced increased membrane fusion (Voets et al., 2001), showing positive role in fusion process for Munc18-1. Also, recently evidence that expression of open-mutation syntaxin 1 cannot bypass the requirement for unc18 (Weimer et al., 2003a), strongly suggests that the role of Munc18 is not only assist the conformation of syntaxin. Therefore, although it is clear that Munc 18-1 plays an essential role in neurotransmitter release, the general physiological role of Munc 18 is not yet clear.

Given that Munc18 is involved in stabilizing the closed conformation of syntaxin 1, how can syntaxin be re-activated? Munc13 is the strongest candidate for releasing syntaxin out of the lock in by Munc 18, by switching the conformation of syntaxin 1 to the Munc18-binding independent open conformation, based on following findings. First, Munc13 localizes selectively in active zone. Second, studies in *Drosophila*, *C. elegans*, and mice suggest that Munc13 functions at a post-

docking step of exocytosis, most likely during synaptic vesicle priming (Aravamudan et al., 1999; Augustin et al., 1999; Brose et al., 1995; Maruyama and Brenner, 1991). Third, from *in vitro* binding assay, the carboxyl terminus of Munc13 binds competitively with Munc 18 to amino terminal region of syntaxin 1, sharing binding domain with Munc 18-1 (Betz et al., 1997; Sassa et al., 1999). Finally, and most importantly, overexpression of constitutively open form of syntaxin rescued the phenotype of unc-13 null *C. elegans*, which strongly suggesting that Munc13 is the protein to switch conformation of syntaxin 1 (Richmond et al., 2001).

RIM is another molecule necessary for switching the conformation of syntaxin 1. RIM1 and RIM2 were found in the search for putative effector molecule of rab3. RIMs bind to rab3 via their zinc finger domains, and via its PDZ domain and C2 domain it can bind phospholipids and Ca^{2+}. Thus, hypothetically, by means of domain structure to function prediction, RIM could bring the vesicles to dock to the membrane.

However, it is not likely that this is the main role of RIMs, since deletion of one of the isoforms, RIM1, caused a much more severe phenotype (severe reduction in neurotransmitter release) than rab3 deletion (Koushika et al., 2001a). RIM1 seems to have its main role as a critical helper for Munc13 because 60% reduction of Munc13 is reported in RIM1 null mice (Schoch et al., 2002). Moreover, disruption of the interaction between RIM1 and Munc13-1 led to a loss of fusion-competent

synaptic vesicles, creating a similar phenotype to Munc13-1-deficient neurons, suggesting that RIM1 is necessary for Munc13-1 to carry out its function in priming (Betz et al., 2001). Correlatively, the phenotype of *C. elegans* lacking RIM can also be rescued by overexpression of syntaxin 1 (Koushika et al., 2001a).

2.7 Ca^{2+} sensing/fusion: synaptotagmins and complexins

Once the SNARE complex is formed, neurotransmitter release is regulated by the increment of intracellular calcium concentration ($[Ca^{2+}]_i$). When an action potential arrives at the presynaptic terminal, high-voltage activated P/Q- and N-type Ca^{2+} channels open, and $[Ca^{2+}]_i$ increases to 10-20 mM, a concentration that triggers vesicular fusion with a 100-200 ms time delay. To meet this time delay, Ca^{2+} channels must be localized in close proximity to the release machinery, and need a very efficient, but low affinity Ca^{2+} sensor. Synaptotagmin 1 is the most attractive candidate since it is a highly conserved synaptic vesicle protein, and binds calcium at physiological concentrations in a complex with negatively charged phospholipids (Brose et al., 1992). Recently, in a reconstitution study involving synaptotagmin and SNAREs, synaptotagmin enhanced both the rate and extent of fusion by binding anionic phospholipids in Ca^{2+}-dependent manner (Tucker et al., 2004). Furthermore, the lack of synaptotagmin 1 led to dramatic deficits in Ca^{2+} triggered synchronous neurotransmitter release but not in asynchronous or Ca^{2+}-independent release, strongly suggesting that synaptotagmin 1 is the major low affinity Ca^{2+}

sensor which mediates Ca^{2+} regulation of synchronous neurotransmitter release in hippocampal neurons (Geppert et al., 1994). Most synaptotagmins bind Ca^{2+} ions through their two C2 domains, which causes secondary acidic phospholipids and/or SNARE protein binding. When a positively charged amino acid residue surrounding the Ca^{2+} binding domain in the C2A region was mutated to alter Ca^{2+} binding affinity without affecting three-dimensional structure of Ca^{2+} binding site, the Ca^{2+} sensitivity of neurotransmitter release was decreased twofold, but spontaneous release or the size of the RRP were not affected (Fernandez-Chacon et al., 2001). On the other hand, mutating the equivalent amino acid residue in the C2B domain (K366Q) caused no change in Ca^{2+}-dependent properties in syntaptotagmin1 or evoked transmitter release. Instead, double point mutation in two serial amino acid residues in polybasic domain of C2B (K326,327A)showed essentially the same phenotype of R233Q mutation in C2A domain (Li et al., unpublished), showing that these two C2 domains have. Results described so far indicate that synaptotagmin I is indeed a Ca^{2+} sensor and it mediates Ca^{2+}-dependent, rapid, synchronous neurotransmitter exocytosis through its C2A and C2B domain.

Complexin I and II, the abundant proteins in the central synapse, are known to bind to the fully assembled SNARE complex and enhance Ca^{2+} sensitivity (Pabst et al., 2000). In double deficient mice, the synchronous component of evoked response

was selectively impaired, while priming and Ca^{2+} independent neurotransmitter release were unaffected (Reim et al., 2001).

2.8 *Short-term plasticity*

Information within neurons is encoded by spike train patterns. At the synapse, these incoming action potentials are transmitted to the receiving neuron by the initiation of neurotransmitter release via fusion of vesicles with the plasma membrane. In response to stimulation at high frequencies, synapses can undergo profound changes in strength, which can be even greater than 10 fold increase or decrease, depending on types of synapses. The efficacy of neurotransmitter release represents the major determinant of how reliable information cross the synapse.

The changes in efficacy of synapses, whether transient or permanent, is referred as synaptic plasticity. Transient or short-term plasticity (STP) critically depends on the rate and duration of incoming action potentials trains and on other factors that may be variable for each presynaptic neuron and each synapse, such as the initial release probability, the number of fusion competent, primed vesicles per synapse.

Various forms of STP, such as short term depression, frequency facilitation, and augmentation govern processes as diverse as sound localization, the generation of oscillatory brain activity, cortical gain control and perhaps many others, even the

terminals made by the same axon on different target cells can show very different short-term plasticity characteristics. Thus it is generally accepted that STP is of central importance for information processing in the brain.

It has long been known that Ca^{2+} ions are the mediators of most forms of short-term plasticity. The function and localization of presynaptic Ca^{2+} channels as well as Ca^{2+} buffers are major contributors to short-term plasticity, because they influence the presynaptic Ca^{2+} dynamics.

As actual functional presynaptic changes during STP, two key determinants have been suggested: **Residual Ca^{2+}** and **pool depletion**. Residual Ca^{2+} hypothesis can explain the facilitation factor during the repetitive stimuli. Since rapid shut off of exocytosis is achieved by rapid removal of Ca^{2+} from the site of action by various mechanisms i.e. diffusion, Ca^{2+} buffering etc., a second stimulus can be influenced by the residual calcium left over from the first Ca^{2+} influx.

The pool depletion factor is mainly governed by vesicle priming rate and the vesicular release probability. Because the number of primed fusion competent vesicles is small, high release probability synapses exhaust the number of available vesicles within a few action potentials. Therefore, replacement of used vesicles with newly primed ones and adaptation of vesicle priming rates during STP will strongly influence how synaptic responses are maintained during trains of action potentials.

As the number of RRP is the limiting factor for short-term plasticity, it valid predicted that the priming factors such as Munc13s and RIMs play crucial roles.

Munc13-1 and –2, especially determine the patterns of short-term plasticity. While Munc13-1 mediates synaptic depression, Munc13-2 causes augmentation by a Ca^{2+}-dependent increase in release probability and RRP size in hippocampal neurons (Rosenmund et al., 2002). In addition, the lack of RIM1 causes short-term facilitation by decreasing vesicular release probability.

2.9 *Specific aim of the study: Syntaxin1- isoforms, structure and function*

Syntaxin1, initially named p35, was first described by biochemical studies as 'two 35-kilodalton proteins' (later known as syntaxin 1a and 1b, respectively) that interact with the synaptic vesicle protein synaptotagmin and N-type calcium channels (Bennett et al., 1992; Bennett et al., 1993). The mammalian syntaxin family consists of 15 different genes on different chromosomes. All of these syntaxins are type II oriented proteins, with amino terminus, the bulk of the polypeptide facing the cytoplasmic side. Most of the syntaxins are distributed ubiquitously while the predominant isoforms syntaxin 1a and 1b together with the less abundant syntaxin 1c, an alternative splicing product of syntaxin 1a (Jagadish et al., 1997), are selectively distributed in neuronal and secretory cells (Teng et al., 2001) . The main secretory cell specific isoforms, syntaxin 1a and syntaxin 1b share more than 75% of homology in protein level, as well as the secondary structure, thus, probably also tertiary structure (Perez-Branguli et al., 2002). Even though there is no direct evidence to prove the functional differences between isoforms, wide range of literature suggest possible functional differences: in the light of their differential distribution in both central and peripheral nervous system (Aguado et al., 1999; Ruiz-Montasell et al., 1996), different Munc18 binding affinities (Perez-Branguli et al., 2002) and isoform-preferential co-localization with synaptobrevin (Perez-Branguli et al., 1999). As Perez-Branguli et al. have shown, syntaxin 1a is preferentially localized with synaptobrevin/VAMP 2, and syntaxin 1b with synaptobrevin/ VAMP 1, meaning

that syntaxin 1a is predominant in the sensory neuron, while syntaxin 1b is exclusively expressed in motor neurons, suggesting that syntaxin 1b would be involved in neuronal networks, which need a very concrete amount of neurotransmitter release in a short time; conversely, syntaxin 1a could be related to a more regulated but slower exocytosis. The study on pancreatic beta cells revealed functional difference as well. In this system, they observed negative regulatory role in insulin release with syntaxin 1a overexpression, whereas insulin release did not show any difference in case of its isoform, syntaxin 1b (Nagamatsu et al., 1996). Biochemical approach on the long-term potentiation in mossy fiber terminals has shown increased expression of syntaxin 1b, together with increased capacity for glutamate release (Helme-Guizon et al., 1998). All of these independent studies on the difference of isoforms correlatively allow the hypothesis that synapses with syntaxin 1a could be more finely regulated, while those with Stx1B would be bigger and/or more immediate responding.

Findings on differential regulation of N-type Ca^{2+} channel between isoforms also support this hypothesis. Coupling of exocytosis with excitation of the presynaptic terminals in brain is dominated by Ca^{2+} influx through N- and P/Q-type Ca^{2+} channels (Takahashi and Momiyama 1993; Wheeler et al., 1994; Bezprozvanny et al., 2000). Syntaxin binds to these Ca^{2+} channels (Bennett et al., 1992) maybe to anchor synaptic vesicles near the Ca^{2+} entry site. Furthermore, syntaxin 1 has been reported to play a role as a negative regulator of the channels. Syntaxin 1 co-

expressed with N- or P/Q-type Ca^{2+} channel in *Xenopus* oocyte, reduced the availability of the channel by stabilizing inactivated channel (Bezprozvanny et al., 1995; Wiser et al., 1996).

Another way of Ca^{2+} regulation by syntaxin 1 is a G-protein mediated manner (Stanley and Goping, 1991; Stanley and Mirotznik, 1997). They showed that expression of syntaxin 1a causes G-protein mediated Ca^{2+} current inhibition in calyx-type nerve terminal of the chick ciliary ganglion synapses, which can be reversed by a preceding depolarization or cleavage of syntaxin 1 with botulinum toxin C1 (BTC1) (Stanley and Mirotznik, 1997). Parallel results were observed in tsA-201 cells. They found negative shift in the steady-state inactivation curve as well as G-protein mediated tonic inhibition. Interestingly, this G-protein mediated Ca^{2+} channel inhibition is caused only by syntaxin 1a, but not syntaxin 1b (Jarvis et al., 2000) (Jarvis et al., 2002). Moreover, when syntaxin 1 was co-expressed with either SNAP-25 or Munc-18 additionally, the negative shift of the steady state inactivation caused by syntaxin 1 disappeared, whereas G-protein mediated tonic inhibition still persists (Jarvis and Zamponi, 2001). Thus, in the physiological condition, where all the interacting molecules of syntaxin 1 are present concomitantly, G-protein mediated regulation by syntaxin 1a could be more important than direct inhibition.

If this isoform-specific regulation of Ca^{2+} channels causes difference in net Ca^{2+} influx at the presynaptic terminal, it would correlate well with the hypothesis

that these two isoforms could bring different efficiency of membrane fusion. To address this question, we studied synapses with only syntaxin 1b as compared to synapses containing both isoforms of syntaxin 1, with respect to the parameters determining neurotransmitter release.

As described in part 2.6, release of syntaxin 1 into an open-conformation is required to allow syntaxin 1 to associate into the SNARE complex (Munson and Hughson, 2002; Weimer et al., 2003b). Since SNAP-25 or synaptobrevin does not have a self-regulatory function, switching conformation of syntaxin 1 is the core determinant of SNARE complex formation. However, in spite of its importance, the functional consequence of syntaxin 1 conformation change from closed to open state is largely not known.

Free syntaxin 1 exists in a dynamic equilibrium state between its open and closed conformations (Margittai et al., 2003b). If this equilibrium can be artificially shifted by genetic manipulations so as to obtain a specific predominant conformation, then the functional significance of such a conformation switch upon SNARE-mediated membrane fusion. Double mutation in the linker domain (L165A, E166A) of syntaxin 1 has been reported to eliminate the default, closed conformation and lock syntaxin in its open conformation, thereby shifting the equilibrium to the constitutively active state. Also, this mutation abolished its binding ability to Munc18-1 (Dulubova et al., 1999). Thus, the second aim of our

study was to understand the physiological consequence of open conformation of syntaxin 1.

To provide a comprehensive and in depth understanding of functional role of open conformation of syntaxin 1 in vesicular docking and membrane fusion, we characterized the mice expressing of syntaxin 1 with constitutively open conformation (double point mutation, L165A, E166A; Gerber and Südhof, unpublished).

As described, the release of syntaxin into its open conformation is believed to be the main role of the essential priming factor, Munc13s. To resolve whether switching conformation of syntaxin 1 is indeed the sole function of Munc13s in membrane fusion, we tested whether activation of Munc13s via the diacylglycerol (DAG) stimulation, causes any further enhancement of neurotransmitter release over and above syntaxin 1 open mutation synapses

.

3. Experimental Procedure

3.EXPERIMENTAL PROCEDURE

3.1 Cell Culture

3.1.1 Microisland Hippocampal Culture As a Model Synapse

Microisland neuronal culture provided excellent experimental model synapse in this study. This central synapse model system is ideal for studying the most important parameters underlying synaptic transmission. In fact, it has been well established that these autaptic neurons are functionally indistinguishable from those *in vivo* including pharmacological kinetics, permeation properties as well as spontaneous activity (Bekkers and Stevens, 1991; Clements et al., 1992).

Moreover, this serves as a powerful tool for highly reliable quantitative estimation of synaptic transmission. Since all synapses originate from a single axon and connect to the same neuron post-synaptically, different synaptic release modes can be quantified, including spontaneous neurotransmitter release activity as well as responses induced by an action potential or hypertonic solutions. All these synaptic parameters are collected from the same cell, which is ideal for parameter cross-correlation, and also helps to reduce variability of data. One of the primary advantages of using this model system is that unlike conventional approaches, where pairs of neurons and electrodes are required, the autaptic system enables the use of a single electrode (Bekkers and Stevens 1991).

To obtain autaptic hippocampal neuronal culture, neurons were cultured on the feeder-layer of astroglial microislands. Culture dishes with microislands of astrocytes were prepared as follows. First, we coated glass cover slips with coating material microdots. Entire sterile round glass cover slips (30 mm in diameter) were first coated uniformly with 0.15% agarose (Type II-A, Sigma, Steinheim, Germany), a substrate upon which cells fails to attach, and placed in 6-well tissue culture plates. Coating material (0.1 mM acetic acid, 0.2 mg/ml collagen, and 0.1 mg/ml poly-D-lysine) is applied on top of the agarose using a rubber stamp with protruding pins to form small "islands", namely microdots, on which cells readily attach. By this method, we could provide distinct microisland area where cells can survive.

Next, astrocytes were enriched and plated using the following procedures. Brain cortexes of wild-type mice were enzymatically digested with a papain solution (20 units/ml of papain, 0.2 mg/ml cystein, 1 mM $CaCl_2$ and 0.5 mM EDTA in Dulbecco's modified Eagle's medium (DMEM; GibcoBRL, Grand island, NY, USA) and bubbled with carbogen gas until the papain dissolved in completely) for an hour, followed by 10 min-incubation in papain-inactivation solution (2.5 mg/ml albumin, 2.5 mg/ml trypsin-inhibitor, and 10% fetal bovine serum in DMEM). Subsequently, the brain tissue was gently triturated so as to obtain a single cell suspension. Cortical cells thus obtained were seeded and grown on ϕ75-mm tissue culture flask with 10% FBS-DMEM until cells became confluent. Once confluent, the culture was vigorously vortexed for 10 min and buoyant cells, which are mainly comprised of microglia, were discarded to enrich the astroglial population.

Adherent cells were collected with trypsin-EDTA and plated on the prepared coated dishes with 10% FBS-DMEM media containing 100 unit/ml of penicillin and 100 μg/ml streptomycin (GibcoBRL, Grand Island, NY, USA). Approximately 100,000 astrocytes were plated in each well of 6-well tissue culture plates. In the substrate forming microdot, astroglial as well as neuronal processes grow within the borders of the coated island but cannot reach outside because of the agarose. When astrocytes formed confluent islands, the anti-mitotic drug, FUDR (0.04 mM 2'-deoxy-5-fluorouridine; 1.0 mM uridine) was applied for 24 hours to prevent astrocytes from overgrowing.

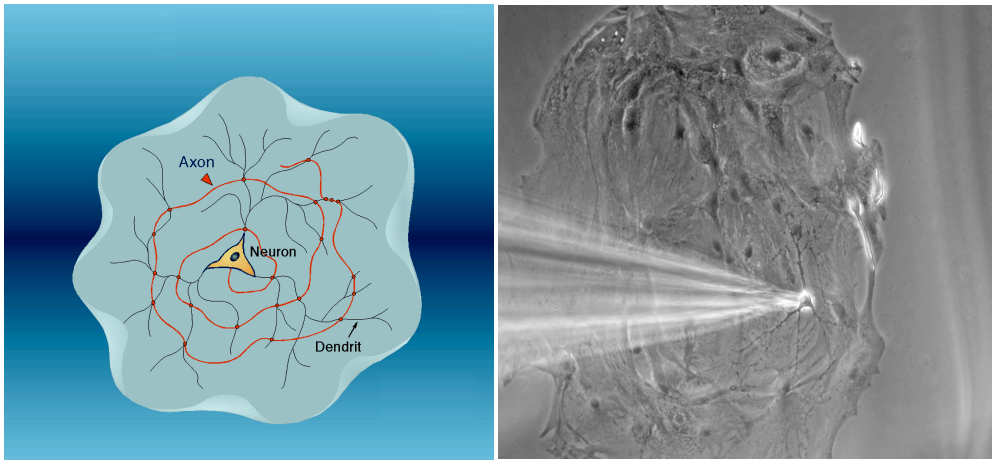

[Figure 4] Schematic diagram (left) and example (right) of autaptic neuron. On top of astroglial island, single neuron was grown to form all of synapses with its own dendrites. This model synaptic system is ideally suited to determine quantitatively the most important parameters underlying synaptic transmission. It is also unique, as all synapses originate from a single axon, which enables quantify different synaptic release modes including spontaneous release an responses by an action potential, by hypertonic solution in this study.

3.1.2Hippocampal Neuron Preparation

Hippocampi were dissected out of neonatal P0 mice brain in ice cold Hanks balanced salt solution (HBSS; GibcoBRL, Grand Island, NY, USA) and incubated with papain solution for 1 hr at 37°C with gentle shaking, followed by incubation with papain-inactivation solution for 10 min. After removal of inhibition solution, the tissue was incubated in neurobasal A medium, with 2% B27 supplement, 1% glutamax I, 20 IU/ml penicillin and 0.02 mg/ml streptomycin (NBA medium) at 37°C with shaking at 900 rpm while genotyping PCR reaction was completed. NBA medium and all of its supplements were purchased from GibcoBRL,Grand Island, NY, USA. Once we knew genotypes of littermates, hippocampi of homozygous mice were mechanically dissociated by gentle trituration in NBA medium. The tubes were allowed to stand for about 2 minutes so as to let the untriturated tissue sink-down by gravity. Dissociated single-cells in supernatant were transferred to fresh tubes, and cell number was determined. Approximately 4,000 to 5,000 single neurons were plated on the prepared confluent microisland astrocyte culture. Cultures were incubated in NBA medium at 37°C, with 5% carbon dioxide and 95% humidity for 9 days or longer before being used for electrophysiological recordings. To reduce possible variation between culture plates, the two different groups of neurons being compared were seeded on the same plate.

3.2 Genotyping

To preserve a homogeneous genetic background, we crossed heterozygote mice. In addition, comparing with control littermates, we were able to reduce the possible variability between different experimental animals. However, that required reliable genotyping of littermates. In order to genotype littermates, genomic DNA was enriched from the tail or fore brain of each animal. Primers for polymerase chain reaction (PCR) were designed to generate PCR products of different length, so that the wild-type and mutant gene were distinguished (S.Gerber and T.Südhof, unpublished).

3.2.1 Genomic DNA Purification

The template DNA was obtained from the tail biopsy from adult animals, or from brain tissue in case of neonatal mice and extracted using phenol/chloroform extraction. Tissues were incubated at 55°C, with 300 µl SNET buffers (20 mM Tris-HCl (pH 8.0), 5 mM Na_2EDTA (pH 8.0), 400 mM NaCl and 1% sodium dodecyl sulfate (SDS)) for lysis of cells, along with 0.17 mg/ml Proteinase K (Roche Diagnostics, Mannheim, Germany) which breaks down polypeptides for better dissolution in phenol. Cell lysates were mixed with the same volume of a 1:1 mixture of phenol and chloroform (USB chemicals, Cleveland, the USA). These organic

solvents precipitate proteins but leave nucleic acid in the aqueous phase. After 15 min of centrifugation at 13,000 rpm, protein molecules are left as a white coagulated mass at the interface between the aqueous and organic phases. The upper aqueous phase containing nucleic acids was transferred into a clean tube.

The DNA in the aqueous phase was precipitated with 0.6 volume of isopropanol and pellets were washed twice with 70% ethanol, and then, dried out in a speed vacuum drier (Eppendorf, Hamburg, Germany). Purified DNA was resuspended in 300 μl Tris-EDTA (10 mM Tris-HCl, 1 mM Na_2EDTA; TE) buffer (pH 8.0) before PCR was performed.

Although the DNA extraction protocol described above (phenol-chloroform extraction) leads to relatively pure and high yield of DNA, it is not suitable to genotype during the preparation of neurons for the cell culture since it requires relatively long time, thereby subjecting the neurons to a suboptimal condition. Thus, phenol-chloroform extraction was used only for genotyping adult mice or confirming the results of genotyping during primary culture. Instead, quicker protocol (on-line genotyping) was used in the case of neonates for the purpose of culturing. Triturated brain was used because of the faster digestibility in this case. The brain tissues left-over after dissecting out the hippocampus from newborn pups were triturated and incubated in 0.5 ml detergent free Tris-Sodium chloride buffer (10 mM Tris-HCl and 100 mM NaCl; TS) with 0.17 mg/ml at 55°C with vigorous

shaking for 10 min. Undigested tissue was spun-down by centrifugation for 2 min, and the proteinase K was inactivated by 5 minute boiling in a heating block. Another centrifugation of 3 minutes at 13,000 rpm was done to spin-down undigested tissue and coagulated matter. 1-1.2 µl of the supernatant was used as a template for the PCR.

3.2.2 Genotyping PCR

Two separate polymerase chain reactions (PCRs) were designed for detecting the type of gene present (S.Gerber and T.Südhof, unpublished). The reactions were performed according to [table 3] using a T-gradient® thermal cycler (Biometra, Goettingen, Germany). The amplified fragments were isolated by means of electrophoresis at 120 - 200 V in a 1.8% agarose gel in Tris-Borate-EDTA (TBE: 100 mM Tris-Cl (pH 8.0), 1 mM Na_2EDTA, 90 mM borate) buffer. Ethidiumbromide (EtBr) was added in the gel and the PCR products were visualized under UV light. All chemicals used for gel electrophoresis were purchased from Life Technologies (Carlsbad, CA, USA), Gibco BRL (Grand Island, NY, USA), Roche (Indianapolis, IN, USA), Invitrogen (Grand Island, NY, USA) or Sigma (Steinheim, Germany).

A Wild type reaction

Sense (SG01459): 5' GAA CGT CAG CTT CAG GCC TTC GCC TGC ATG 3'
Antisense (SG01460):5'CCA GCT AGG GAA TAA TTA GAC TAG GCG 3'

Syntaxin 1A knock out reaction

Sense (SG00368): 5'CAT AGC CTG AAG AAC GAG ATC AGC AGC CTC 3'
Antisense (SG00395): 5'CTG CCT TTC CTG TGC CCT TAG GGG AAA GCC 3'

B

wild-type reaction			knock-out reaction		
Temp (°C)	Time (m:s)		Temp (°C)	Time (m:s)	
95	3:00		95	3:00	
95	0:50		95	0:30	
58	1:10	40 cycles	66	1:10	40 cycles
72	2:45		72	1:00	
72	5:00		72	3:00	

C Wild type/ stx1B$_{of}$ knock-in reaction

Sense: 5' CAA GGA CCG AAT CCA GAG GCA G 3'
Antisense :5' GCT CAC ATC ATC AGT GAA GAT GGC 3'

D

wild-type reaction		
Temp (°C)	Time (m:s)	
94	3:00	
95	0:30	
58	0:45	40 cycles
72	0:45	
72	2:00	

E PCR-Mix

per 25µl Reaction

2.5 µl 10x Soriano Buffer
0.3 µl dNTPs (25 mM)
2.5 µl Primer 1 (10 pmol/µl)
2.5 µl Primer 2 (10 pmol/µl)
0.2 µl Promega Taq (5 unit/µl)
9.3 µl H_2O
1.0 µl DNA-Template

10x Soriano-Buffer

166 mM Ammoniumsulphate
670 mM Tris-HCl pH 8.8
67 mM $MgCl_2$
50 mM ß-Mercaptoethanol
67 µM EDTA
in H_2O

[Table 2] Polymerase chain reaction for genotyping. For genotyping of Stx1A KO and Stx1Bof mice line, primers were designed as shown in A and C to generate different product in size. The reaction was performed in the condition described in B and D. The composition of PCR mixture was described in E.

3.3 Protein assays

3.3.1 Immunoblot Analysis

Immunoblot analysis allows quantitative estimation on the expression of a protein of interest. In the present study, this method was used to evaluate the amount of each isoform of Stx1. Extracted hippocampi were homogenized in lysis buffer (150 mM NaCl, 5 mM EDTA (pH 8), 1% Triton X-100, 10 mM Tris-Cl (pH 7.4)), containing protease inhibitors (0.2 mM PMSF, 2 μg/ml each of aprotinin, pepstatin and leupeptin). Total protein concentrations of mice hippocampal lysates were determined by Bradford method (BioRad, Hercules, CA) using bovine serum albumin (BSA) as a standard. 20 μg of total protein was boiled in sample buffer (25% glycerol, 2% SDS, 14.4 mM 2-mercaptoethanol, 3 mg/ml bromophenyl blue, and 60 mM Tris-HCl (pH6.8)) for 10 min to make proteins have uniformed conformation and charge, eventually to resolve proteins only according to their molecular weight. Denatured proteins were resolved by sodium dodecyl sulfate – polyacrylamide gel electrophoresis (SDS-PAGE) and electrically transferred onto nitrocellulose membranes together with prestained molecular markers (Kaleidascope marer, Bio-Rad, Hercules, CA, USA). To confirm proper transfer of proteins, the membrane was reversibly stained with Ponceau S (Sigma, Steinheim, Germany). The blotted membrane was incubated with blocking solution (5% skim milk, 5% goat serum,

0.05% Tween20 in Tris-buffered saline) for one hour at room temperature for blocking the membrane from non-specific protein binding and incubated either with monoclonal anti-Stx1A antibody (Cl. 78.1) or polyclonal Stx1B antibody, diluted 1:1000 in blocking solution. These antibodies were kindly provided by R. Jahn, MPI for biophysical chemistry and Synaptic System, Göttingen, Germany. The membranes were incubated with primary antibodies overnight at 4°C and then washed three times in TBS-T (0.05% Tween20 in Tris-buffered saline). Subsequently they were incubated with horseradish peroxidase-conjugated secondary antibody for an hour at room temperature (1:10,000; Jackson Immunoresearch laboratories, Pennsylvania, USA). After second wash in TBS-T, chemiluminescent detection was performed using ECL plus (Amersham, Uppsala, Sweden) and membranes were exposed to X-ray film (Amersham, Uppsala, Sweden).

3.3.2 Immunohistochemistry

We investigated a possible change in tissue distribution of syntaxin 1a and structural alteration of hippocampus caused by the lack of syntaxin 1b using immunohistochemistry. To reduce developmental differences, age-matched mice were used. Anaesthetized mice were intercardially perfused with 5-10 ml of ice cold heparinized saline, immediately followed by 50 ml of fixative solution (4% paraformaldehyde in 0.1 M sodium phosphate buffer). Then, the whole brain of each

experimental group was extracted, and incubated with fixative solution for 30 min before being frozen. 14 μm thick slices from the fixed and frozen brains were incubated with monoclonal anti-syntaxin 1a and polyclonal anti-syntaxin 1b antibodies (Synaptic system, Göttingen, Germany) and probed with Alexa Fluor 488 dye-conjugated anti-mouse antibody and Alexa Fluor 568 dye-conjugated anti-rabbit antibody. Primary and secondary antibodies were applied with 0.3% Triton X-100 to increase cellular penetration. As negative controls, wild-type brain slices were sustained using the same procedure with no primary antibody incubation. The processed slides prepared were mounted with mounting solution (1.5% N-propyl gallate, 60% glycerol in PBS) and analyzed by Confocal microscopy.

3.4 Electrophysiology

Electrophysiological recordings were done using the hippocampal autaptic neuron model system (figure 4: see part 3.1, *Cell culture* in this section). Around the same number of cells from each experimental group were recorded in a day to even out possible changes in synaptic release properties during development.

3.4.1 Experimental Condition

All electrophysiological recordings were carried out at room temperature (23-25°C). Cultured autaptic neurons were perfused with the standard recording solution at a flow of 1 ml/min approximately. The solution in the dish was kept at a

constant volume by a low-pressure aspiration system. Pharmacological agents and other solutions were applied using a fast flow application system, which allowed reliably rapid exchange of solutions in as little as 20-50 ms. The patch pipettes were prepared using a horizontal puller (model p-87, Sutter of instrument, Novato, USA) from glass capillaries (type GB150F-8P, Science Products, Hofheim, Germany). Pipettes were pulled to a tip opening corresponding to about 2.2-3 MΩ in chloride-based internal solution.

3.4.2 Data acquisition

Currents were filtered at 5 kHz and recorded using a patch-clamp amplifier (Axopatch 200A; Axon Instruments, Union city, CA, USA), and were digitalized at 10 kHz using Digidata 1321A and Clampex 8.03 software (Axon Instruments, Union city, CA, USA) and subsequently analyzed using Axograph 4.5 software (Axon Instruments, Union city, CA, USA).

3.4.3 Standard external and internal solutions for electrophysiology

The standard external solution consists of 140 mM NaCl, 2.4 mM KCl, 10 mM HEPES, 10 mM glucose, 4 mM $CaCl_2$, 4 mM $MgCl_2$. Osmolarity and pH were adjusted to about 300 mOsm and 7.4 respectively to maintain physiological conditions during recording. The internal solution was made as following: 12 mM phosphocreatin, 0.3 mM GTP-Na, 4 mM ATP-Mg, 50 units/ml creatin-phosphokinase, 0.6 mM $MgCl_2$, 1 mM potassium-EGTA, 136 mM KCl, 17.8 mM

HEPES, solution was adjusted to pH 7.4 and 300 mOsm.

3.4.4 Stimulation Protocols and Electrophysiological parameters

3.4.4-1 Evoked response

As the standard procedure, EPSCs were recorded every 5s to monitor the quality of voltage clamping and evaluate non-specific changes in EPSC amplitude such as the influence of time-dependent run-down, leaky seals etc. Neurons were somatically voltage-clamped in the whole cell patch clamp configuration at a holding membrane potential of −70 mV. The cells were depolarized to 0 mV for 2 ms using a 0.2 Hz stimulation protocol to evoke action potentials, leading to an immediate Na^+ inward current followed by K^+ outward current (figure 5 *left*). As described in *Introduction (part 2.1)*, depolarization of membrane and subsequent action potential propagation induces Ca^{2+} influx in the presynaptic terminal which triggers a cascade of events evoking neurotransmitter release which can be detected as a post synaptic inward transient of quantal events normally with a 2-3 ms synaptic delay (EPSC in case of excitatory cells; Figure 5). The height of the peak and integration of the postsynaptic response were measured for EPSC amplitude and charge respectively.

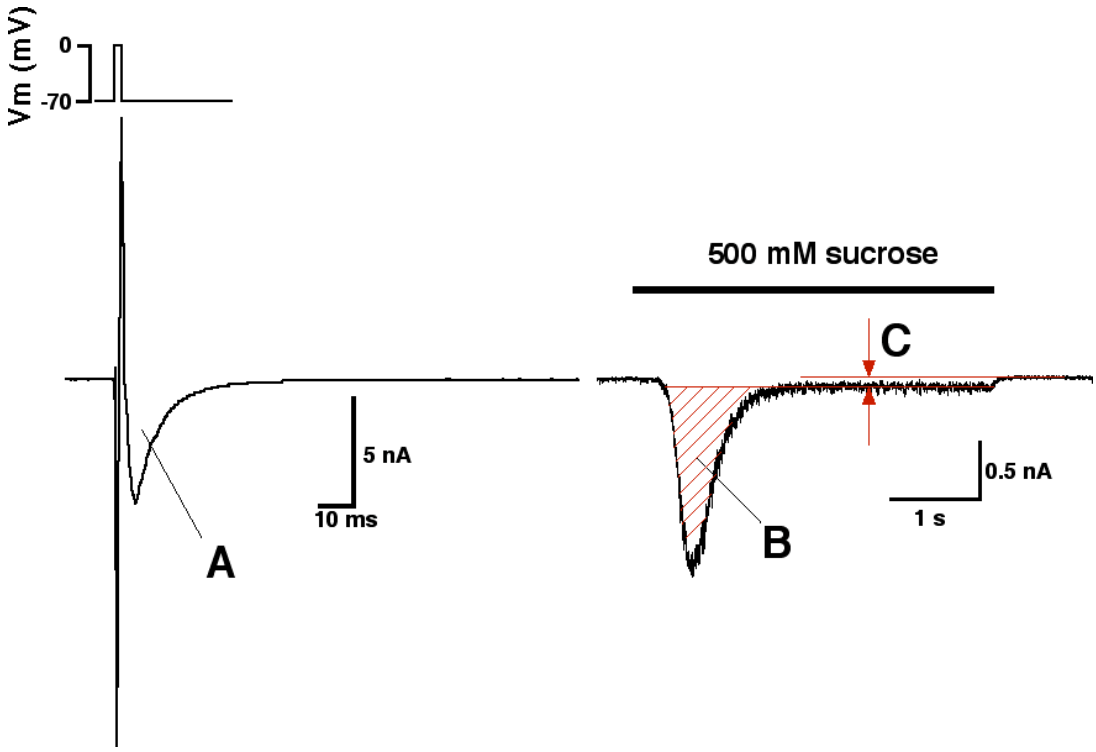

[Figure 5] EPSC, RRP and calculation of vesicular release probability. Left, Depolarization induced Na^+ inward and K^+ outward, and excitatory post synaptic currents (**EPSC ;A**). **Right,** Hypertonic solution (500 mM sucrose for 4 s)-evoked Inward transient current signifying the release of a readily releasable pool (**RRP; B**) of quanta (presumably corresponding to the primed synaptic vesicles) and followed by a steady state component representing equilibrium state between release and refilling. The mean amplitude of the steady state component quantifies refilling **C** (Rosenmund and Stevens, 1996). The charge of the EPSC (**A** in the figure) divided by the charge of RRP (**B** in the figure) gives the vesicular release probability.

3.4.4-2 Determining the size of readily releasable pool and vesicular release probability

As a manner of determining the total charge of RRP, the charge induced by hypertonic solution was measured as described in (Rosenmund and Stevens, 1996). 500 mM sucrose was extracellularly applied for more than 3 s using the fast flow application system. This application induces release of RRP, which leads to a transient followed by a steady state inward current (Figure 5, *right*). Since the transient part consists of a burst-like release of all fusion-competent, primed vesicles, the integral of the transient component after subtraction of steady state component give the total charge of the RRP (Figure 5 B). The sustained component induced by sucrose application is believed to represent the release of vesicles that have just been primed into the RRP (Figure 5 C; Reim et al., 2001).

To determine the vesicular release probability, 500 mM sucrose were applied for 4 sec, 3 sec after evoking the action potential. The vesicular release probability was calculated as the charge released by an action potential divided by total charge of the RRP [Figure 5].

3.4.4-3 Short-term plasticity

Cells were stimulated at 10 or 20Hz frequencies so as to reveal the short-term plasticity characteristics. Peak amplitudes of EPSCs during each train were measured and averaged. Furthermore, to reduce cell-to-cell variation in amplitude, every measured response was normalized to the amplitude of the first EPSC, and then averaged.

3.4.4-4 Calcium Sensitivity of evoked neurotransmitter release

The efficiency of the Ca^{2+}-triggered neurotransmitter release is one of the most important factors that decide the vesicular neurotransmitter release probability. Thus, to evaluate possible changes in the relationship between EPSCs and the external Ca^{2+} concentration by a given mutation, we studied neurotransmitter release as a function of external Ca^{2+} concentration.

The sensitivity of synaptic responses to various concentrations of external Ca^{2+} was measured at constant Mg^{2+} concentrations (1 mM). To control for the run-down of synaptic responses, individual test measurements were preceded and followed by EPSC measurements under standard conditions, namely 4 mM $[Ca^{2+}]_{ex}$ and 4 mM $[Mg^{2+}]_{ex}$. EPSCs in various $[Ca^{2+}]_{ex}$ are taken after being stabilized, and compared to mean EPSC amplitudes of preceding and following standard conditions. As an example, in figure 6, the level of EPSC change was determined as 2B/ (A+C). A represents the averaged EPSC amplitude of a standard condition (4

mM Ca^{2+} and 4 mM Mg^{2+}) before varying $[Ca^{2+}]_{ex}$; B shows mean EPSC amplitude under experimental condition (12 mM Ca^{2+} and 1 mM Mg^{2+} in figure 6) and C signifying average EPSC in standard condition after changing $[Ca^{2+}]_{ex}$.

The change in Ca^{2+}-sensitivity of neurotransmitter release will lead to alterations in the level of potentiation at high $[Ca^{2+}]_{ex}$ and also reduction of EPSC at low $[Ca^{2+}]_{ex}$.

On the other hand, in case Ca^{2+}-independent vesicular release probability is changed (even without affecting Ca^{2+}-sensitivity), level of potentiation can be expected to be altered because high probability of release limits the potential for any further enhancement while lower release probability allows a greater degree of potentiation.

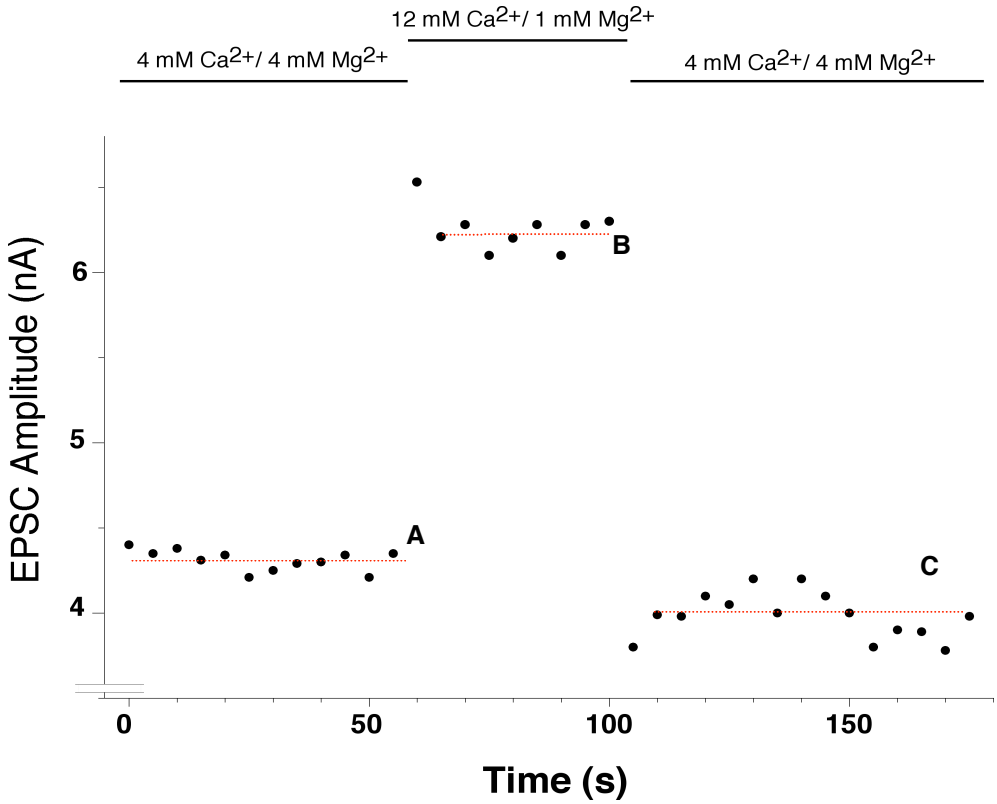

[Figure 6]Calculation of EPSC change in various Ca^{2+} concentrations. The sensitivity of synaptic responses to various $[Ca^{2+}]_{ex}$ (12 mM in this figure) was measured at constant Mg^{2+} concentrations (1 mM). To control the rundown of synaptic responses, individual test measurement was preceded and followed by EPSC measurements under standard control conditions, 0.2 Hz, in 4 mM $[Ca^{2+}]_{ex}$ and 4 mM $[Mg^{2+}]_{ex}$.Dashed lines show averages of each measurement under standard (before **(A)** and after **(C)**) and experimental **(B)** conditions. The level of augmentation was calculated as **2B / (A+C).**

3.4.4-5 Synaptic release probability

Synaptic release probability differs from vesicular release probability by the probability that any vesicle, no matter how many, at a given synapse is released during an action potential, note that vesicular release probability is the ratio of the charge released by an action potential to that of RRP. This can be different because of non-uniform size and structure of synaptic terminal. As a way of measuring synaptic release probability, the NMDA component of EPSC was measured with 100 - continuous action potentials in presence of MK-801, the irreversible NMDA open channel blocker. Since the antagonist will only be able to lock the pore of the receptor channel, only channels opened before are blocked. Thus, if the release probability of a given synapse is high, more post-synaptic NMDA channels will be open, and the progressive block should be faster (Rosenmund et al., 1993).

NMDA-EPSCs were revealed in external solution containing 2.7 mM-external Ca^{2+} and 10-mM glycine, without any added Mg^{2+} (see glutamate receptors in *introduction* part 2.2.3). This modified external solution allowed us to measure both AMPA and NMDA component of EPSC.

The amplitude of the NMDA component was measured by 100 successive stimuli at every 5 seconds in presence of 5 μM MK-801. The rate of progressive block of NMDA-EPSCs was estimated to evaluate synaptic release probability over synapses of entire neuron (Rosenmund et al., 1993).

Since this protocol takes relatively long time, there could be significant run-down of synaptic response in addition to decaying by MK-801. To compensate for the non-specific change of EPSC amplitude, every peak current of AMPA component of the individual response was set to one and normalized NMDA currents were measured by the mean amplitude between 50 ms and 100 ms (or later, depending on the size of the AMPA component).

3.4.4-6 Spontaneous release

Miniature EPSCs (mEPSCs or minis) were recorded at –70 mV at least for 50s with 0.3 μM tetradotoxin (TTX) to completely block the possibility of undesired action-potentials. A template-based detection program within the function of Axograph 4.5 was used for detecting and analyzing the miniature events. The template of mEPSC was determined as the following equation and criteria:

$$f(t) = \exp(-t/\text{rise time}) - \exp(-t/\text{decay time})$$

Template amplitude = -20 pA, template rise time = 0.5 ms, decay time = 5 ms, base line before events = 5 ms, and total template length = 30 ms. When the amplitude or charge was evaluated, events spaced within 10 ms of one another were discarded. Detection threshold was set to –3.5 fold of the noise standard deviation. Detected events were reselected based on their amplitude, rise time, and half-width. Events within the range of 10 to 100 pA in amplitude, 0 to 1 ms in rise time, and 0 to 5 ms in

half-width were considered as mini events. Selected events of individual cell were averaged to determine the mean amplitude and charge.

The number of vesicles in the RRP was calculated by dividing the integrated charge of the transient burst component in the sucrose response by the mean mEPSC charge measured for each cell. By comparing the frequency of events to the number of vesicles in RRP, spontaneous release activity was normalized for variation in size of RRP, which defines the spontaneous release probability (pool unit/s).

3.4.4-7 Somatic Calcium Current

Somatic calcium currents were measured in the external solution containing 0.5 μM tetradotoxin (TTX) which blocks the sodium current and 10 mM tetraethyl ammonium (TEA) to obstruct potassium current and we used Cesium-gluconate based internal solution to block potassium conductance. Cells were held at –70 mV and depolarized to 0 mV for 10 ms. Traces were subtracted by the current with external 200 μM cadmium, which completely blocks all types of Ca^{2+} current without affecting the Na^{+} or K^{+} current, to rule out possible interferences of other ionic flow.

Because mainly P/Q- and N-type Ca^{2+} channels govern the Ca^{2+} influx in the presynaptic terminal (see (Catterall, 1999)), 3 μM nifedipine was applied to eliminate the L-type channel dependent calcium current out of total Ca^{2+} current to provide better resolution of presynaptic Ca^{2+} current.

3.4.4-8 Kinetics of sucrose responses

To get a preliminary idea on neurotransmitter release, the release time course during sucrose application was analyzed. First, averaged shapes of sucrose responses were gained. Before averaging, each sucrose response was aligned at its peak of the transient component to determine width of the response. In another side, the evoking time delay was measured independently from individual sucrose response. Average shapes of sucrose responses were shifted according to the average time to evoke. To avoid artifacts resulting from improper application of the solution, comparable numbers of cells were analyzed on a given day and responses delayed by more than one second from the point of digital switching, were ruled out in this study. To compare release properties of each group, sucrose responses were integrated with a zero line as the sustained component and normalized by the total charge of the pool in each cell to standardize different RRP sizes.

Then, for more accurate analysis of hypertonic sucrose solution-evoked responses, the time-to-peak, half-width, 10-90% rise time, and time-to-onset of individual transient components were analyzed using Axograph 4.5 (Axon instruments, Union city, CA, USA). Responses with values lying outside of three

times standard deviation in any of the mentioned parameters were ruled out in this study.

3.4.4-9 Osmotic pressure-dependent neurotransmitter release

Neurons with greater release rates require less energy to have the same charge of transient component, since the transient component of a hypertonic solution-induced response represents the faster depletion factor in comparison to the sustained component. We therefore compared 250 and 350 mM sucrose-evoked transient component between the experimental groups. The charge was measured in the same way depicted in figure 5 and the released charge was normalized by the RRP charge of individual cells.

3.4.4-10 Maximum release rate

The maximum slope of the integrated sucrose response was determined in terms of maximum pool units released per second and used to compare the efficiency of neurotransmitter release by mechanical force. To compare neurotransmitter release rate as a function of various osmotic pressures, cells were subjected to 100, 250, 350, 500 mM sucrose solutions. To calculate the maximum release rate by 250, 350 and 500 mM sucrose, each transient component of sucrose response was integrated after baselining at the sustained component, and then normalized by the total charge of RRP judged by the released charge of the transient component during a 500 mM sucrose application, to even out various

RRP sizes. To measure the relese rate triggered by 100 mM sucrose, we used miniature events detection program within the function of Axograph 4.5 as described in *spontaneous release* section and calculated release rate based on the frequency of mini events. Measured frequency in presence of 100 mM sucrose was divided by the corresponding number of vesicles in RRP (calculated as charge of transient component caused by 500 mM divided by mean charge of spontaneous release).

3.4.4-11 Rate of vesicle turn over or refilling of readily releasable pool

The rate of replenishment of the RRP was compared by two different methods. The mean amplitude of the sustained component of a sucrose response was determined as the refilling amplitude, since the steady state sustained amount of release after depleting RRP is believed as the release from the vesicles just primed. The values were normalized to the total charge of the RRP of individual cell to compare refilling portion of the pool in a second (pool unit/s). However, this measurement is often not feasible, because of relatively low signal to noise ratio.

To overcome this problem, a paired pulse of sucrose application protocol was used. Two pulses of sucrose were applied onto the cell at variable time intervals. Then, the refilling rate during a time interval between two sucrose applications was determined by the ratio of the second release over the first release.

3.4.4-12 PDBU-induced augmentation

Augmentation of neurotransmitter release by β-phorbol ester (β-PE), a functional analogue of the endogeneous second messenger, diacyl glycerol (DAG) had been believed as a consequence of protein kinase C activation before it was found that no augmentation can be achieved by β-PE in neurons expressing mutant Munc13 deficient in DAG binding (Rhee et al., 2002). Since it is now well accepted that the β-PE induced augmentation is mediated by Munc13s, the level of augmentation was measured to examine whether Munc13 plays an additional role besides switching the conformation of syntaxin to the open state.

After obtaining baseline EPSC in standard condition, 1 μM β-PE was applied for 1 min, during 0.2 Hz stimulation, and then the effect of washing it out was measured for another 5 min. All of measured EPSCs were normalized to initial baseline EPSC and then averaged. The degree of augmentation was determined from the augmented EPSC after it reached steady state.

To resolve whether decreased augmentation in $Stx1B_{of}$ is caused by increased initial release probability, the levels of augmentation caused by β-PE for both groups was plotted in a graph as a function of vesicular release probability for each cell. Exponential fits were gained using a curve fit function of Kaleidagraph 3.0.

3.5 Experimenter bias minimization

Having prepossession during experiment and analysis of data can make significant effect on the results. To rule out any artifact that the experimenter could make by prejudice, all electrophysiological recordings and analysis were performed without knowledge of genetic background of the culture to eliminate experimenter bias artifact. A. Meyer regularly analyzes the genotyping results and assigned the mice of the different genotypes as letters A, B, C etc.

3.6 Data display and Statistics

All data shown represent the mean ± S.E.M. Statistical comparisons were performed using *Mann-Whitney Test* using statistical software Instat version 2.03 (GraphPad software, USA). A p values below 0·05 was regarded as a statistically significant difference.

4. Results

4. RESULTS

Being an integral component of the SNARE complex, syntaxin 1 plays a major role in neurotransmitter release via SNARE-mediated synaptic vesicle fusion. As described in the ***Introduction*** (part 2.9) syntaxin (Stx) has 15 different isoforms, and Stx1A and Stx1B are the two major isoforms expressed exclusively in secretory cells. Previous experiments showed differences between Stx1A and Stx1B including differences in distributions, co-localization with other SNARE partners, Ca^{2+} channel regulation, binding affinity to Munc18-1 (Aguado et al., 1999; Jarvis et al., 2000; Jarvis and Zamponi, 2001; Lu et al., 2001; Perez-Branguli et al., 2002; Perez-Branguli et al., 1999; Ruiz-Montasell et al., 1996). Although these studies suggest the possibility of functional differences between Stx1A and Stx1B, it is not yet documented whether these isoforms indeed have distinct roles in neurotransmitter release.

Stx1 is implicated to be the key determinant in regulating actual formation of SNARE complexes by its conformational switch (Duluvoba et al., 1999, Margittai et al., 2003a, Richmond et al., 2001). However, the physiological outcome of open-conformation of Stx1 remains unclear. Furthermore, in spite of the elegant study in *C.elegans* showing that opening of Stx is the sole function of Unc13 (Richmond et al., 2001), it has not yet been documented in mammalian system.

To address these questions, we characterized two genetically manipulated mouse lines, namely Stx1A null mice (Stx1AKO) and double mutant mouse

expressing the constitutively open conformation of StxIB and lacking StxIA ($StxIB_{of}$) using interdisciplinary methods including western blotting, immunohistochemical and electrophysiological techniques.

4.1 Mutant mouse strains, StxIAKO

To examine the possible isoform-specific functional differences of Stx1 by characterizing synapses exclusively expressing StxIB against those expressing both isoforms, we used StxIA null mice. Furthermore, it is necessary to identify the effects of eliminating StxIA to provide a proper control for the second part of the study, which explores the physiological consequences of open-form Stx1 by studying the synaptic release properties of $StxIB_{of}$.

StxIAKO mice were generated and provided by S. Gerber and T.Südhof at UT Southwestern, Dallas, TX, U.S.A. The line was maintained as heterozygotes to obtain mutant and wild-type in any given litter to eliminate possible litter-to-litter differences.

Homozygous StxIAKO mice are viable and fertile with no detectable abnormality in behavior or in gross anatomy (S.Gerber and T.Südhof, unpublished).

4.2 Expression of StxIA and StxIB in wild-type, heterozygote and knock out mice

To confirm these mouse models, we had to verify that the deletion of the gene leads to complete abolishment of StxıA expression. Therefore, we used western blot analysis against StxıA to verify the absence of StxıA at the protein level. Also to evaluate possible changes of expression level of StxıB protein, we quantified expression of StxıB in the absence of StxıA protein. The same amount of hippocampal extract was separated on SDS-PAGE electrophoresis and blotted onto nitrocellulose membrane. Blots were probed with isoform specific antibodies.

Figure 7 *left* shows that expression of StxıA was notably reduced in heterozygote mice (HZ) and completely abolished in StxıAKO mice. However, the lack of StxıA apparently did not affect the expression of StxıB (Figure 7 *right*). We conclude that in StxıA KO mice, StxıA protein is completely eliminated whereas StxıB expression remains unchanged, and the total amount of Stxı protein is reduced.

Since StxıAKO mice did not show any notable deficits in survival, behavior or anatomy, this demonstrates that neither absence of StxıA nor reduction in total amount of Stxı critically affected normal development and survival of mice.

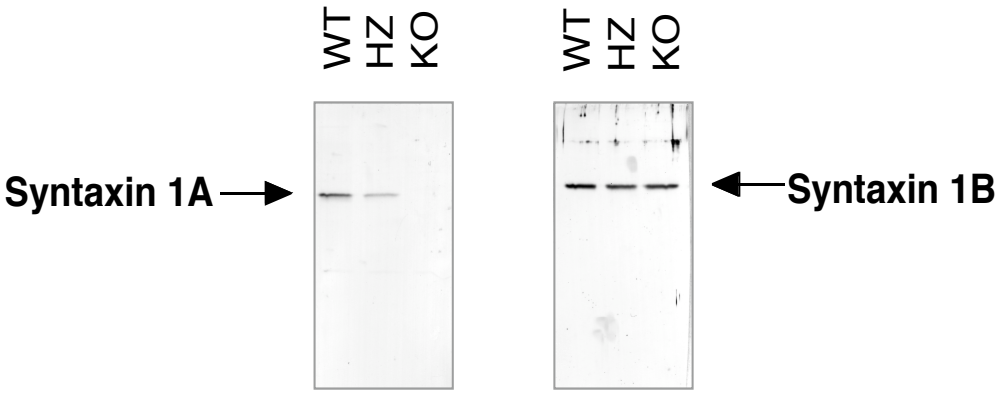

[Figure 7] Western blotting analysis Expressions of syntaxin 1a (left panel) and syntaxin 1b (right panel) were analyzed using western blotting in wild type (WT), Stx1A heterogygotes (HZ) and Stx1A knock out (KO) mice. 20 μg of total protein extracts were loaded in each lane, separated by SDS-PAGE and probed with monoclonal Stx1A (Cl. 78.1; left) or polyclonal Stx1B antibody (right). As expected the level of Stx1A expression was decreased in heterozygotes by half and knocked out in null mice, while expression of Stx1B is essentially constant.

4.3 Tissue distribution of StxIA and StxIB in hippocampus

To verify the complete elimination of StxIA and to test out possible changes in brain structure or distribution of StxIB by deletion of StxIA protein, we performed immunohistochemical staining experiments on slices from adult hippocampus. Fixed and frozen brains of age-matched adult mice were sliced at 14 μm thick and probed with anti-StxIA and 1B antibodies. As a negative control for non-specific staining, we stained wild-type brain slices using the same procedure omitting out the primary antibody incubation. Figure 8a shows distribution of these two isoforms in wild-type brain, in contiguity with the previous report of Ruiz-Montasell (Ruiz-Montasell et al., 1996). The signal of StxIA was significant reduced in the brain of heterozygote mice and signal detected in StxIAKO brain was comparable to that of negative control, which confirms the complete absence of StxIA in StxIAKO brain. We observed no obvious structural changes neither in the HZ nor the StxIAKO brains (n = 2), implying that absence of StxIA does not significantly affect development of brain structure.

This result, along with that of western blot analysis consistently shows that genetic ablation of StxIA leads to complete absence of the protein and proves that our genotyping assay is reliable. Furthermore, we found that removal of StxIA does not alter the expression of StxIB gene. Therefore, we could conclude that StxIAKO mouse line serves an ideal experimental system to investigate isoform-specific

function of Stx1. In addition, it allows direct comparison between synapses exclusively using wild-type Stx1B versus those using Stx1B with open-form mutation, in the second part of the study.

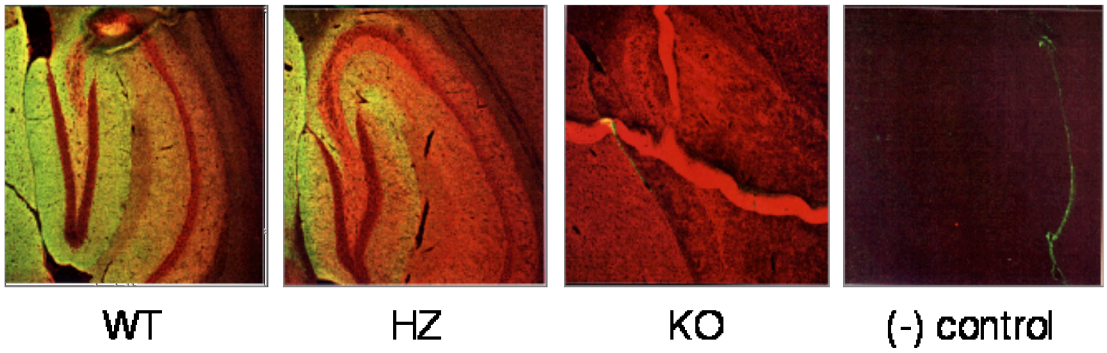

[Figure 8] Distribution of Stx1A and Stx1B in hippocampus. Fixed and frozen whole brains were sliced in 14 μm-thick sections, and incubated with monoclonal Stx1A (Cl. 78.1), ***green;*** and polyclonal anti-Stx1B, ***red;*** followed by with secondary antibodies. Wild-type (WT), heterozygotes (HZ) and knock out (KO). Negative control is gained from the same protocol omitting primary antibody incubation.

4.4 *Basic Characteristics in release efficacy of Stx1A KO*

To study synaptic neurotransmitter release properties of synapses using only Stx1B in comparison to those using Stx1A and Stx1B, we performed voltage-clamp recording on cultured individual hippocampal neurons from newborn pups (Bekkers and Stevens, 1991). We focused our analysis on excitatory glutamatergic neurons because they are more numerous, in addition, inhibitory GABAergic neurons show different molecular properties of vesicle release (Augustin et al., 1999). GABAergic neurons can be easily distinguishable from glutamatergic neurons by their time course of evoked neurotransmitter release. Neurons were voltage clamped at –70 mV and synaptic responses were evoked by 2 ms of somatic depolarization.

Our comparison of the mean amplitudes of the EPSCs between Stx1AKO mice and the control wild-type littermates, showed no obvious change in synaptic amplitude (figure 9A, 9B: 7.0 ± 0.6 nA, n=76 for WT; 7.3 nA ± 0.6, n=77 for Stx1AKO, p=0.9253). This data indicate that complete removal of Stx1A isoform lead to no significant impact on amplitude of evoked responses.

Next, we compared mean EPSC charge to detect possible changes in EPSC time course. If knocking out Stx1A caused major alteration of EPSC time course, for an example increases in asynchronous component, charge of EPSC could be altered, while the peak amplitude remains constant. Also, the EPSC

charge provided crucial information for calculating vesicular release probability. The measured mean EPSC charge was not affected upon removal of Stx1A (54 ± 5 pC, n= 76 for WT and 55.8 ± 0.7 pC, n= 77 for Stx1AKO, p=0.9824), supporting the conclusion that the lack of Stx1A does not bring about considerable alteration of evoked synaptic neurotransmitter responses.

Another important factor that determines the efficiency of neurotransmitter release is that total number of vesicles available for fusion, readily releasable pool (RRP). RRP can be quantified in autaptic neurons by pulsed application of hypertonic solution.

Four-second application of the hypertonic solution causes a transient followed by the steady state inward current. The transient component subtracted by the sustained component represents RRP and the sustained component represents the release of vesicles, which newly become available (Rosenmund and Stevens, 1996). We integrated the transient component of hypertonic sucrose response to define the RRP size and found no significant difference in their size between the Stx1AKO and their WT littermates (figure 9D and 9E: 690± 80 pC, n=68 for WT; 690 ± 80 pC, n=65 for KO, p=0.9534).

Knowing the charge of EPSCs as well as the charge of RRP, we can directly calculate which fraction of the RRP is released during the single action potential. This number is defined as vesicular release probability and it can be easily calculated by forming the ratio of the evoked response charge and RRP charge. We calculated vesicular release probability for each cell and found as expected that the vesicular

release probability was unchanged in the Stx1A deficient neurons (0.104 ± 0.007, n = 68 for WT; 0.101 ± 0.006, n = 65 for Stx1AKO, p=0.9193, Figure 9F). This finding indicates that regardless whether Stx1A is present or absent, an action potential releases synaptic vesicles with the chance of approximately 10%.

4.5 Short-term plasticity characteristics in Stx1AKO neurons

Presynaptic short-term plasticity is critically governed by changes in the vesicular release probability, along with other parameters such as action poteinal-induced Ca^{2+} influx and accumulation, RRP size, and pattern of stimulation (see (Zucker and Regehr, 2002)). Synapses with high probability of neurotransmitter release tend to depress during tetanic stimulation because limited number of fusion-competent vesicles are more quickly consumed than replenished. This phenomenon is clearly elucidated in the case of synapses expressing Munc13-1 H567K, point mutant knock-in mice that render Munc13-1 insensitive to diacylglycerol/β-phorbol ester, which showed stronger depression of synaptic responses during trains of action potentials because of their initially higher release probability in comparison to wild-type littermates (Rhee et al., 2002). On the other hand, low release probability synapses like those lacking complexin 1,2 or expressing mutant synaptotagmin (R233Q), which have 2-fold apparent decrease in Ca^{2+} sensitivity of release and thus reduced vesicular release probability, tend to facilitate (Fernandez-Chacon et al., 2001; Reim et al., 2001), probably because of accumulated residual presynaptic Ca^{2+}

(Schneggenburger et al., 2002). In contrast, wild-type hippocampal autaptic neurons consistently show approximately 50% of depression under identical condition.

Therefore, to further confirm the effect of Stx1A removal protein on initial release probability and subsequently on synaptic depression, we analyzed the normalized synaptic responses of amplitude during 50 trains of action potentials at a frequency of 10Hz.

We quantified peak current of each evoked response of the spike train and plotted the mean amplitude of all cells recorded (Figure 9G). In addition, we normalized EPSCs to amplitude of the first EPSC to reduce the cell-to-cell scatter in amplitude and then averaged (Figure 9H). As shown in figure 9G and 9H, both groups exhibited a typical short-term plasticity pattern of wilt-type neuron, prominent depression of EPSC during 10 Hz trains, which reach equilibrium at 45% for WT and 48% for Stx1AKO of the initial amplitude. Therefore, the patterns of short-term plasticity during 10 Hz in hippocampal neuronal autapses with and without Stx1A are essentially the same as expected by the finding concerning vesicular release probability.

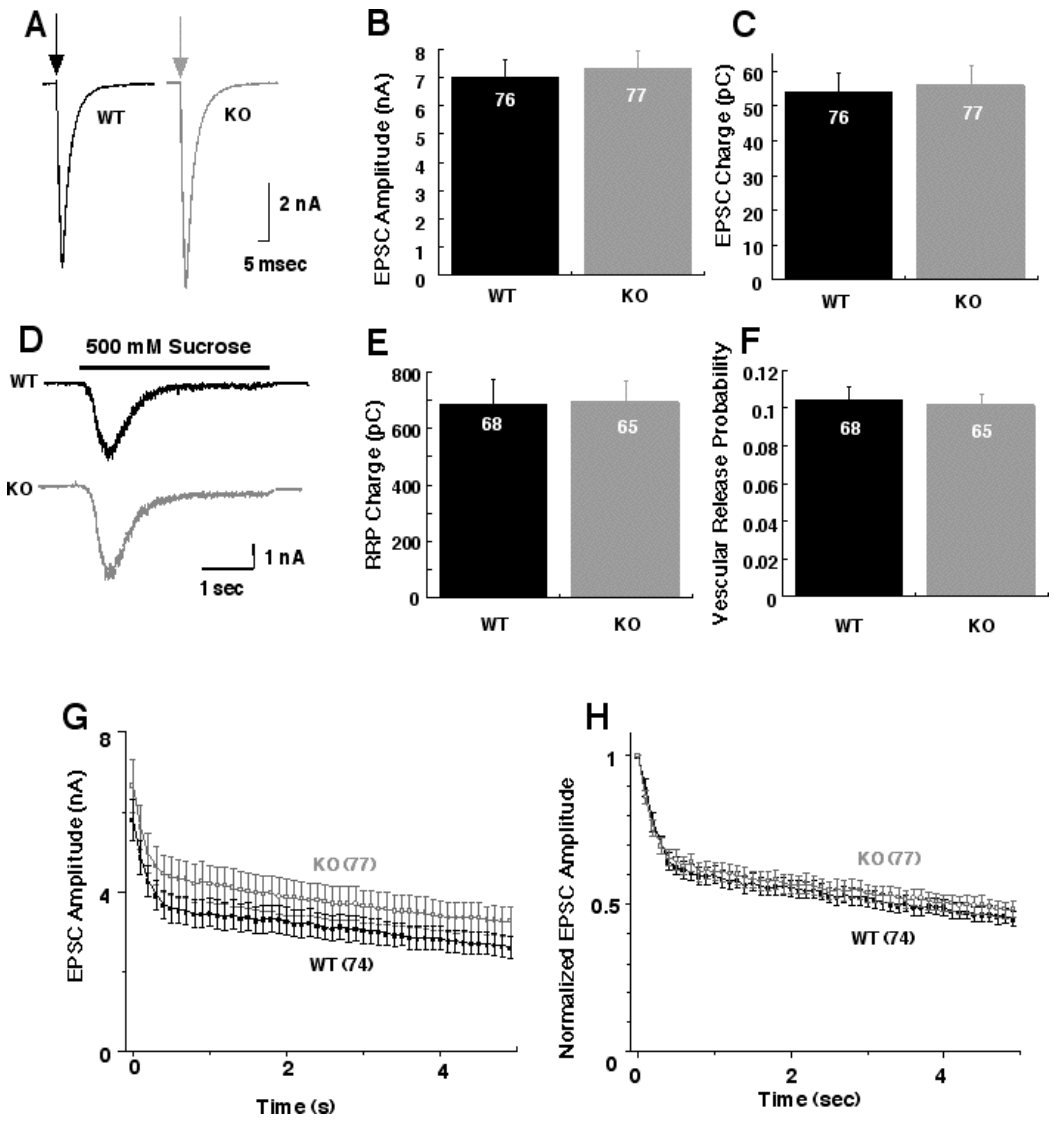

[Figure 9] Release efficacy and short-term plasticity of wild-type (WT) and syntaxin 1a knock-out (KO) neurons. Sample traces of wild-type (black) and Stx1AKO (gray) are shown in **A**. Arrows indicate the point of AP were evoked. Mean amplitude **(B)** and charge **(C)** of EPSC are compared between WT and KO in autaptic hippocampal neuronal culture. Neither charge nor amplitude of EPSC shows significance in difference **(B, C)**. To determine the RRP size, 500 mM sucrose was applied for 4s, and the transient component of inward current was integrated and determined as RRP (Rosenmund and Stevens, 1996). Examples of sucrose responses are shown in **D.** Black bar above traces shows time the sucrose was applied. **E** shows bar plot of mean RRP charges of two groups. **F,** Vesicular release probability, as calculated from the ratio of charge released by a single action potential to the charge released by sucrose application, was not changes by the Stx1A. **G, H,** Change of EPSC during 10Hz trains**.** The averaged actual amplitudes **(G)** and average normalized amplitude during tetanic stimulation **(H)**. Both WT and KO amplitudes show approximately 50% depression, compared to the first of the train. Numbers in bars (B, C, E and F) and in blanket in G, H shows *n*.

4.6 Calcium Sensitivity of EPSC

The sensitivity of EPSC amplitude to external Ca^{2+} is a parameter of importance, since evoked neurotransmitter release is tightly governed by the triggering molecule, Ca^{2+}.

To access whether there is any basic change in the sensitivity to external Ca^{2+} concentration ($[Ca^{2+}]_{ex}$), we used a simple experimental manipulation. Sensitivity to Ca^{2+} and saturation of release efficacy was monitored by measuring the level of potentiation of EPSC caused by increasing Ca^{2+}concentration in the external medium. As explained before (see part 2.8 and 3.4.4-4), the relationship between release probability and $[Ca^{2+}]_{ex}$ shows sigmoid shape. In other words, once release probability reaches plateau state, increasing $[Ca^{2+}]_{ex}$, henceforth, cannot cause any further increase in the release probability. Based on the principles of this relationship, manipulation of $[Ca^{2+}]_{ex}$ can be used for estimating release probability. The cells with high release probability will show less potentiation in response to elevation of $[Ca^{2+}]_{ex}$, because they are more saturated in terms of release probability. On the other hand, more potentiation is expected for the cell with initially low release probability.

External solution containing 12 mM Ca^{2+} and 1 mM Mg^{2+} (12 Ca^{2+}/1 Mg^{2+}) was applied, and the potentiation in EPSC was analyzed. To even out the run-down

of amplitude, EPSC measuring in 12 Ca^{2+}/1 Mg^{2+} was preceded and followed by standard external solution containing 4 mM Ca^{2+} and 4 mM Mg^{2+}, at least for 60s. Mean amplitude in 12 Ca^{2+}/1 Mg^{2+} was compared to average of control measurement before and after. Typical wild-type autapses show approximately 50%-70% of potentiation in response to this manipulation.

12 Ca^{2+}/1 Mg^{2+} induced approximately 1.6 fold potentiation of EPSC amplitude both in the WT and Stx1AKO groups (1.6 ± 0.3, n=43 for wild-type; 1.6 ± 0.1, n=38 for Stx1AKO, p=0.5671; Figure 10). This result indicates that Ca^{2+} sensitivity of neurotransmitter release machinery is not significantly altered, thereby, further corroborating the fact that the Stx1AKO neurons show classical release efficacy.

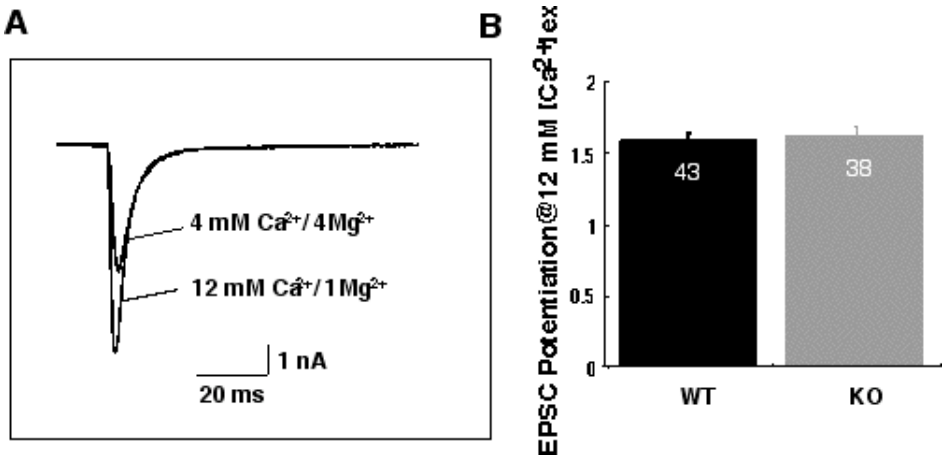

[Figure 10] EPSC potentiation by 12 mM $[Ca^{2+}]_{ex}$. Potentiation of EPSC by high Ca^{2+} concentration (12 mM Ca^{2+} and 1 mM Mg^{2+}) was measured in comparison to EPSC in normal external solution containing 4 mM Ca^{2+} and 4 mM Mg^{2+}. **A,** Representative raw traces for each condition **B,** Averaged potentiation in EPSC, showing the same ~ 1.6 fold increase in both WT and KO groups.

4.7 *Spontaneous Neurotransmitter Release in Stx1AKO*

Another critical aspect of synaptic function is Ca^{2+}-independent, spontaneous neurotransmitter release (mEPSC or minis). In spite of having no significant effect on the Ca^{2+}- dependent release properties such as vesicular release probability and short-term plasticity, the removal of Stx1A from neurons could induce possible changes in the spontaneous activity. In principle, the amplitude and kinetics of minis provide information about postsynaptic responsiveness, charge of minis shows vesicular load or the quantal size, and the frequency of mini conveys information about Ca^{2+} independent release efficacy. In order to detect changes in any of those parameters as a consequence of the Stx1A deletion, mEPSCs were recorded and analyzed. Recording of mini events was performed in the presence of 0.3 μM tetrodotoxin (TTX) at holding potential of −70 mV, which is close to neuronal resting membrane potential. The amplitude, charge and frequency of mini events were analyzed using template-based miniature detecting program.

No significant change was found in the amplitude (WT = 24.6 ± 1.1 pA, n = 39: KO = 26.3 ± 1.2 pA, n = 40, p = 0.4473), charge (0.106 ± 0.006, n = 39 for WT; 0.110 ± 0.005, n = 40 for KO, p = 0.3317), or frequency (WT = 7.5 Hz ± 0.7, n = 39 and KO = 6.1 ± 0.6, n = 40, p = 0.1551) of the mEPSC as shown in the Figure 11.

Therefore, from this observation, it can be concluded that knocking out Stx1A does not lead to any change in either evoked or spontaneous neurotransmitter release.

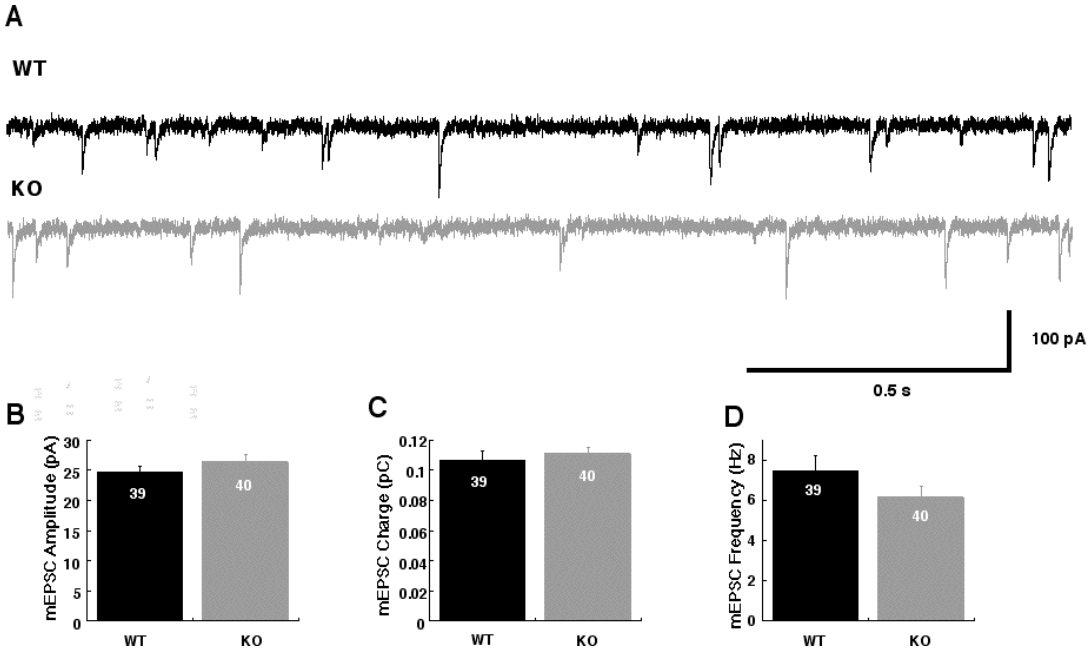

[Figure 11] Spontaneous neurotransmitter release in WT and Stx1AKO. A , Sample traces of miniature release in WT (black) and Stx1AKO (gray) neurons. To compare Ca^{2+} independent neurotransmitter release between WT and KO neurons, amplitude **(B),** charge **(C)** and frequency **(D)** of spontaneous neurotransmitter release were analyzed. Template shape based detection program was used for this analysis. Detected events were averaged in every cell for estimating charge and amplitude. None of the measured parameters *vis-à-vis* mean amplitude, charge or frequency shows significant alteration from wild type behavior. Numbers in bars show number of cells tested.

4.8 Turnover rate of readily releasable pool in StxIA KO

It has been consistently found that the various parameters of vesicle fusion, vis-à-vis evoked response, RRP size, vesicular release probability, short-term plasticity, Ca^{2+}-senstivity as well as spontaneous response remained unaffected by the removal of StxIA.

In view of these findings, attention was shifted to the pre-fusion stages, in order to study the effect of StxIA deletion on rate of the vesicular pool turnover, the efficiency of synaptic vesicle translocation, docking and priming to active zone of synapse. As described in *experimental procedure*, typically sucrose response is composed of a fast, transient component, which stands for the release of the RRP, followed by a sustained steady state component, which provides a measure for the refilling rate of the RRP.

Average refilling rate of RRP was determined by measuring the mean amplitude of the sustained component of the sucrose response. To quantify variance in the pool size of individual cells, mean amplitudes of the sustained components were normalized to the charge of the respective sucrose transients within the cell. Thus, the values show the turnover rate, refilled proportion of the RRP per unit time (in pool units/s) and the reciprocal of these values represent the time needed for refilling one pool unit. In the comparison between WT and StxIAKO, no difference

was observed (0.14 ± 0.02 pool unit/s for WT and 0.14 ± 0.01 pool unit/s for Stx1AKO, p=0.5502; Figure 12). This result of RRP turnover rate correlates well with the previously reported rate of WT hippocampal autaptic neurons (Reim et al., 2001), implying that Stx1A loss did not considerably affect the rate of vesicle translocation, docking and priming.

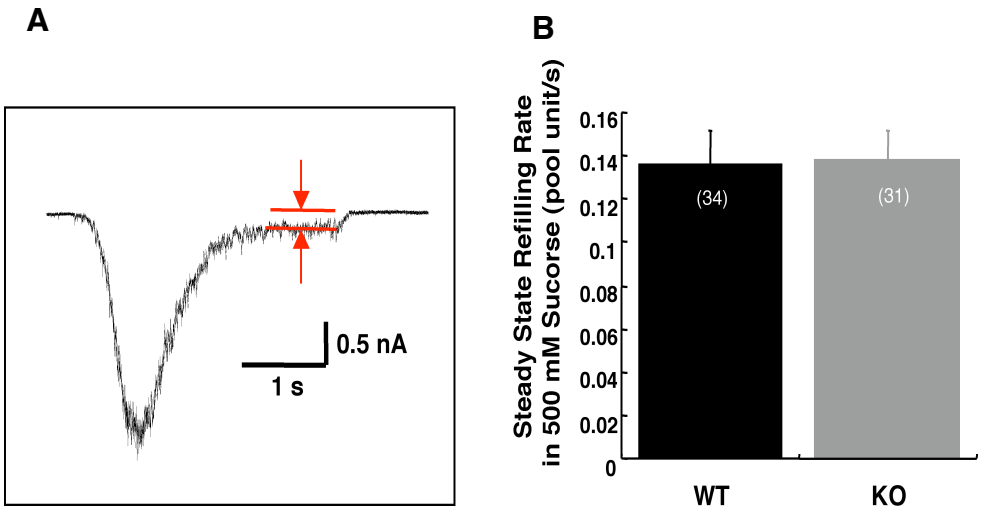

[Figure 12] Turnover rate of readily releasable pool. Sustained component of sucrose response stands for refilling rate of the RRP after depletion. **A.** Representative sucrose response and the way of measuring mean amplitude of sustained component **(red arrows). B.** Average of mean amplitude in sustained component of the response. Refilling rates obtained from the mean amplitude of sustained component show no difference between wild-type (WT) and knock-out (KO). Numbers in bars show the number of cells measured.

4.9 Stx1A KO cells as a control for comparison with syntaxin 1b open-form mutants

It has been establised through these studies comparing the fundamental parameters of neurotransmitter relase of the murine hippocamal Stx1AKO neurons to their wild-type counterparts, that their phenotypes are essentially the same with respect to Ca^{2+}-dependent as well as Ca^{2+}-independent neurotransmitter release, Ca^{2+} sensitivity, and turnover rate of the RRP.

Therefore, we concluded that it is acceptable to regard neurons from Stx1A KO mice as a control for analysis of double mutant mice with Stx1B open-form mutation and Stx1A knock-out ($Stx1B_{of}$).

4.10 Basic Characteristics of double mutant mice expressing constitutively open conformation of syntaxin 1b and syntaxin 1a null ($Stx1B_{of}$).

Stx1 has been implicated as the only SNARE component, which switches to open-conformation, exposing its core complex region, so as to regulate the actual formation of SNARE complex (Dulubova et al., 1999). This implies that syntaxin is the key molecule that controls the critical step of membrane fusion.

However, in spite of the importance of the molecule in regulation of neurotransmitter release, the functional significance of its conformational switching,

by which it actually exercises this regulation remains poorly understood (Dulubova et al., 1999; Jarvis et al., 2002). In the present study, characterization of double mutant mice expressing constitutively open conformation of Stx1B, lacking Stx1A ($Stx1B_{of}$) was carried out to address this crucial issue.

$Stx1B_{of}$ mice were provided by S.Gerber and T.Südhof and maintained as heterozygotes. At birth $Stx1B_{of}$ homozygote mice had similar body weight compared to control but usually developed seizure at the onset age of two weeks, and eventually died approximately a month after birth. However, the $Stx1B_{of}$ mice did not display significant abnormalities in gross anatomy, or brain structure (S.Gerber and T.Südhof, unpublished).

4.11 Characterization of Vesicular Release efficacy in $Stx1B_{of}$

In hippocampal autaptic neurons from $Stx1B_{of}$, amplitude and charge of EPSC, RRP were measured and vesicular release probability was calculated in the same manner as in the Stx1A null study.

Mean amplitude and charge of EPSCs from $Stx1B_{of}$ and Stx1A KO (control) of the same age *in vitro* show no significant difference (Figure 13 A, B, and C; Measured EPSCs amplitude were 7.7 ± 0.4 nA, n=171 for control; 7.8 ± 0.4 nA, n=185 for $Stx1B_{of}$, p=0.9824 and EPSCs charge were 57 ± 4 pC and 57 ± 4 pC for control and $Stx1B_{of}$, p=0.6802). These results indicate that basic machinery for

membrane docking and fusion are not destroyed by constitutive opening of Stx1B and time course of EPSC was not dramatically changed.

However, the open-form mutation in Stx1B causes reduction of RRP size to half of the control; 480 ± 70 pC, n=147 in $Stx1B_{of}$ compared to 760 ± 60 pC, n=167 for control: $p<0.0001$). Thus, vesicular release probability of $Stx1B_{of}$ becomes approximately 2.2 fold as high as control, because this is the ratio of constant EPSC charges to half-reduced RRP (Pvr=8.9 ± 0.4%, n=146 for control; 19.7 ± 0.9%, n=167 for $Stx1B_{of}$, $p<0.0001$: see figure 13D and F).

4.12 Short-term plasticity of $Stx1B_{of}$

As described above, short-term plasticity is a very useful tool for comparison of release probability. To confirm the increased vesicular release probability in $Stx1B_{of}$, synaptic amplitudes during trains of action potentials at frequencies of 10Hz and 20Hz were compared. The short-term plasticity of $Stx1B_{of}$ showed dramatically faster depression and greater depletion in both frequencies of trains (Figure 14), confirming the increased vesicular release probability in $Stx1B_{of}$ neurons (Figure 13).

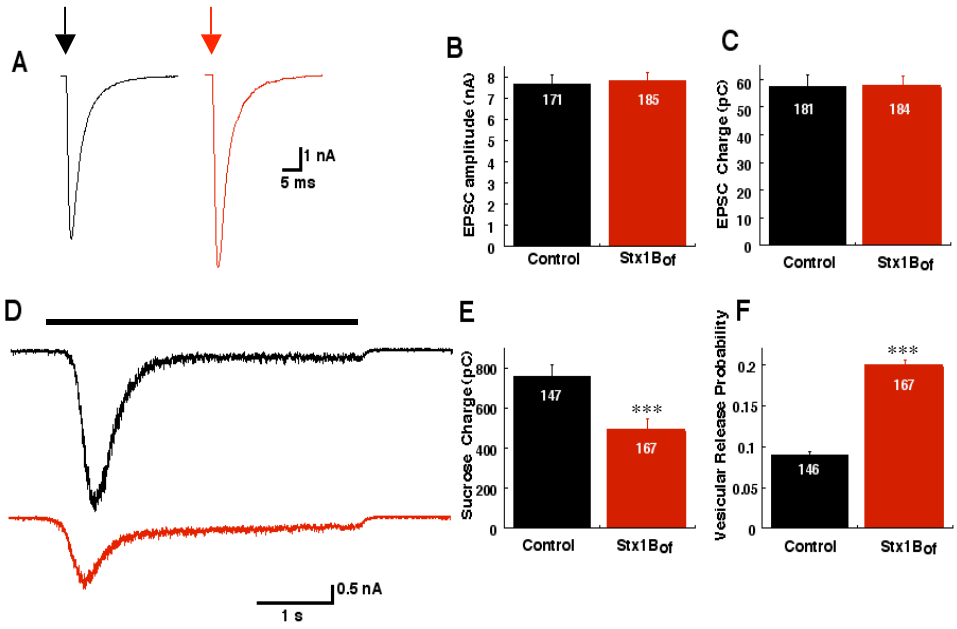

[Figure 13] Vesicular release probability of syntaxin 1b open-form mutant ($Stx1B_{of}$). **A,** Sample traces of evoked postsynaptic responses for control (black) and $syt1B_{of}$ (Red). Arrows indicate the point AP was evoked. **B,C,** While EPSC of $Stx1B_{of}$ is the same in amplitude and charge with syntaxin 1a knock out cell (control). **D,** Raw traces of sucrose reponse for controal and $Stx1B_{of}$ (black, red respectively). Black bar above traces represents application of hypertonic sucrose solution. **E,** The charge released by 500 mM sucrose (RRP) was reduced approximately by half ***p<0.0001**. F,** Thus, the release probability, calculated by these two factors, is increased approximately two folds. Number in each column shows number of cells tested, and error bars show S.E.M. ***p<0.0001

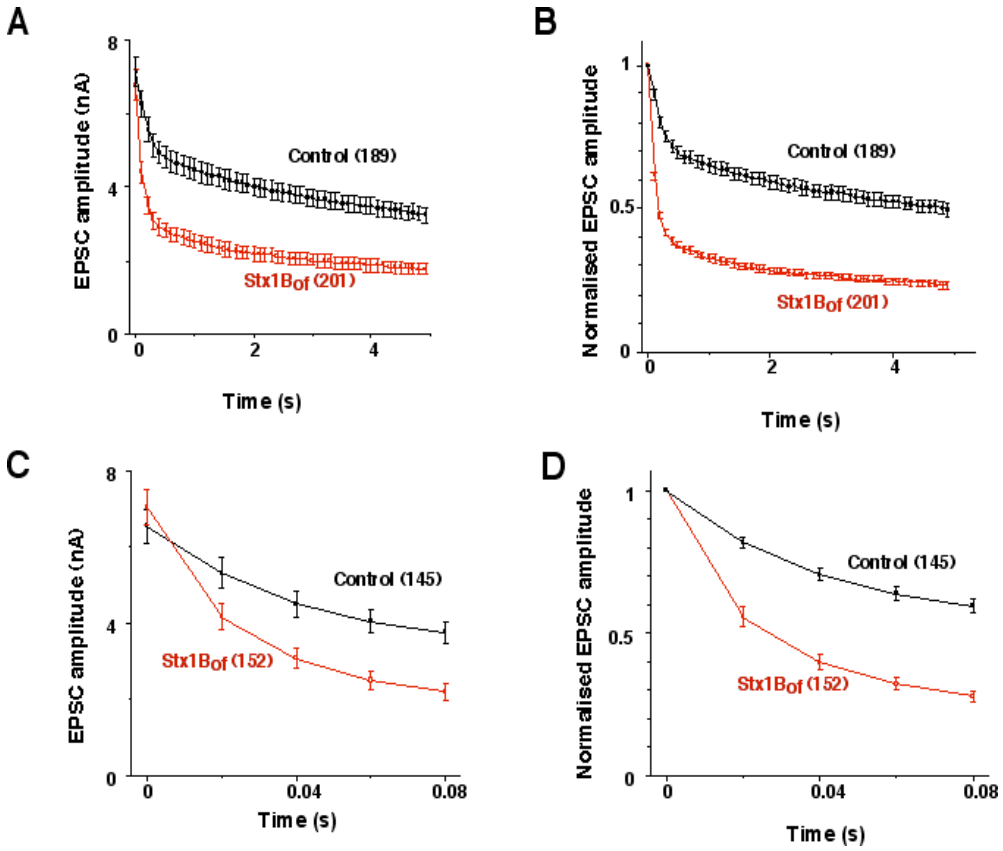

[Figure 14] Short-term plasticity characteristics of Stx1B$_{of}$. Synaptic amplitudes during trains of action potential at frequencies of 10 Hz **(A)** and 20Hz **(C)** were observed. EPSC amplitudes by tetanic stimulation were normalized to the one by the first stimulus in 10 Hz **(B)** and 20 Hz **(D)**. In both trains, Stx1B$_{of}$ shows dramatically faster depression, as well as the greater depletion, in contiguity with increased vesicular release probability. Numbers in blanket show number of cells tested and error bars show S.E.M.

4.13 Synaptic release probability

So far, we have shown the probability of individual vesicle to fuse by an action potential, so called, vesicular release probability is increased in $Stx1B_{of}$ neurons. Also, it was revealed that overall synaptic response was not changed and RRP size was rather decreased by the mutation. Since synaptic release probability is proportional to two different factors, vesicular release probability and number of vesicles in RRP (Dobrunz and Stevens, 1997), our results are indicating that both factor that increases efficiency as well as decrease efficiency of synaptic transmission are occurring with open-form mutation of Stx1B. To analyze the efficiency using completely independent method that depends on synaptic output, we used MK-801 method.

The underlying principle of this technique is based on the irreversible block of postsynaptic open NMDA receptors by MK-801. The rate at which synaptic NMDA-EPSCs are blocked is dependent upon the probability that any vesicle at given synapses is released during an action potential. Thus, the higher the synaptic release probability, the faster is the MK801 induced blockage of the NMDA-EPSC (Rosenmund et al., 1993).

To measure the NMDA mediated EPSCs, extracellular solution was modified. Mg^{2+} was removed, Ca^{2+} was decreased to 2.7 mM and glycine was added at a concentration of 10 μM (Rosenmund et al., 1993). Under this condition, we can simultaneously measure the AMPA-mediated and the NMDA-mediated EPSC. The AMPA mediated EPSC was the fast component of dual component of EPSC, while the NMDA mediated EPSC was slower component. After initial measurement of EPSC period, the extracellular solution was switched to the solution containing 5 μM MK-801. The dual components of EPSCs were recorded during 100 consecutive action potentials and we used AMPA receptor-dependent fast component as internal normalization factor for possible presynaptic run-down of the EPSC.

When we compared the normalized NMDA decay constant for $Stx1B_{of}$ with control, we noticed that initial, rapid phase of NMDA component decay was slightly faster but not quite significant in $Stx1B_{of}$ than in control ($\tau = 3.5 \pm 0.2$ stimuli, n = 16 for control and 3.0 ± 0.1 stimuli for $Stx1B_{of}$ n = 20; $p = 0.0721$) and ultimately, come to the same level during the later slow decay phase. This result was consistent with heterogeneous synaptic release probability in hippocampal autaptic cultures (Rosenmund et al., 1993). Also, our data indicate that the increase in vesicular release probability was compensated by decrease in number of fusion-competent vesicles in RRP keeping the overall synaptic output at low frequency stimulation relatively stable.

Based on our findings (A) synaptic output remains unchanged, (B) synaptic release probability is almost not changed; we can conclude that the increase in vesicular release probability has been compensated by the decrease in number of vesicles in the RRP. These result is further supported by faster depression and greater depletion of EPSC during trains of action potentials because of the reduced number of vesicles per active zone.

.

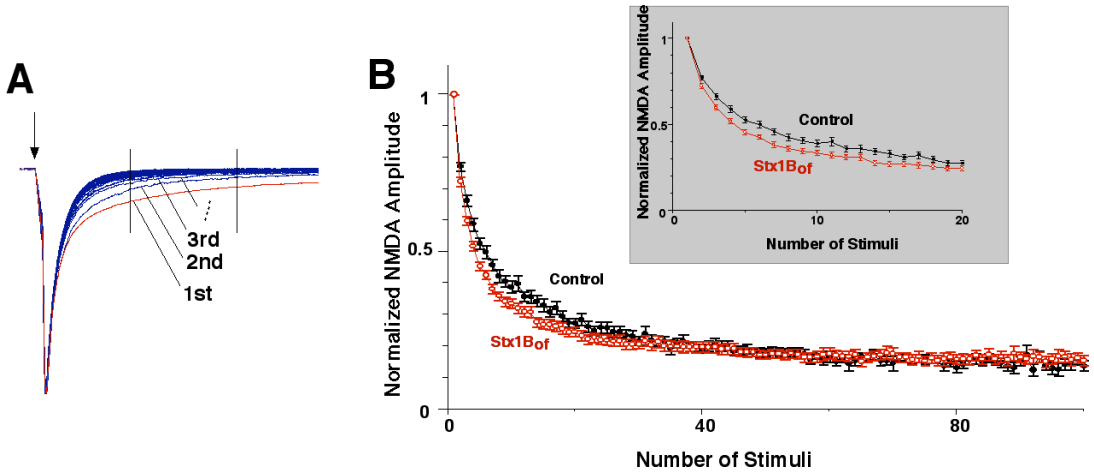

[Figure 15] Determining Synaptic release probability as given by the decay of NMDA (N-methyl-D-aspartate) dependent current in the presence of MK-801. Dual components of AMPA- and NMDA-mediated were activated every 5 sec by somatic depolarization with 10 μM glycine and 2.7 mM [Ca^{2+}] in the absence of external Mg^{2+}. Amplitudes of NMDA component were measured during consecutive 100 stimuli at every 5 sec in presence of 5 μM MK-801. During the successive stimulation, activated proportion of the channel is shown as decay. NMDA currents were determined as mean amplitude between 50-100 ms, in most cases. In the cells that have big AMPA current, time window was shifted accordingly. **A,** Sample traces of NMDA current during spike train with MK-801. Arrow shows the point where action potential was evoked. AMPA component of EPSC was used as internal control of presynaptic run-down **B,** Average normalized NMDA EPSC during 100 stimuli. At the beginning of stimulation, $Stx1B_{of}$ shows slightly faster but not significant decay in NMDA current and ultimately, reach same level during the later slow decay phase (p=0.7619). First 20 responses were magnified in inset.

4.14 Calcium sensitivity to neurotransmitter release

Our results so far lead to the conclusion that constitutive opening of Stx1B leads to an increase in the release probability of vesicles. One possible explanation of this increased vesicular release probability could be that the calcium sensitivity of the release apparatus was increased by the open-form mutation of Stx1B, alternatively, the mutation induced greater calcium influx. To evaluate these possibilities, first, EPSC amplitude was measured in the varying external concentrations of calcium (1, 2, 4, 8 and 12 mM), holding magnesium at constant concentration (1 mM). Each mean EPSC at the testing concentrations was normalized to the mean EPSC amplitude under the standard concentration (4 mM $[Ca^{2+}]_{ex}$, 4 mM $[Mg^{2+}]_{ex}$; see figure 6)

As shown in [Figure 16], as compared to the control (Stx1AKO), EPSC amplitudes of $Stx1B_{of}$ were less reduced at lower concentrations of external calcium (EPSC of control and $Stx1B_{of}$ at 1 mM $[Ca^{2+}]_{ex}$ was respectively 0.36 ± 0.03 (n=16) and 0.52 ± 0.04 (n=19) of EPSC in standard condition (p=0.0103)). Also, a smaller degree of potentiation was observed in $Stx1B_{of}$ at 12 mM $[Ca^{2+}]_{ex}$, EPSC of control potentiated 1.70 ± 0.09 (n=15) while $Stx1B_{of}$showed 1.38 ± 0.04 (n=15; p=0.014).

As a consequence, the overall relationship between EPSC and Ca^{2+}- dose showed an obvious left shift. However, this apparent left shift is not necessarily

indicative of increased Ca^{2+} sensitivity of release apparatus but it also can interpreted by the overall increase in Ca^{2+}-independent release probability (see part 3.4.4-4 and 4.16).

4.15 Somatic Calcium Current

Next, to analyze whether the mutation was directly affecting Ca^{2+} regulating function of Stx1, we assessed Ca^{2+} channel function. The possible alteration in Ca^{2+} regulation by open-mutation of Stx1 has been suggested by some previous reports that voltage-gated calcium channels are regulated by Stx1 and this regulation depends on conformations of Stx1 (Jarvis and Zamponi, 2001). Since our culture system does not allow for direct recording of presynaptic terminal because of its small size, we analyzed Ca^{2+} current at soma. It is known that the soma contains similar types of channels that are present at the presynapse (N- and P/Q-types) and also Stx1 is present at the plasma membrane of soma.

To record Ca^{2+} current specifically, voltage-dependent conductance of Na^{+} and K^{+} was blocked by using Cs-based internal solution and external solution containing 0.5 μM TTX and 10 mM TEA. We measured somatic Ca^{2+} current by depolarizing the neuronal somatic membrane from –70 mV to 0 mV for 10 msec. In addition, to remove L-type Ca^{2+} channel-dependent conductance, which contributes little at neurotransmitter release, we added L-type Ca^{2+} channel antagonist,

nifedipine (3 μM) to the extracellular solution.

When we averaged the mean somatic calcium currents with and without L-type channel contribution in the control and $Stx1B_{of}$ neurons, we found no significant difference. I_{ca} with L-type channel contribution was 0.66 ± 0.10 nA, n=15 for control; 0.65 ± 0.07 nA, n=16 for $Stx1B_{of}$, p=0.6213 and I_{ca} without L-type channel contribution was 0.40 ± 0.05 (n=12) for control and 0.40 ± 0.07 (n=11) for $Stx1B_{of}$, respectively (p=0.9274). Even though further studies on presynaptic Ca^{2+} current are needed for a definite conclusion, a possible putative change in presynaptic Ca^{2+} current is unlikely to be the main cause of a 2.2 fold increase in the vesicular release probability and the left shift of the apparent sensitivity of the EPSC to external Ca^{2+} concentration [Figure 17].

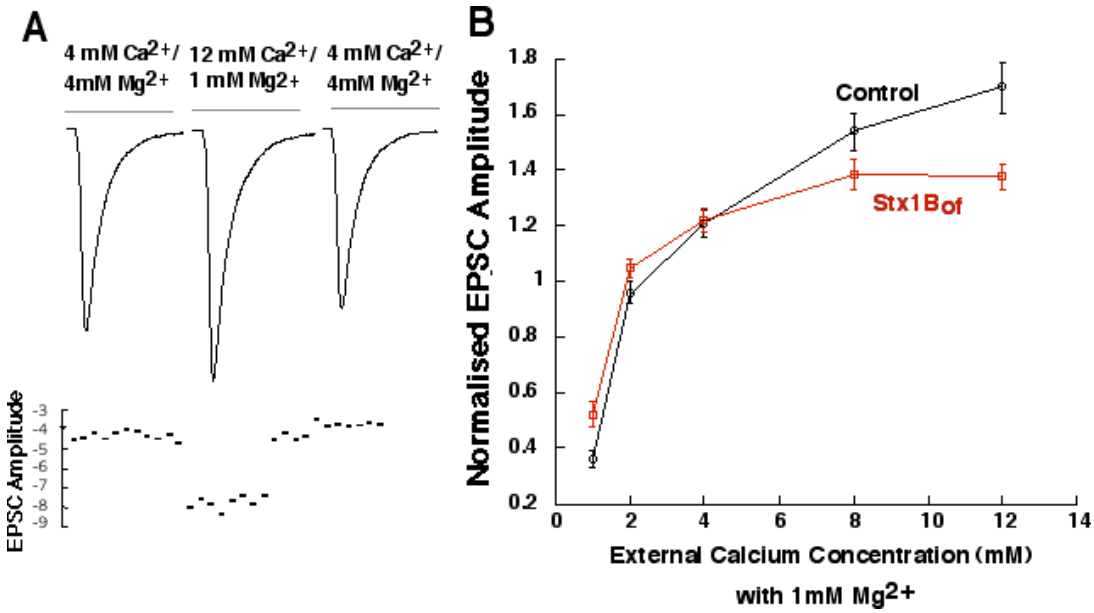

[Figure 16] Dependency of EPSC amplitude upon external Ca^{2+} concentration. EPSC amplitudes were measured at 0.2 Hz at various concentration of external calcium (1-12 mM), with constant 1 mM Mg^{2+}. To compensate the rundown effect and variability of EPSC between cells, we scaled EPSC in standard condition (4 mM Ca^{2+}, 4mM Mg^{2+}) before and after the individual test recording. The responses at various concentrations of external Ca^{2+} were normalized to EPSC's under standard condition. Note that responses in $Stx1B_{of}$ less increase at lower $[Ca^{2+}]_{ex}$ and also decreased less at higher $[Ca^{2+}]_{ex}$ in comparison to KO group. Change of normalized EPSC by 1 mM and 12 mM Ca^{2+} showed significant difference p=0.0103 and 0.0114, respectively. Error bars show S.E.M.

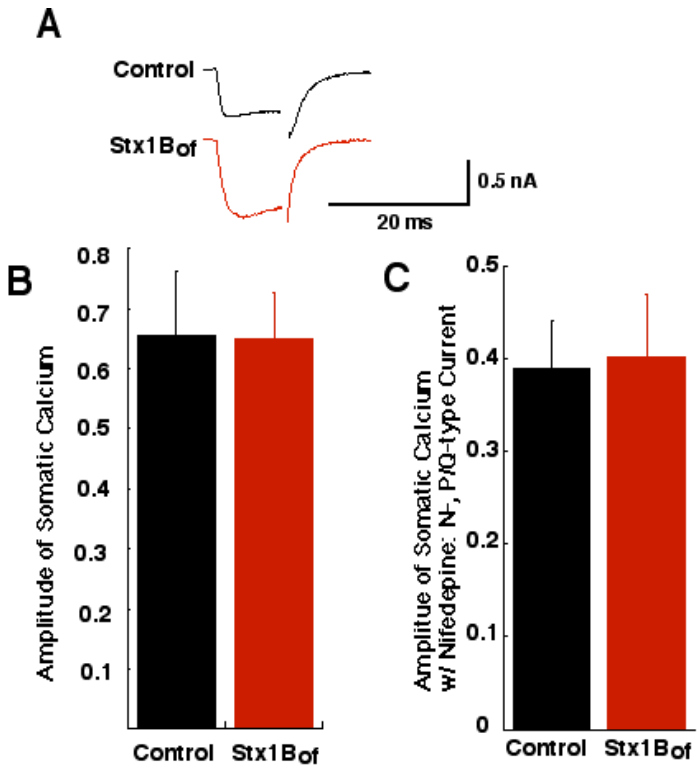

[Figure 17] Somatic Ca^{2+} current comparison between control and $Stx1B_{of}$neurons. To measure somatic Ca^{2+} current, cells were depolarized for 10 ms to 0 mV in presence of internal Cs and external 0.5 μM TTX and 10 mM TEA **A,** Leak subtracted sample trace of each group. Total somatic Ca^{2+} current as well as the amplitude L-type dependent current subtracted by 3 μM Nifedipine. **B,** No significantly different amplitude of the currents were observed in both with and without L-type Ca^{2+} channel conductance.

4.16 Spontaneous Neurotransmitter Release

So far our data indicates that the open-form mutation of Stx1B leads to an enhanced vesicular release probability, in addition to a shift of EPSC sensitivity to external Ca^{2+}. These data could mean that overall sensitivity to Ca^{2+} is increased; alternatively, this could be the consequence of a shift in the Ca^{2+}-independent release probability, which is not dependent on Ca^{2+} sensing (see 3.4.4-4). One way of resolving these possibilities would be to test whether spontaneous neurotransmitter release is affected by the open-form mutation. If we observe the enhanced spontaneous release frequency, which is by definition a Ca^{2+}-independent neurotransmitter release, we would gain evidence for more efficient Ca^{2+}-independent fusion of vesicles. In addition, it can be also interpreted as a reduced energy barrier for the fusion process itself. This analysis also conveys information about the possible changes in postsynaptic receptor responsiveness or loading of neurotransmitter into vesicles. Hence, we analyzed amplitude, charge, and frequency of miniature EPSCs in $Stx1B_{of}$ neurons as well as Stx1AKO control neurons in the presence of 0.3 μM TTX to eliminate any action potential or spontaneous Ca^{2+}-driven release.

Our analysis of mEPSC between the two groups showed that neither average amplitude nor charge of mini events was significantly different between

control and $Stx1B_{of}$ neurons, showing that constitutive opening of Stx1B does not affect post synaptic or quantal parameters. The mean amplitudes of mEPSCs were 23 ± 1 pA, n=69 for control and 25 ± 1 pA, n=68 for $Stx1B_{of}$, (p=0.1235); and the mean charge of mEPSC were 0.106 ± 0.005 pC, n=69 for control and 0.094 ± 0.005 for $Stx1B_{of}$ (p=0.1704; Figure 18 B and C).

However, the average frequency of the spontaneous neurotransmitter release was significantly increased in $Stx1B_{of}$ neurons (Figure 18D: 5.3 ± 0.5 Hz, n=70 for control, 7.3 ± 0.6 Hz, n=68 for $Stx1B_{of}$, p=0.0099). Since we measured mEPSC frequencies and RRP size in the same neuron, we could determine the spontaneous vesicular release probability from these neurons. The 'spontaneous vesicular release probability' was calculated by dividing the frequency of mini events by the number of vesicles in RRP. Because RRP size of $Stx1B_{of}$ neurons was significantly reduced, we observed dramatic increase in probability of spontaneous release. The calculated spontaneous release probabilities were for control 0.0015 ± 0.0004 s^{-1} (n=62) and 0.0033 ± 0.0004 s^{-1} (n=62) in $Stx1B_{of}$ neurons (p<0.0001) as shown in Figure 18 E. The level of increase in spontaneous release probability was approximately as large as the increase in the vesicular release probability of evoked responses (2.2 fold increase in both vesicular release probability as well as spontaneous release probability). Based on this finding, there is a possibility that the increased vesicular release probability of evoked responses may be caused, at least in large part, by this enhanced Ca^{2+}-independent neurotransmitter release efficiency.

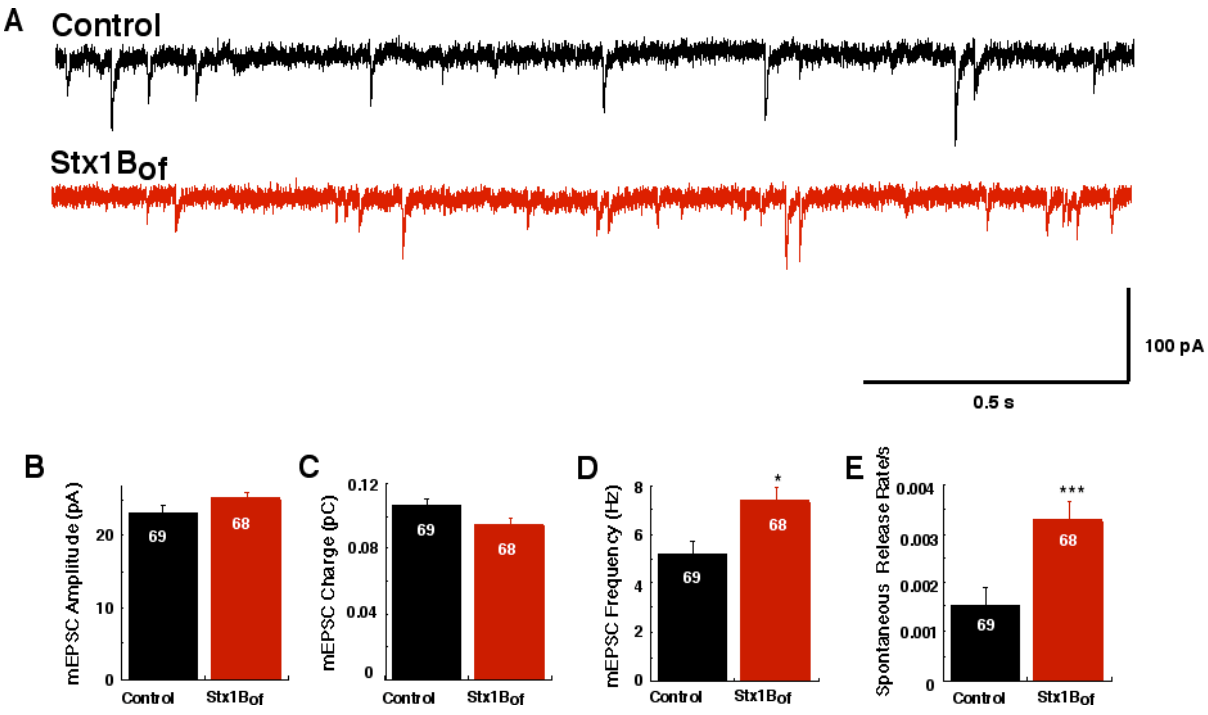

[Figure 18] Spontaneous neurotransmitter release efficiency in Stx1B$_{of}$ neurons. Spontaneous neurotransmitter release was measured at –70 mV, in presence of 0.3 μM TTX. **A,** Black and red traces represent sample trances for spontaneous neurotransmitter release of control and Stx1B$_{of}$ neurons respectively. **B, C,** While amplitude and charge of mini events remain unchanged **D**, frequency of spontaneous events was significantly increased in Stx1B$_{of}$. **E.** To compare the frequency of events per number of vesicles in RRP, we calculated spontaneous release probability as the frequencies of mini events divided by the number of vesicles in RRP in each cell. Note that the spontaneous release probability was increased as much as vesicular release probability (2.2 fold). *p<0.05, ***p<0.0001, Numbers in bars show the number of cells tested.

4.17 Neurotransmitter release time course by osmotic pressure

To test the hypothesis that the increased efficiency of spontaneous release is responsible for that of evoked responses, we systematically analyzed the time course of neurotransmitter release by osmotic pressure in more detail. Since hypertonic solutions are known to release the fusion-competent vesicles in a Ca^{2+} independent manner, if this hypothesis is correct, then vesicles would be released with greater ease. In other words, when the same amount of force, (for example, osmotic pressure) is applied to the synapse, a reduction in the energy threshold for neurotransmitter release, as may be the case for the $Stx1B_{of}$, would cause an earlier onset and faster release of vesicles.

Firstly, to have a preliminary idea for the kinetics of the hypertonicity-induced response from each group, every trace was aligned at the peak point of the response and averaged to compare their width as described in the *Experimental Procedure* section. As expected, the responses of $Stx1B_{of}$ neurons are narrower than control (Figure 19A). Then, to retrieve the information altered during the trace alignment process, concerning onset of the response, we measured the time point of onset of the responses without alignment from individual cells. Since the onset of the responses varies depending on the geometry of the cell and overgrowth of the astrocyte, responses with longer than 1s of time-to-onset were excluded in this study.

The analysis showed that timing of the onset of hypertonic response was significantly decreased from 0.59 ± 0.02s (n=53) to 0.52 ± 0.02s (n=68) by the open mutation (p=0.0318). Subsequently, knowing the onset time, we adjusted the positioning of the averaged sucrose responses according to measured onset time to directly compare the time course of the sucrose responses. As depicted in figure 19A, our preliminary results suggested possible changes in half-width and rise time. In addition, we noticed that sucrose response of $Stx1B_{of}$ has greater inward steady state component, which is indicative of faster refilling. This will be dealt with in the *priming rate of vesicles* section.

For allowing estimation in terms of pool unit released per given time (rate of release of PU), we integrated transient components of these averaged responses and then normalized by the total charge of the RRP (Figure 19B). As shown in figure 19 B, release by sucrose in $Stx1B_{of}$ appears to have decreased time for complete release.

The maximum slope of the sucrose transient integral, which basically represents the release activity at the peak of the response, directly indicates release rate in pool unit/s caused by a constant degree of osmotic pressure. From this estimation, control neurons had 1.699 pool unit/s, while $Stx1B_{of}$ neurons had 2.275 pool unit/s for $Stx1B_{of}$, implying that there may be approximately a 30% increase in the maximum release rate in response to hypertonic sucrose.

Next, we analyzed hypertonic solution (500 mM sucrose) –evoked responses from individual cells. In order to detect any change in the kinetics of the response, we analyzed four parameters from each sucrose transient: time-to-peak, half width, 10-90% rise time and time to onset of the transient sucrose response. The responses with values lying outside of three times standard deviation in any parameter were not considered in this study. As expected by an average sucrose response curve in figure 19A, sucrose responses of Stx1B$_{of}$ showed narrower transients and required less time to reach the peak of release (figure 19C). Time-to-peak was significantly reduced from 1.01 ± 0.03 sec (n=53) to 0.91 ± 0.02 sec (n=68) by the open-form of Stx1B (p=0.0078). Half width of the response was also notably reduced by the mutation (0.38 ± 0.02 sec (n=53) for control; 0.31 ± 0.01 (n=68) for Stx1B$_{of}$; p=0.0029), while 10-90% rise time was slightly but not significantly reduced (0.219 ± 0.009 sec, n=53 for control and 0.197 ± 0.005, n=68; p=0.1639 for Stx1B$_{of}$).

These data support our hypothesis that the open-form mutation of Stx1B increases the kinetics of hypertonic solution-mediated neurotransmitter release; therefore, it provides direct evidence for a shift in the energetics of Ca^{2+}-independent neurotransmitter release.

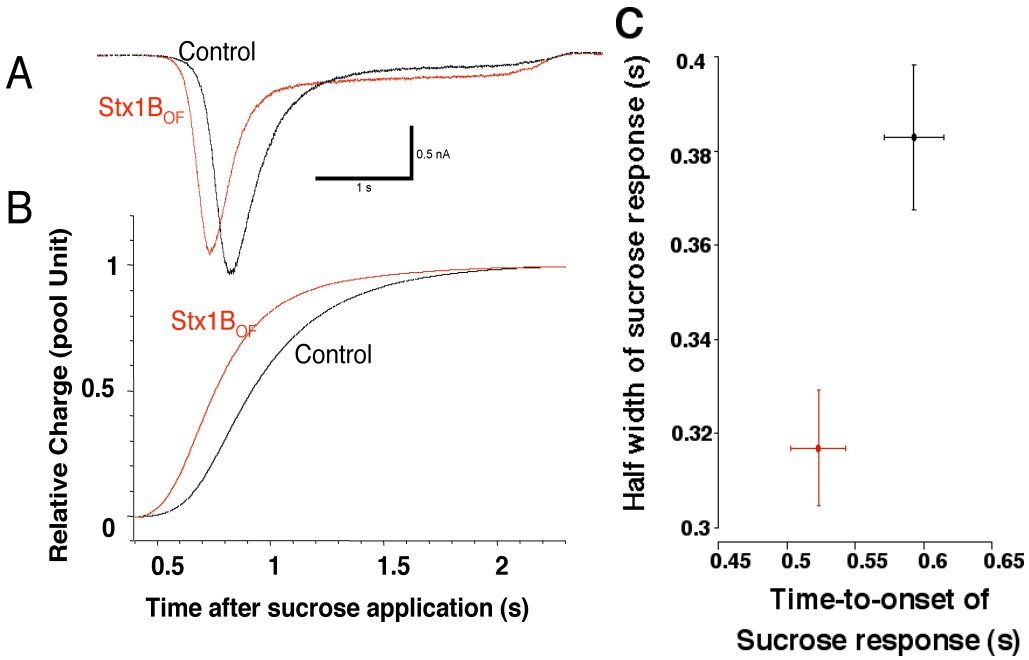

[Figure 19] Time courses of neurotransmitter release by 500 mM sucrose. A, To obtain an average sucrose responses curve in each group. First, the sucrose responses were aligned to time of the peak location to compare average shape, and then shifted according to the average time of onset to elucidate changes in release kinetics. **B,** The averaged sucrose responses were integrated and normalized to total charge to compare cumulative released charge from the pool. By this comparison, a narrower and a leftward shift in average sucrose response was gained in Stx1B$_{of}$ neurons. Cumulative charge vs time curve of Stx1B$_{of}$ shows an earlier onset as well as a faster time course of release in response to the same osmotic pressure compared to control (p<0.005). **C,** Half-width and time-to-onset were measured from individual sucrose responses. Responses that deviated more than three times S.D. from average were ruled out.

4.18 Neurotransmitter release by smaller osmotic pressure

For further confirmation of increased spontaneous efficiency for fusion, we designed a set of follow-up experiments. First, we compared the ratio of transient component charge caused by lower osmotic pressure (250, 350 mM sucrose) to RRP charge for control and $Stx1B_{of}$. Since the transient inward component induced by hypertonic osmotic pressure represents the faster depletion factor than the steady state refilling component, neurons with increased release rate require smaller osmotic pressure for producing the same charge of transient component.

The result depicted in [Figure 20 B] firmly supports the hypothesis that less energy is required in $Stx1B_{of}$ to release fusion-competent vesicles. While 250 mM sucrose hypertonic solution induced release as much as 20 ± 3% of the RRP in control (n=21), up to 54 ± 6% of RRP was released in $Stx1B_{of}$ neurons (n=20; $p<0.0001$). Also, the response evoked by 350 mM sucrose was 52 ± 4% of the RRP in control (n=25), as against 79 ± 6% of response evoked by 500 mM in $Stx1B_{of}$ (n=22; $p=0.0016$). As expected, the same mechanical force applied to $Stx1B_{of}$ containing synapses caused release of a greater fraction of the pool.

However, current transient at particularly lower hypertonicity is hard to detect as the responses reach the steady state without forming a peak. We therefore determined vesicular release rate as a function of hypertonic pressure. Cells were

subjected to different doses of sucrose hypertonic solution (100, 250, 350, and 500 mM) and calculated release rate of responses in each concentration.

For measurement of maximum release rate by 250 mM, 350 mM and 500 mM sucrose, we integrated the transient component of each response and normalized by the charge released by 500 mM sucrose hypertonic solution, which termed as RRP for direct comparison across neurons. From this normalized integral, maximum slope was fitted.

For measurement of release rate at 100 mM sucrose, we used miniature events detection program and the release rates calculated based on the frequency of the events. 100 mM sucrose was applied for 50s and the frequency of minis under this condition was monitored. Release rate by 100 mM sucrose was calculated from the respective mEPSC rates divided by the corresponding number of vesicles in the RRP of each cell. [Figure 20C]. With these methods of analysis in hand, we were able to directly measure the maximum vesicular release rate in pool unit/s.

As expected when $Stx1B_{of}$ neurons have higher efficiency of Ca^{2+} - independent membrane fusion, we observed the $Stx1B_{of}$ group showed faster vesicular release rate in every concentration of sucrose tested [Figure 20C]. Except for the vesicular release rate at 100 mM (0.015 ± 0.002 pool unit/s, n=22 for control and 0.024 ± 0.003 pool unit/s, n=19 for $Stx1B_{of}$, p=0.0515), $Stx1B_{of}$ mutation led to enhanced release rate. The maximum release rate at 250 mM sucrose showed 0.10 ± 0.02 pool unit/s (n=17) for control, 0.37 ± 0.07 for $Stx1B_{of}$ (n=18; p<0.0001). In

response to 350 mM sucrose, 0.40 ± 0.04 pool unit/s (n=17) and 0.90 ± 0.10 pool unit/s (n=18) were released (p=0.0010). For 500 mM sucrose, 1.24 ± 0.04 pool unit/s (n=17) and 1.64 ± 0.10 pool unit/s (n=17; p=0.0109) was observed in control and Stx1B$_{of}$, respectively.

We also added the spontaneous release rate at 0 mM hypertonicity into the plot to show that even without any external force, the release rate is enhanced and therefore the behavior of Stx1B$_{of}$ at rest is consistent with our finding with stimulation of hypertonic solution. As previously described, spontaneous release rates (without hypertonicity) were drastically enhanced by constitutive opening of Stx1B (0.0015 pool unit/s ± 0.0004 (n=62) in control and 0.0033 ± 0.0004 pool unit/s (n=62) in Stx1B$_{of}$; p<0.0001). Therefore, we can conclude that open-mutation of Stx1B enhanced Ca^{2+} independent release rate both in spontaneous release activity as well as in the accelerated kinetics by hypertonic pressure.

In summary, it is likely that, at least in larger part, the observed increase in vesicular release rate during evoked responses in Stx1B$_{of}$ is caused by a reduced energy barrier for Ca^{2+}-independent fusion of the vesicles.

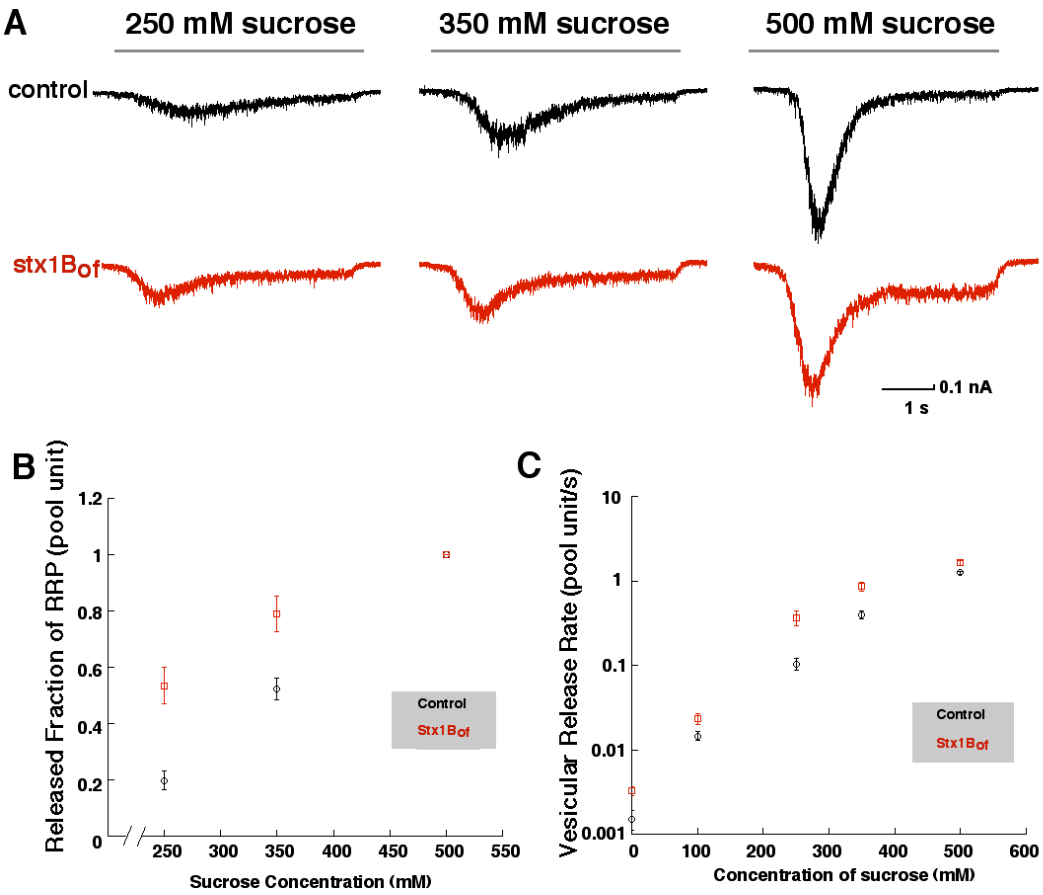

[Figure 20] Determination of an energy barrier for fusion by released fraction of RRP and maximum released pool unit/s. To test the possibility that the open-form mutation leads to a lower energy barrier for fusion osmotic pressure lower than 500 mM sucrose was applied. The relative pool units released and release rate at various concentration of hypertonic solution (0-500 mM) were compared. **A,** Representative sample traces of responses evoked by 250, 350 and 500 mM hypertonic sucrose solution. Gray bars above traces show time hypertonic solution was applied. **B,** Relative charge released in response to 250 and 350 mM sucrose to charge of RRP **C,** Calculated pool unit per second in various concentrations of sucrose. Released pool unit/s at 250, 350 and 500 mM was determined as maximum slope of normalized, integrated transient component. Release rate at 0 and 100 mM were gained by the mini frequencies over total number of vesicles in RRP.

4.19 Priming rate of vesicles

So far, we have analyzed the effect of open-form mutation on the efficiency of neurotransmitter release. Since switching conformation of Stx1 is one of the major events during the priming reaction, one of the initial questions was whether switching conformation of Stx1 indeed improves efficiency of priming rate.

As mentioned previously, mean amplitude of the steady state component of the sucrose response conveys information about the refilling rate, thus, priming efficiency of RRP. We have already pointed out that $Stx1B_{of}$ neurons show larger steady state inward current from the averaged shape of sucrose response (figure 19) compared to Stx1AKO control, which behaves like wild-type (figure 12).

Assuming that refilling is a linear process, the mean amplitude divided by the charge of RRP depicts estimated refilling pool unit per second. Absolute current-induced steady state inward activity was slightly but not significantly larger in $Stx1B_{of}$ cells (Figure 21B; 120 ± 10 pA, n=66 for control; 180 ± 20 pA, n=96, p=0.0933). Taking the overall smaller pool size in $Stx1B_{of}$ into consideration, the difference was strongly significant. (Figure 21C; 0.116 pool unit/s ± 0.008 n= 66 for control and 0.370 pool unit/s ± 0.030, n=96 for $Stx1B_{of}$; p<0.0001).

A more reliable evaluation for rate of pool refilling is to apply pairs of 500 mM sucrose at varying inter-pulse intervals (1, 4, 7 and 10 sec). The first application of sucrose depletes the RRP, while the second sucrose response shows refilled fraction of the RRP during the inter-pulse interval. As can be correlated with the previous result from the measurement of steady state inward current of the sucrose response (figure 19 and figure 21), refilling kinetics of the pool is notably faster in $Stx1B_{of}$ group (τ=2.3255s in control: τ= 1.082s in $Stx1B_{of}$; figure 22). For example, one second after pool depletion, RRP of $Stx1B_{of}$ was refilled as much as 0.50 ± 0.04 of the total pool (n=18), while 0.30 ± 0.02 pool unit (n=18) was replenished in the control state (p=0.0003).

These results concerning the rate of RRP refilling imply that the opening of Stx1 may be one of time limiting steps in the priming reaction.

4.20 Diacylglycerol/β-phorbol ester induced augmentation

According to current hypotheses, opening of Stx1 is mediated by essential priming factor, Munc13 (Augustin et al., 1999; Richmond et al., 2001). If the only role of Munc13 in exocytosis is to open Stx1, its role of Munc13 in the $Stx1B_{of}$ neuron, should have become concealed. Besides being an essential priming factor, Munc13s are also the sole target of diacylglycerol (DAG)/β-phorbol ester (β-PE) mediating augmentation of neurotransmitter release (Rhee et al., 2002). We used this property

to test whether Munc13 is still acting on the priming/release process. If β-PE still causes potentiation of the synaptic response in $Stx1B_{of}$ neurons, this would indicate that Munc13 does more than opening Stx1. In contrast, if Munc13 only opens Stx1 as its sole role in regulation of exocytosis, β-PE should not induce any change in synaptic responsiveness in $Stx1B_{of}$ neurons.

We, therefore, measured potentiation of synaptic responses upon application of 1 μM β–phorbolester dibutyrate (PDBU). After obtaining base line responses 1 μM PDBU was applied for 1 min and was subsequently washed out for 5 min. Amplitudes of EPSCs in PDBU were normalized to the initial base line, and the degree of potentiation was measured by EPSCs after augmented responses reach steady state. While control cells show 2.44 ± 0.13 fold enhanced neurotransmitter release (n=45), $Stx1B_{of}$ cells show much reduced enhancement of 1.45 ± 0.05 fold by PDBU (n=43, $p<0.0001$; figure 23A). This data, depicting that $Stx1B_{of}$ still shows sensitivity in response to PDBU, leads to the conclusion that apart from opening Stx1, Munc13 indeed plays additional roles in the synaptic release process.

Furthermore, the reduced PDBU response could be the consequence of the intrinsic high release probability of $Stx1B_{of}$, while the EPSC of $Stx1B_{of}$ is as sensitive as control to PDBU, implying that although Munc13 may exercise part of its function by switching the conformation of Stx1, PDBU-stimulated Munc 13 could employ a different mechanism to enhance neurotransmitter release.

To evaluate this possibility we correlated the degree of augmentation of EPSC as a function of vesicular release probability. If high vesicular release

probability was the cause of the reduction in PDBU augmentation, we would see inverse correlation between the two parameters.

Figure 23B shows the combination of vesicular release probability and PDBU augmentation measured from both control and Stx1B$_{of}$ neurons. Stx1B$_{of}$ (red dots) have intrinsically higher vesicular release probability and smaller degree of potentiation in comparison to control (black dots; figure 23C). However, a continuously distributed inverse correlation appears to form between these two parameters. Based on this finding, we would propose that the reduction in degree of potentiation by PDBU in Stx1B$_{of}$ is due to intrinsically high vesicular release probability rather than impaired interaction of Munc13 with its target in changing neurotransmitter release probability.

However, in all cases, the augmentation of neurotransmitter release in Stx1B$_{of}$ neurons suggest that Munc 13-1 has a role alternative to that of switching the conformation of Stx1 in response to PDBU and thus to DAG.

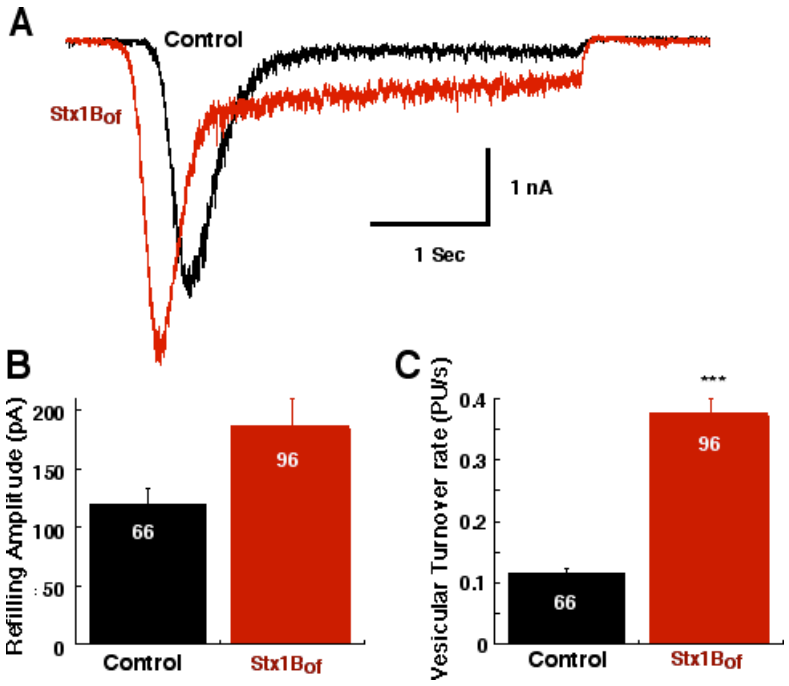

[Figure 21] Steady state amplitude of sucrose response. Sustained component of sucrose response was termed refilling amplitude. **A,** Representative traces (Black-control; red-Stx1B$_{of}$) **B,** Average of mean amplitude in sustained component **C,** Mean amplitude of steady state component was divided by the charge of RRP to standardize various pool size (refilling pool unit/s). Refilling of RRP in Stx1B$_{of}$ cells were significantly faster than control. ***p<0.0001

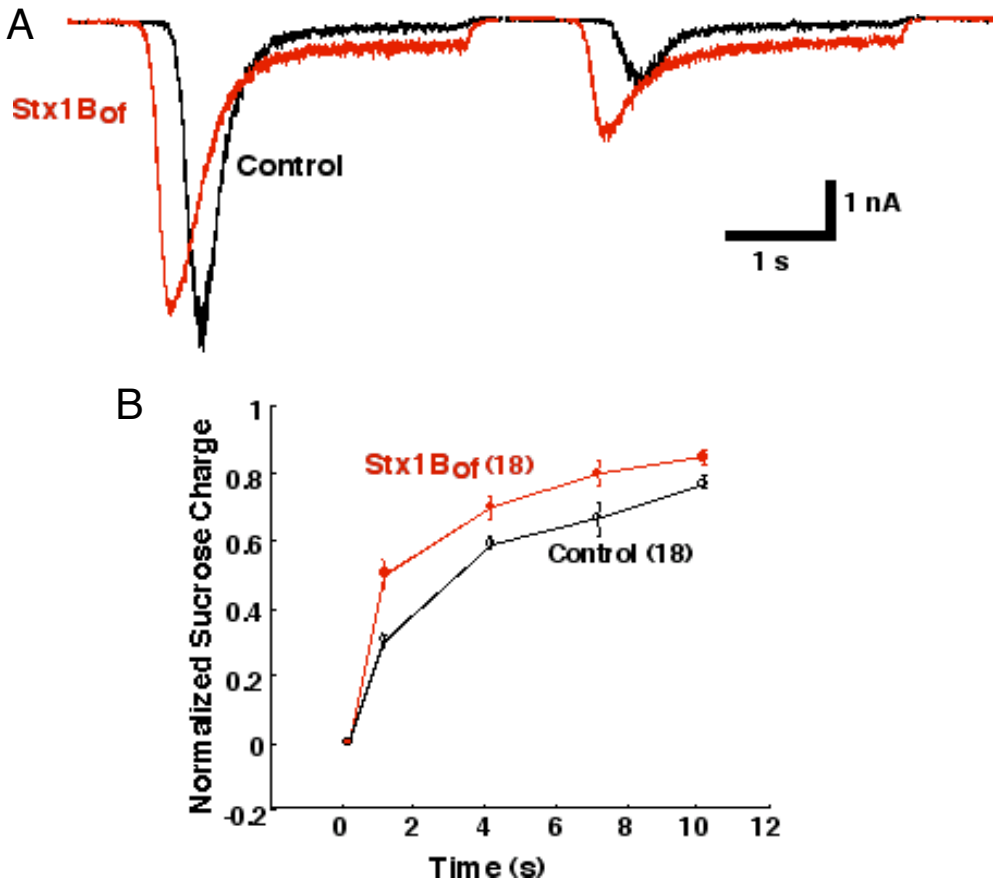

[Figure 22] Comparison of priming rate between control and Stx1B$_{of}$ neurons. To compare priming rate of vesicles into the RRP, paired sucrose responses were compared. After a certain time from depletion of the pool by first sucrose application, sucrose was re-applied and the ratio for refilled charge compared to the first is determined as refilling of the time internal. **A,** Sample traces for each group (Black-control; Red-Stx1B$_{of}$). **B,** After 1s of depletion around half of RRP was refilled in Stx1B$_{of}$ cell, while only 30% of the pool is refilled in control. This difference correlates well with the finding from the sustained component of sucrose response. It should be noted from the identical offset points of the sucrose responses in the control and Stx1B$_{of}$ raw traces that the faster onset is due to inherent release properties of Stx1B$_{of}$ and not the fast flow application system.

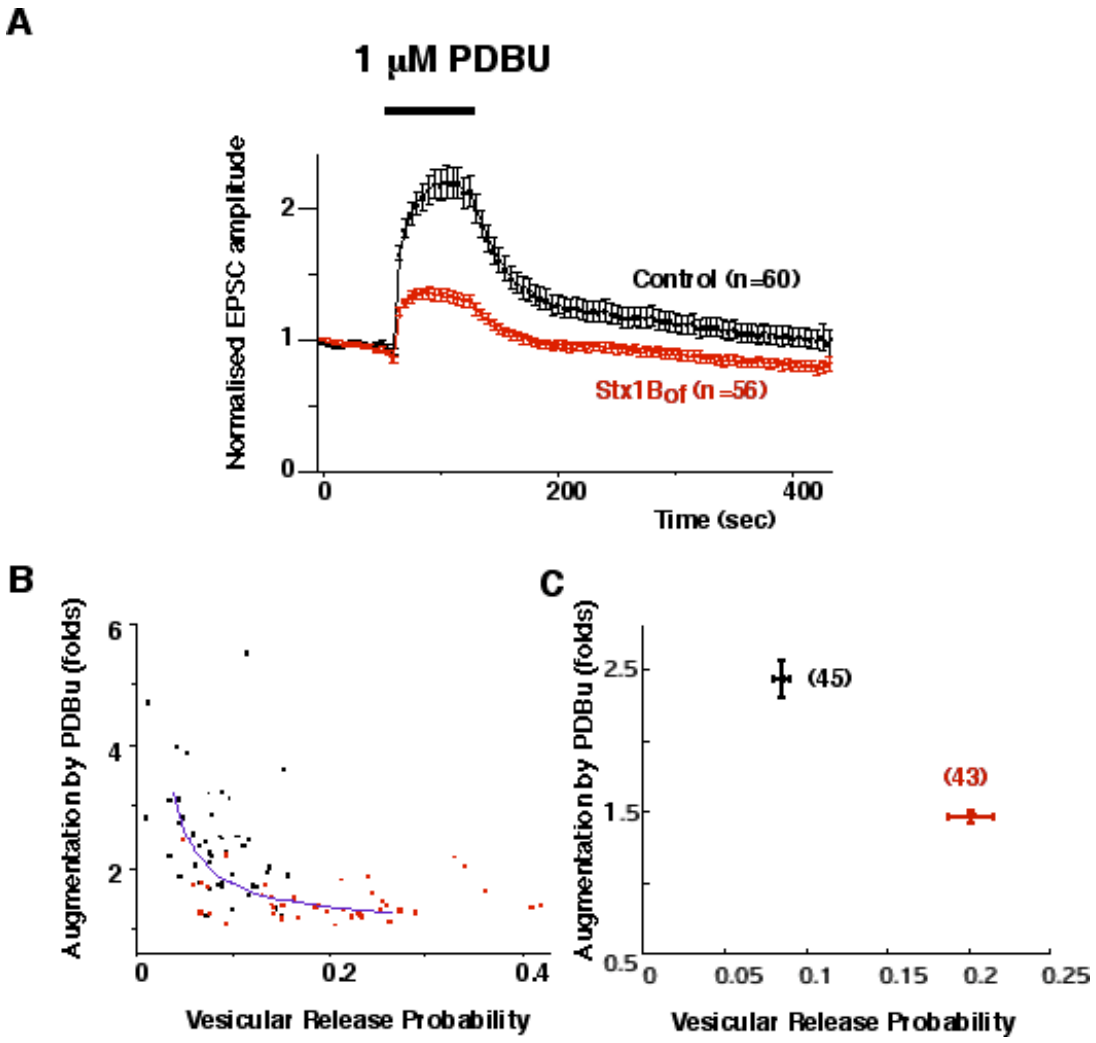

[Figure 23] Alternative role of Munc13 in vesicle priming/fusion. A, To examine whether Munc13-1 has different role than switching conformation of Stx1, the level of augmentation by PDBU was measured. While control neurons show 2.44 ± 0.13 fold enhanced EPSCs, $Stx1B_{of}$ neurons have 1.45 ± 0.08 fold augmentation in response to PDBU. **B.** To resolve whether reduced degree of potentiation in $Stx1B_{of}$ is due to intrinsically high release probability, the degree of augmentation was plotted as a function of release probability (Black-control; Red-$Stx1B_{of}$). Note that two groups fall in a continuous distribution forming inverse correlation between these two parameters. **C.** Mean release probability and potentiation are plotted. Error bar shows S.E.M. Numbers in blanket shows number of cells tested.

5. Discussion

DISCUSSION

The purpose of this study was, first, to identify functional differences between Stx1A and Stx1B and secondly, to study the physiological impact of mutation of SNARE molecule, Stx1 that has been found in biochemical experiment to lock the conformation of Stx1 in open form and prevent the formation of closed conformation.

We initially characterized synaptic properties of mice lacking Stx1A and found that synapses lacking Stx1A do not lead to any obvious defects in neurotransmission in comparison to wild-type synapses. Subsequently, Stx1AKO mice were crossed with $Stx1B_{of}$ mutant mice to obtain homogeneous conformation of Stx1 to direct compare between Stx1B wild-type and $Stx1B_{of}$. Mice expressing an open mutation of Stx1B on a Stx1A knock out background exhibited a 2.2 fold increase in release efficacy most likely caused by a reduction in the energy barrier for membrane fusion. In addition, synapses containing the constitutively open conformation of Stx1B led to significantly faster vesicle priming.

Despite lines of evidence predicting functional differences between the two major secretory cell-specific isoforms of syntaxin, namely, Stx1A and Stx1B, including differential distribution, binding affinity to Munc18 and inhibitory roles on

voltage-gated Ca^{2+} channel (see *introduction part 2.9*), StxIA null mice showed typical hippocampal synaptic release properties of wild-type mice.

A possible explanation for this finding might be the presence of StxIB as the dominant endogenously expressed isoform in the hippocampal neurons was considered. However, in keeping with previous studies, our immunohistochemistry result shown in the present study indicates that these two isoforms are natively expressed throughout the hippocampal area (see figure 8 and (Ruiz-Montasell et al., 1996)). Therefore StxIB cannot be the predominant isoform in hippocampus.

In general, deletion of one isoform may lead to an enhanced expression of the other. However, the lack of StxIA does not detectably affect the expression of StxIB. This can be explained by the presence of alternative isoforms of syntaxin other than StxIB, as a compensatory measure for the absence of StxIA. Alternatively and more likely, StxIA may not functionally differ from StxIB and there can be substantially great amounts of total Stx1 present in hippocampal neurons as has been shown previously by Hu et al. (Hu et al., 2002).

To provide a clearer answer for the functional differences between the two isoforms, we would need to compare the synapses using only StxIA and StxIB, respectively. The comparison between neurons from anterior lobes of pituitary gland where no StxIB was found (Ruiz-Montasell et al., 1996) and that of StxIAKO

mice may provide a better resolution. Furthermore, the parallel analysis of Stx1B null mice, or characterization of the double knock out synapses rescued by either of those isoforms will be needed.

As previously described in the *introduction (part 2.9)*, Stx1 has at least two conformations: a closed conformation in which core complex domain is masked by the N-terminal Habc domain, so that it is unable to form SNARE complexes, and an open conformation, where the SNARE motif of Stx1 is exposed and ready to form SNARE complexes, possibly through an intermediate conformation. However, it has not yet been verified what can be caused from the open conformation of Stx1.

Since a conformational switch to the open state is believed to be a key step in the priming reaction, an enhanced priming rate in $Stx1B_{of}$ (Figure 21, 22) is not too surprising. Vesicles docked at active zones in $Stx1B_{of}$ most likely have a higher probability to face an active Stx1 (open-conformation of Stx1), without having to wait for being acted upon by the priming proteins. We also discovered that the vesicles primed with Stx1B that are constitutively open have higher fusion efficiency than the vesicles with wild-type Stx1B. Since even in the wild-type context, all the primed vesicles are, in any case, supposed to have open Stx1, this observation was rather unforeseen.

The increased vesicular release probability was determined by two independent measurements. The bigger population of vesicles was released by an action potential and secondly the short-term plasticity experiment revealed much stronger depression, which is an indicative of higher release probability.

Nevertheless, we observed that the total synaptic output per action potential per synapse was identical between the Stx1AKO control and the open-form mutant. This was demonstrated by similar amplitudes of EPSC (Figure 13) as well as by unchanged synaptic release probability, measured using the MK-801 method (Figure 15). Based on these findings, together with the same size of EPSC, we could conclude that the increased vesicular release probability and decreased size of RRP compensates each other to hold the same synaptic strength as in wild-type neurons.

These two findings correlate well with decreased RRP size in $Stx1B_{of}$ neurons (Figure 13). Reduced RRP size was also rather surprising because we noticed that the vesicle priming rate is actually enhanced. If the equilibrium between the priming and umpriming is relevant for size of the RRP, we would expect the opposite, an increase in pool size. Thus, we suggest that the reduced RRP size is a compensatory mechanism to preserve the size of EPSC in the effective range so as to maintain consistency of synaptic transmission.

The cause of increased release efficacy can be explained by reduced activation energy of the fusion reaction, based on the following findings: (1) increased level of vesicular release probability coincides with that of spontaneous release probability [figure 13 and 18]. (2) early onset, and narrower half width of the sucrose responses indicating faster kinetics and increased efficiency of vesicular fusion by given constant osmotic pressure [figure 19]. (3) a larger fraction of the pool was released at lower concentration of sucrose, implying ease of fusion [figure 20 B] (4) increased release rate (higher pool unit/s) by every given concentration of sucrose [figure 20C]. Similar phenomena were observed in the previous studies by β-PE stimulation (Stevens and Sullivan, 1998) and by high frequency stimulation (Stevens and Wesseling, 1999)

One of the possible explanations would be following. Stx1 continuously switches its conformation with binding to either Munc13 or Munc 18-1, reaching equilibrium between the open and closed state. The greater the portion of the core complex region exposed, the more completely the SNARE complex forms. Hence, a greater part of the unstable hemifusion intermediate is stabilized energetically. In the open form mutant, because the equilibrium is set to the fully open state, every SNARE formed is a complete one. Thus, intermediate states are stabilized to a greater extent, which drives the fusion process more easily. However, a half-formed SNARE has not been reported so far in the literature and it is not known whether Munc13 binding is reversible, hence, this idea cannot be evidently theorized.

Another possible explanation for the increased release can be suggested based on an observed obvious left shift in sensitivity of release machinery to external Ca^{2+} concentration as a cause of phenotype. Elevation of external Ca^{2+} in $Stx1B_{of}$ caused reduced potentiation and the synapses using $Stx1B_{of}$ have less sensitivity to reduction of external Ca^{2+}, which is consistent with higher sensitivity to Ca^{2+}.

As explained above, Stx1 has a negative regulatory effect on Ca^{2+} channels. If introduction of the mutation in Stx1 molecule causes des-inhibition of Ca^{2+} channel function, then it will subsequently lead to a greater Ca^{2+} influx and enhanced sensitivity to external Ca^{2+}. The possibility of altered regulation of Ca^{2+} channels is supported by the evidence that transiently transfected tsA-201 cells with an open conformation of Stx1 did not show a hyperpolarizing shift in the half-inactivation potential of N-type Ca^{2+} channel (Jarvis et al., 2002).

Since the preparation we used in this study does not allow direct measurement of Ca^{2+} current at the presynaptic terminal, we measured somatic Ca^{2+} current to verify this possibility. Furthermore, for providing a better resolution, the L-type-dependent Ca^{2+} current, which normally contributes little in neurotransmission, was blocked using nifedipine and the amplitude of the P/Q- and N- type channel-dependent current was compared. We found that both in the presence and absence of the L-type Ca^{2+} channel contribution, the somatic current remained unchanged (Figure 17). In spite of this finding, the possible influence of

Stx1 open mutation on Ca^{2+} channel inhibition cannot be completely ruled out, since one has to consider the fact that reliable electrical control of the presynaptic Ca^{2+} current is hard to achieve. The membrane of neuronal processes is normally to some extent isolated from the electrode leading to separation by an axial access resistance-depending on the distance between the membrane and the electrode. This introduces significant voltage-drop or space clamp error, leading to inaccuracy in estimation of actual presynaptic Ca^{2+} current. Therefore, further studies involving direct measurement of the presynaptic Ca^{2+}current, such as Calyx of Held (Felmy et al., 2003), will be needed to overcome this problem.

In the light of these ideas, undetected difference in Ca^{2+} influx at the presynaptic terminal could indeed explain the increased release probability, and enhanced priming rate, but not the parallel observations of increased rate of spontaneous release or the kinetic change of sucrose response. In addition, based on the finding that the level of increased spontaneous release probability correlates with increased vesicular release probability, differential regulation of Ca^{2+} channels cannot be the major cause.

The most reasonable explanation would be that in $Stx1B_{of}$, there are increased numbers of SNARE complexes per vesicle and this causes the observed phenotype. Under physiological conditions, free Stx1 switches its conformation to establish equilibrium between the open and closed conformations in a short time

(Margittai et al., 2003b) and the open-form mutation shifts the equilibrium towards the open state.

In order to sustain the open, active conformation, Stx1 needs extra interaction with regulatory proteins such as Munc 13 and RIM (Koushika et al., 2001b; Richmond et al., 2001). This requirement for interactions decrease the chances of having open-form Stx1 in comparison to the $Stx1B_{of}$ situation, where all of the Stx1 molecules are already in their open and active state. The number of SNARE complexes critically depends on the proportion of open-form Stx1. The more open-form of Stx1, the larger number of assembled SNARE complexes are formed between the plasma and vesicle membrane. Accordingly, more SNARE complexes could be formed per vesicle, and each of the complexes may provide the energy needed to drive fusion (Lin and Scheller, 1997). Such vesicles with inherently open form of Stx1 need to overcome lower threshold energy for fusion and therefore they fuse with noticeably higher release probability and accelerated fusion kinetics.

The results presented so far have shown that opening of Stx1, known to be a functional consequence of interaction with Munc13-1, makes vesicles more ready for priming, as well as for fusion. This raises the question whether enhancing the function of Munc13-1 in wild-type neurons can lead to similar phenomena i.e. enhanced release probability. Recent unpublished data from our laboratory, as well as a previous report show that PDBU application causes similar phenomena with open mutation of Stx1, in terms of earlier onset of sucrose response, and faster pool

unit depletion by sucrose (J.Basu and C. Rosenmund, personal communication (Stevens and Sullivan, 1998)). Based on the finding that Munc13 is the sole molecular target for β-PE mediated augmentation of neurotransmitter release (Rhee et al., 2002), we can conclude that such a functional enhancement of Munc13 indeed showed similar release properties to those of Stx1B$_{of}$, which, in turn, support the hypothesis that Munc13-1 is the molecule switching the conformation of Stx1.

Now, focus can be directed to answer the question whether conformational switching Stx1 is the only role of Munc13. This issue can be addressed by exploring whether Munc13 can still exert its function for neurotransmitter release in the neuron expressing open-form of Stx1. If the role of Munc13 in neurotransmitter release was nothing more than that of opening up Stx1, then the effect of PDBU upon Munc13 would not persist in this mutation, and subsequently, augmentation of neurotransmitter release would not be expected. By applying PDBU onto Stx1B$_{of}$ cells, Munc13 was stimulated and potentiation of EPSC was observed. Although the level of PDBU-mediated augmentation was significantly reduced in Stx1B$_{of}$ as compared to its control counterpart, enhanced neurotransmitter release was observed (Figure23).

One possible interpretation of this result is that there is another molecule (or other molecules) that can mediate PDBU-induced augmentation, recruiting a mechanism(s) alternative to that of Munc13. However, this is very unlikely because

mutation of Munc 13 for lacking phorbol ester interaction (H567K mutation) led to completely abolished augmentation under the same experimental condition (Rhee et al., 2002).

Alternatively, considering that PDBU is indeed acting upon Munc13 only, and that level of augmentation in the $Stx1B_{of}$ is reduced, PDBU mediated Munc13 stimulation exerts its effect on neurotransmitter release via a different mechanism, independent of Stx1 opening. In this case, Munc13 does not open Stx1 to potentiate the release but acts upon a different target in the fusion process for facilitating the release at least in response to PDBU. Therefore, $Stx1B_{of}$ cells would show the same level of augmentation with that of wild-type. However, as emphasized by our results, PDBU-mediated augmentation is significantly reduced. This may be because the intrinsically higher, and more saturated vesicular release probability, as seen in the $Stx1B_{of}$ neurons, may not allow the same degree of PDBU augmentation. Alternatively, it can be also explained if Munc13 exerts its role in potentiate EPSC, partially by opening Stx1, in addition to alternative pathway.

To check this possibility, the augmentation level was plotted against vesicular release probability of the cell (figure 23 B, C). If the assumption is correct, overlapped negative correlation between the two factors is expected. In this study, as plotted in figure 23 B, these two parameters showed relatively weak but overlaid negative correlation between each other. Therefore, we would suggest that the

reduced augmentation by PDBU is rather the consequence of intrinsically higher release probability.

However, our results so far do not clearly resolve whether the role of Munc13 in response to β-PE is to mediate, solely a mechanism that is alternative to opening of Stx1 or both the opening of Stx1 in addition to the other mechanism. To provide an answer of this question, further study addressing β-PE response in $Stx1B_{of}$ neurons, with artificially lowered release probability equivalent to that of control e.g. by modifying external Ca^{2+} concentration, is required.

The hypothesis that Munc13 has a different way of enhancing neurotransmitter release, other than opening Stx1 conflicts with the finding in *C. elegans*, demonstrating that overexpression of constitutively open form of Stx1 bypasses the need of unc13 (Richmond et al., 2001). Recently, the same overexpression experiment has been performed in a mouse system. An open mutation of Stx1 overexpressed in Munc13 double knockout mouse hippocampal neuron culture showed partial rescue of neurotransmitter release. Although EPSCs were found in this system, these releases showed very rapid run-down, suggesting that the rescue is far from being complete (Rhee and Rosenmund, unpublished data). This finding provides another line of evidence suggesting additional role of Munc13 besides opening of Stx1. This difference between nematode and mammalian data can be explained by the redundancy and complexity of Munc13 function in the mammalian system. However, this preliminary data requires very careful

interpretation, since overexpression of wild-type Stx1 can cause Ca^{2+} channel inhibition and defects in transmission (Bezprozvanny et al., 2000; Stanley, 2003; Zamponi, 2003). Therefore, tightly controlled expression of $Stx1B_{of}$, ideally under endogenous gene expression, is required to test this hypothesis.

When taken together, our present study suggests that, the individual conformations of Stx1 control the probability of formation of the SNARE complex, and thereby act as crucial regulators of Ca^{2+}-independent membrane fusion efficacy and important determinants of short-term plasticity of synaptic transmission.

6. References

REFERENCES

Aguado, F., Majo, G., Ruiz-Montasell, B., Llorens, J., Marsal, J., and Blasi, J. (1999). Syntaxin 1A and 1B display distinct distribution patterns in the rat peripheral nervous system. Neuroscience *88*, 437-446.

Aravamudan, B., Fergestad, T., Davis, W. S., Rodesch, C. K., and Broadie, K. (1999). Drosophila UNC-13 is essential for synaptic transmission. Nature Neuroscience *2*, 965-971.

Augustin, I., Rosenmund, C., Südhof, T. C., and Brose, N. (1999). Munc13-1 is essential for fusion competence of glutamatergic synaptic vesicles. Nature *400*, 457-461.

Bekkers, J. M., and Stevens, C. F. (1991). Excitatory and inhibitory autaptic currents in isolated hippocampal neurons maintained in cell culture. Proc Natl Acad Sci U S A *88*, 7834-7838.

Bennett, M. K., Calakos, N., and Scheller, R. H. (1992). Syntaxin: a synaptic protein implicated in docking of synaptic vesicles at presynaptic active zones. Science *257*, 255-259.

Bennett, M. K., Garcia-Arraras, J. E., Elferink, L. A., Peterson, K., Fleming, A. M., Hazuka, C. D., and Scheller, R. H. (1993). The syntaxin family of vesicular transport receptors. Cell *74*, 863-873.

Betz, A., Okamoto, M., Benseler, F., and Brose, N. (1997). Direct interaction of the rat unc-13 homologue Munc13-1 with the N terminus of syntaxin. Journal of Biological Chemistry *272*, 2520-2526.

Betz, A., Thakur, P., Junge, H. J., Ashery, U., Rhee, J. S., Scheuss, V., Rosenmund, C., Rettig, J., and Brose, N. (2001). Functional interaction of the active zone proteins Munc13-1 and RIM1 in synaptic vesicle priming. Neuron *30*, 183-196.

Bezprozvanny, I., Scheller, R. H., and Tsien, R. W. (1995). Functional impact of syntaxin on gating of N-type and Q-type calcium channels. Nature *378*, 623-626.

Bezprozvanny, I., Zhong, P., Scheller, R. H., and Tsien, R. W. (2000). Molecular determinants of the functional interaction between syntaxin and N-type Ca2+ channel gating. Proceedings of the National Academy of Sciences of the United States of America *97*, 13943-13948.

Binz, T., Blasi, J., Yamasaki, S., Baumeister, A., Link, E., Südhof, T. C., Jahn, R., and Niemann, H. (1994). Proteolysis of SNAP-25 by types E and A botulinal neurotoxins. Journal of Biological Chemistry *269*, 1617-1620.

Blasi, J., Chapman, E. R., Yamasaki, S., Binz, T., Niemann, H., and Jahn, R. (1993). Botulinum neurotoxin C1 blocks neurotransmitter release by means of cleaving HPC-1/syntaxin. EMBO Journal *12*, 4821-4828.

Brenner, S. (1974). The genetics of Caenorhabditis elegans. Genetics *77*, 71-94.

Broadie, K., Prokop, A., Bellen, H. J., O'Kane, C. J., Schulze, K. L., and Sweeney, S. T. (1995). Syntaxin and synaptobrevin function downstream of vesicle docking in Drosophila. Neuron *15*, 663-673.

Brose, N., Hofmann, K., Hata, Y., and Südhof, T. C. (1995). Mammalian homologues of Caenorhabditis elegans unc-13 gene define novel family of C2-domain proteins. J Biol Chem *270*, 25273-25280.

Brose, N., Petrenko, A. G., Südhof, T. C., and Jahn, R. (1992). Synaptotagmin: a calcium sensor on the synaptic vesicle surface. Science *256*, 1021-1025.

Catterall, W. A. (1999). Interactions of presynaptic Ca2+ channels and snare proteins in neurotransmitter release. Ann N Y Acad Sci *868*, 144-159.

Clements, J. D., Lester, R. A., Tong, G., Jahr, C. E., and Westbrook, G. L. (1992). The time course of glutamate in the synaptic cleft. Science *258*, 1498-1501.

Deitcher, D. L., Ueda, A., Stewart, B. A., Burgess, R. W., Kidokoro, Y., and Schwarz, T. L. (1998). Distinct requirements for evoked and spontaneous release of neurotransmitter are revealed by mutations in the Drosophila gene neuronal-synaptobrevin. J Neurosci *18*, 2028-2039.

Dick, O., tom Dieck, S., Altrock, W. D., Ammermuller, J., Weiler, R., Garner, C. C., Gundelfinger, E. D., and Brandstatter, J. H. (2003). The presynaptic active zone protein bassoon is essential for photoreceptor ribbon synapse formation in the retina. Neuron *37*, 775-786.

Dobrunz, L. E., and Stevens, C. F. (1997). Heterogeneity of release probability, facilitation, and depletion at central synapses. Neuron *18*, 995-1008.

Dulubova, I., Sugita, S., Hill, S., Hosaka, M., Fernandez, I., Südhof, T., and Rizo, J. (1999). A conformational switch in syntaxin during exocytosis: role of Munc18. The EMBO Journal *18*, 4372-4382.

Fasshauer, D. (2003). Structural insights into the SNARE mechanism. Biochim Biophys Acta *1641*, 87-97.

Felmy, F., Neher, E., and Schneggenburger, R. (2003). The timing of phasic transmitter release is Ca2+-dependent and lacks a direct influence of presynaptic membrane potential. Proc Natl Acad Sci U S A *100*, 15200-15205.

Fernandez, I., Ubach, J., Dulubova, I., Zhang, X., Südhof, T. C., and Rizo, J. (1998). Three-dimensional structure of an evolutionarily conserved N-terminal domain of syntaxin 1A. Cell *94*, 841-849.

Fernandez-Chacon, R., Konigstorfer, A., Gerber, S. H., Garcia, J., Matos, M. F., Stevens, C. F., Brose, N., Rizo, J., Rosenmund, C., and Südhof, T. C. (2001). Synaptotagmin I functions as a calcium regulator of release probability. Nature *410*, 41-49.

Geppert, M., Goda, Y., Hammer, R. E., Li, C., Rosahl, T. W., Stevens, C. F., and Südhof, T. C. (1994). Synaptotagmin I: a major Ca2+ sensor for transmitter release at a central synapse. Cell *79*, 717-727.

Harlow, M. L., Ress, D., Stoschek, A., Marshall, R. M., and McMahan, U. J. (2001). The architecture of active zone material at the frog's neuromuscular junction. Nature *409*, 479-484.

Hata, Y., Slaughter, C. A., and Südhof, T. C. (1993). Synaptic vesicle fusion complex contains unc-18 homologue bound to syntaxin. Nature *366*, 347-351.

Helme-Guizon, A., Davis, S., Israel, M., Lesbats, B., Mallet, J., Laroche, S., and Hicks, A. (1998). Increase in syntaxin 1B and glutamate release in mossy fibre terminals following induction of LTP in the dentate gyrus: a candidate molecular mechanism underlying transsynaptic plasticity. European Journal of Neuroscience *10*, 2231-2237.

Hu, K., Carroll, J., Fedorovich, S., Rickman, C., Sukhodub, A., and Davletov, B. (2002). Vesicular restriction of synaptobrevin suggests a role for calcium in membrane fusion. Nature *415*, 646-650.

Jagadish, M. N., Tellam, J. T., Macaulay, S. L., Gough, K. H., James, D. E., and Ward, C. W. (1997). Novel isoform of syntaxin 1 is expressed in mammalian cells. Biochemical Journal *321*, 151-156.

Jahn, R., Lang, T., and Südhof, T. C. (2003). Membrane fusion. Cell *112*, 519-533.

Jarvis, S. E., Barr, W., Feng, Z. P., Hamid, J., and Zamponi, G. W. (2002). Molecular determinants of syntaxin 1 modulation of N-type calcium channels. Journal of Biological Chemistry *277*, 44399-44407.

Jarvis, S. E., Magga, J. M., Beedle, A. M., Braun, J. E., and Zamponi, G. W. (2000). G protein modulation of N-type calcium channels is facilitated by physical interactions between syntaxin 1A and Gbetagamma. Journal of Biological Chemistry *275*, 6388-6394.

Jarvis, S. E., and Zamponi, G. W. (2001). Distinct molecular determinants govern syntaxin 1A-mediated inactivation and G-protein inhibition of N-type calcium channels. Journal of Neuroscience *21*, 2939-2948.

Kandel, E. R., Schwartz, J. H., and Jessell, T. M. (2000). Principles of Neural Science, 4th EDITIOIN edn (New York, McGraW-Hill).

Koushika, S. P., Richmond, J. E., Hadwiger, G., Weimer, R. M., Jorgensen, E. M., and Nonet, M. L. (2001). A post-docking role for active zone protein Rim.[see comment]. Nature Neuroscience *4*, 997-1005.

Lin, R. C., and Scheller, R. H. (1997). Structural organization of the synaptic exocytosis core complex. Neuron *19*, 1087-1094.

Lu, Q., AtKisson, M. S., Jarvis, S. E., Feng, Z. P., Zamponi, G. W., and Dunlap, K. (2001). Syntaxin 1A supports voltage-dependent inhibition of alpha1B Ca2+ channels by Gbetagamma in chick sensory neurons. Journal of Neuroscience *21*, 2949-2957.

Margittai, M., Fasshauer, D., Jahn, R., and Langen, R. (2003a). The Habc domain and the SNARE core complex are connected by a highly flexible linker. Biochemistry *42*, 4009-4014.

Margittai, M., Widengren, J., Schweinberger, E., Schroder, G. F., Felekyan, S., Haustein, E., Konig, M., Fasshauer, D., Grubmuller, H., Jahn, R., and Seidel, C. A. (2003b). Single-molecule fluorescence resonance energy

transfer reveals a dynamic equilibrium between closed and open conformations of syntaxin 1. Proc Natl Acad Sci U S A *100*, 15516-15521.

Maruyama, I. N., and Brenner, S. (1991). A phorbol ester/diacylglycerol-binding protein encoded by the unc-13 gene of Caenorhabditis elegans. Proc Natl Acad Sci U S A *88*, 5729-5733.

Misura, K. M., Scheller, R. H., and Weis, W. I. (2000). Three-dimensional structure of the neuronal-Sec1-syntaxin 1a complex.[see comment]. Nature *404*, 355-362.

Morihara, T., Mizoguchi, A., Takahashi, M., Kozaki, S., Tsujihara, T., Kawano, S., Shirasu, M., Ohmukai, T., Kitada, M., Kimura, K., *et al.* (1999). Distribution of synaptosomal-associated protein 25 in nerve growth cones and reduction of neurite outgrowth by botulinum neurotoxin A without altering growth cone morphology in dorsal root ganglion neurons and PC-12 cells. Neuroscience *91*, 695-706.

Munson, M., and Hughson, F. M. (2002). Conformational regulation of SNARE assembly and disassembly in vivo. J Biol Chem *277*, 9375-9381.

Murthy, V. N., and Stevens, C. F. (1999). Reversal of synaptic vesicle docking at central synapses. Nat Neurosci *2*, 503-507.

Nagamatsu, S., Fujiwara, T., Nakamichi, Y., Watanabe, T., Katahira, H., Sawa, H., and Akagawa, K. (1996). Expression and functional role of syntaxin 1/HPC-1 in pancreatic beta cells. Syntaxin 1A, but not 1B, plays a negative role in regulatory insulin release pathway. Journal of Biological Chemistry *271*, 1160-1165.

Nonet, M. L., Saifee, O., Zhao, H., Rand, J. B., and Wei, L. (1998). Synaptic transmission deficits in Caenorhabditis elegans synaptobrevin mutants. Journal of Neuroscience *18*, 70-80.

Novick, P., Field, C., and Schekman, R. (1980). Identification of 23 complementation groups required for post-translational events in the yeast secretory pathway. Cell *21*, 205-215.

Ohtsuka, T., Takao-Rikitsu, E., Inoue, E., Inoue, M., Takeuchi, M., Matsubara, K., Deguchi-Tawarada, M., Satoh, K., Morimoto, K., Nakanishi, H., and Takai, Y. (2002). Cast: a novel protein of the cytomatrix at the active zone of synapses that forms a ternary complex with RIM1 and Munc13-1. J Cell Biol *158*, 577-590.

Osen-Sand, A., Catsicas, M., Staple, J. K., Jones, K. A., Ayala, G., Knowles, J., Grenningloh, G., and Catsicas, S. (1993). Inhibition of axonal growth by SNAP-25 antisense oligonucleotides in vitro and in vivo. Nature *364*, 445-448.

Osen-Sand, A., Staple, J. K., Naldi, E., Schiavo, G., Rossetto, O., Petitpierre, S., Malgaroli, A., Montecucco, C., and Catsicas, S. (1996). Common and distinct fusion proteins in axonal growth and transmitter release. J Comp Neurol *367*, 222-234.

Otto, H., Hanson, P. I., and Jahn, R. (1997). Assembly and disassembly of a ternary complex of synaptobrevin, syntaxin, and SNAP-25 in the membrane of synaptic vesicles. Proceedings of the National Academy of Sciences of the United States of America *94*, 6197-6201.

Pabst, S., Hazzard, J. W., Antonin, W., Südhof, T. C., Jahn, R., Rizo, J., and Fasshauer, D. (2000). Selective interaction of complexin with the neuronal SNARE complex. Determination of the binding regions. J Biol Chem *275*, 19808-19818.

Perez-Branguli, F., Muhaisen, A., and Blasi, J. (2002). Munc 18a binding to syntaxin 1A and 1B isoforms defines its localization at the plasma membrane and blocks SNARE assembly in a three-hybrid system assay. Molecular & Cellular Neurosciences *20*, 169-180.

Perez-Branguli, F., Ruiz-Montasell, B., and Blasi, J. (1999). Differential interaction patterns in binding assays between recombinant syntaxin 1 and synaptobrevin isoforms. FEBS Letters *458*, 60-64.

Rao, S. S., Stewart, B. A., Rivlin, P. K., Vilinsky, I., Watson, B. O., Lang, C., Boulianne, G., Salpeter, M. M., and Deitcher, D. L. (2001). Two distinct effects on neurotransmission in a temperature-sensitive SNAP-25 mutant. Embo J *20*, 6761-6771.

Reim, K., Mansour, M., Varoqueaux, F., McMahon, H. T., Südhof, T. C., Brose, N., and Rosenmund, C. (2001). Complexins regulate a late step in Ca2+-dependent neurotransmitter release. Cell *104*, 71-81.

Rhee, J. S., Betz, A., Pyott, S., Reim, K., Varoqueaux, F., Augustin, I., Hesse, D., Südhof, T. C., Takahashi, M., Rosenmund, C., and Brose, N. (2002). Beta phorbol ester- and diacylglycerol-induced augmentation of transmitter release is mediated by Munc13s and not by PKCs. Cell *108*, 121-133.

Richmond, J. E., Weimer, R. M., and Jorgensen, E. M. (2001). An open form of syntaxin bypasses the requirement for UNC-13 in vesicle priming. Nature *412*, 338-341.

Rizo, J., and Südhof, T. C. (2002). Snares and Munc18 in synaptic vesicle fusion. Nat Rev Neurosci *3*, 641-653.

Rosenmund, C., Clements, J. D., and Westbrook, G. L. (1993). Nonuniform probability of glutamate release at a hippocampal synapse. Science *262*, 754-757.

Rosenmund, C., Rettig, J., and Brose, N. (2003). Molecular mechanisms of active zone function. Curr Opin Neurobiol *13*, 509-519.

Rosenmund, C., Sigler, A., Augustin, I., Reim, K., Brose, N., and Rhee, J. S. (2002). Differential control of vesicle priming and short-term plasticity by Munc13 isoforms. Neuron *33*, 411-424.

Rosenmund, C., and Stevens, C. F. (1996). Definition of the readily releasable pool of vesicles at hippocampal synapses. Neuron *16*, 1197-1207.

Ruiz-Montasell, B., Aguado, F., Majo, G., Chapman, E. R., Canals, J. M., Marsal, J., and Blasi, J. (1996). Differential distribution of syntaxin isoforms 1A and 1B in the rat central nervous system. European Journal of Neuroscience *8*, 2544-2552.

Sassa, T., Harada, S., Ogawa, H., Rand, J. B., Maruyama, I. N., and Hosono, R. (1999). Regulation of the UNC-18-Caenorhabditis elegans syntaxin complex by UNC-13. Journal of Neuroscience *19*, 4772-4777.

Schikorski, T., and Stevens, C. F. (1997). Quantitative ultrastructural analysis of hippocampal excitatory synapses. J Neurosci *17*, 5858-5867.

Schluter, O. M., Schmitz, F., Jahn, R., Rosenmund, C., and Südhof, T. C. (2004). A complete genetic analysis of neuronal Rab3 function. J Neurosci *24*, 6629-6637.

Schneggenburger, R., Sakaba, T., and Neher, E. (2002). Vesicle pools and short-term synaptic depression: lessons from a large synapse. Trends Neurosci *25*, 206-212.

Schoch, S., Castillo, P. E., Jo, T., Mukherjee, K., Geppert, M., Wang, Y., Schmitz, F., Malenka, R. C., and Südhof, T. C. (2002). RIM1alpha forms a protein scaffold for regulating neurotransmitter release at the active zone. Nature *415*, 321-326.

Schoch, S., Deak, F., Konigstorfer, A., Mozhayeva, M., Sara, Y., Südhof, T. C., and Kavalali, E. T. (2001). SNARE function analyzed in synaptobrevin/VAMP knockout mice. Science *294*, 1117-1122.

Schulze, K. L., Broadie, K., Perin, M. S., and Bellen, H. J. (1995). Genetic and electrophysiological studies of Drosophila syntaxin-1A demonstrate its role in nonneuronal secretion and neurotransmission. Cell *80*, 311-320.

Serra-Pages, C., Medley, Q. G., Tang, M., Hart, A., and Streuli, M. (1998). Liprins, a family of LAR transmembrane protein-tyrosine phosphatase-interacting proteins. J Biol Chem *273*, 15611-15620.

Siegel, G. J., Agranoff, B. W., Albers, R. W., Fisher, S. K., and Uhler, M. D. (1999). Basic Neurochemistry, Sixth Edition edn (Philadelphia, Lippincott Willians & Wilkins).

Stanley, E. F. (2003). Syntaxin I modulation of presynaptic calcium channel inactivation revealed by botulinum toxin C1. European Journal of Neuroscience *17*, 1303-1305.

Stanley, E. F., and Goping, G. (1991). Characterization of a calcium current in a vertebrate cholinergic presynaptic nerve terminal. J Neurosci *11*, 985-993.

Stanley, E. F., and Mirotznik, R. R. (1997). Cleavage of syntaxin prevents G-protein regulation of presynaptic calcium channels. Nature *385*, 340-343.

Stevens, C. F., and Sullivan, J. M. (1998). Regulation of the readily releasable vesicle pool by protein kinase C. Neuron *21*, 885-893.

Stevens, C. F., and Wesseling, J. F. (1999). Identification of a novel process limiting the rate of synaptic vesicle cycling at hippocampal synapses. Neuron *24*, 1017-1028.

Südhof, T. C. (2000). The synaptic vesicle cycle revisited. Neuron *28*, 317-320.

Südhof, T. C., and Scheller, R. (2001). Mechanism and Regulation of Neurotransmitter Release. In Synapses, W. M. Cowan, T. C. Südhof, and C. F. Stevens, eds. (Baltimore, The Johns Hopkins University Press), pp. 177-215.

Sutton, R. B., Fasshauer, D., Jahn, R., and Brunger, A. T. (1998). Crystal structure of a SNARE complex involved in synaptic exocytosis at 2.4 A resolution.[see comment]. Nature *395*, 347-353.

Sweeney, S. T., Broadie, K., Keane, J., Niemann, H., and O'Kane, C. J. (1995). Targeted expression of tetanus toxin light chain in Drosophila specifically eliminates synaptic transmission and causes behavioral defects. Neuron *14*, 341-351.

Takahashi, T., and Momiyama, A. (1993). Different types of calcium channels mediate central synaptic transmission. Nature *366*, 156-158.

Teng, F. Y., Wang, Y., and Tang, B. L. (2001). The syntaxins. Genome Biology *2*, REVIEWS3012.

Tucker, W. C., Weber, T., and Chapman, E. R. (2004). Reconstitution of Ca2+-regulated membrane fusion by synaptotagmin and SNAREs. Science *304*, 435-438.

Verhage, M., Maia, A. S., Plomp, J. J., Brussaard, A. B., Heeroma, J. H., Vermeer, H., Toonen, R. F., Hammer, R. E., van den Berg, T. K., Missler, M., *et al.* (2000). Synaptic assembly of the brain in the absence of neurotransmitter secretion. Science *287*, 864-869.

Voets, T., Toonen, R. F., Brian, E. C., de Wit, H., Moser, T., Rettig, J., Südhof, T. C., Neher, E., and Verhage, M. (2001). Munc18-1 promotes large dense-core vesicle docking. Neuron *31*, 581-591.

Washbourne, P., Thompson, P. M., Carta, M., Costa, E. T., Mathews, J. R., Lopez-Bendito, G., Molnar, Z., Becher, M. W., Valenzuela, C. F., Partridge, L. D., and Wilson, M. C. (2002). Genetic ablation of the t-SNARE SNAP-25 distinguishes mechanisms of neuroexocytosis. Nat Neurosci *5*, 19-26.

Weber, T., Zemelman, B. V., McNew, J. A., Westermann, B., Gmachl, M., Parlati, F., Sollner, T. H., and Rothman, J. E. (1998). SNAREpins: minimal machinery for membrane fusion. Cell *92*, 759-772.

Weimer, R. M., Richmond, J. E., Davis, W. S., Hadwiger, G., Nonet, M. L., and Jorgensen, E. M. (2003a). Defects in synaptic vesicle docking in unc-18 mutants. Nature Neuroscience *6*, 1023-1030.

Wheeler, D. B., Randall, A., and Tsien, R. W. (1994). Roles of N-type and Q-type Ca2+ channels in supporting hippocampal synaptic transmission. Science *264*, 107-111.

Wiser, O., Bennett, M. K., and Atlas, D. (1996). Functional interaction of syntaxin and SNAP-25 with voltage-sensitive L- and N-type Ca2+ channels. EMBO Journal *15*, 4100-4110.

Wu, M. N., Fergestad, T., Lloyd, T. E., He, Y., Broadie, K., and Bellen, H. J. (1999). Syntaxin 1A interacts with multiple exocytic proteins to regulate neurotransmitter release in vivo.[erratum appears in Neuron 2000 Mar;25(3):735]. Neuron *23*, 593-605.

Yang, B., Steegmaier, M., Gonzalez, L. C., Jr., and Scheller, R. H. (2000). nSec1 binds a closed conformation of syntaxin1A. Journal of Cell Biology *148*, 247-252.

Yoshihara, M., and Littleton, J. T. (2002). Synaptotagmin I functions as a calcium sensor to synchronize neurotransmitter release. Neuron *36*, 897-908.

Zamponi, G. W. (2003). Regulation of presynaptic calcium channels by synaptic proteins. Journal of Pharmacological Sciences *92*, 79-83.

Zhen, M., and Jin, Y. (1999). The liprin protein SYD-2 regulates the differentiation of presynaptic termini in C. elegans. Nature *401*, 371-375.

Zucker, R. S., and Regehr, W. G. (2002). Short-term synaptic plasticity. Annu Rev Physiol *64*, 355-405.

Acknowledgements:

I would like to thank all of the members of department of Membrane Biophysics for their scientific and professional support. I am extremely grateful to Professor Erwin Neher for being an exceptional model of my life as a scientist and for his constant support I am also indeed grateful for Professor Christian Rosenmund for their excellent guidance and encouragement.

Foremost, I acknowledge my past and present lab mates for their cooperative help and friendship. Especially, I am thankful for Dr. Alexander Meyer who provided me with brilliant suggestions and criticisms of my research. I wish to thank René Wiese, Albrecht Sigler, Susann Kaufmann and Michael Mansour for their sincere friendship and kind help for my German life. Also, I am more than happy to be with Jayeeta Basu, Mingshan Xue, Liyi Li, Dr. Jeong-Seop Rhee and Dr.Shutaro Katsurabayashi at our new lab in Houston. I cannot forget technical and administrative support of Ina Herfort, Ralf Nehering and Irmgard Barteczko.

I would also like to take this opportunity to thank my parents. Their endless love and belief created an environment that spurred my curiosity for research.

I dedicate this dissertation to my wife, Jiwon.

RAH, JONG-CHEOL

Mai 7 1974	Geboren in Seoul, Korea Sohn von Choong-Kyun Rah MBA und Choon-Hee Ban BSc.
Februar 1993 – Februar 1999	BSc. (Biologie/ Biochemie) an der Sogang University, Seoul, Korea
Juli 1995 – Dezember 1996	Wehrdienst in der koreanischen Armee
September 1999 – Februar 2000	Austauschstudent am Imperial College of London, London, UK Betreuung: Prof. Mustafa Djamgoz PhD
Maerz 2000 – Februar 2002	MSc (Pharmakologie) an der Seoul National University, Seoul, Korea Betreuung: Prof.Yoo-Hun Suh, MD. PhD.
Oktober 2001 – Februar 2002	Austauschstudent am Imperial College of London, London, UK Betreuung: Prof. Mustafa Djamgoz PhD
Februar 2002 –	Dissertation in der Abteilung Membranbiophysik, Arbeitsgruppe PD Dr.Christian Rosenmund, am Max-Planck-Institut für biophysikalische Chemie, Göttingen, unter Betreuung von PD Dr. Christian Rosenmund und Prof. Dr. Erwin Neher

Publikationen

Jong-Cheol Rah, Stefan Gerber, Alexander Meyer, Jeong-Seop Rhee, Thomas Sudhof, Christian Rosenmund, Constitutively open conformation of syntaxin 1B enhances vesicle priming and membrane exocytosis (in Vorbereitung)

Jong-Cheol Rah, Hye-Sun Kim, Sung Su Kim, Jae-Hyung Bach, Sung-Jin Jeong, Ji-Heui Seo, Cheol Hyoung Park, Yong-Sik Kim, and Yoo-Hun Suh, Effects of the carboxyl-terminal fragment of Alzheimer's amyloid precursor protein and amyloid b-peptide on the production of cytokines and nitric oxide in glial cells. *FASEB J. 2001 Jun 15(8): 1463-1465.*

JH Kim, **Jong-Cheol Rah**, SP Fraser, KA Chang, MB Djamgoz, YH Suh Carboxyl-terminal peptide of beta-amyloid precursor protein blocks inositol 1,4,5-

trisphosphate-sensitive Ca2+ release in *Xenopus laevis* oocytes.. *J Biol Chem. 2002 Jun 7; 277(23):20256-63.*

JH Seo, **Jong-Cheol Rah**, SH Choi , JK Shin, K Min, HS Kim, CH Park, S Kim, EM Kim, SH Lee, S Lee, SW Suh, YH Suh a-Synuclein regulates neuronal survival via Bcl-2 family expression and PI3/Akt kinase pathway. *FASEB J. 2002 Nov; 16(13):1826-1826. Epub 2002 Sep 05.*

CH Park, SH Choi, CH Kim, JH Seo, JW Koo, **Jong-Cheol Rah**, HS Kim, SJ Jeong, WS Joo, YJ Lee, YS Kim, MS Kim, YH Suh. General pharmacology of indole [2',3':3,4]pyrido[2,1-b]quinazolinium-5,7,8,13-tetrahydro-14-methyl-5-oxo-chloride, a new anti-dementia agent. *Arzneimittelforschung. 2003;53(6):393-401.*

JH Bach, HS Chae, **Jong-Cheol Rah**, MW Lee, SH Choi, JK Choi, YS Kim, KY Kim, WB Lee, YH Suh and SS Kim:C-terminal fragment of Amyloid Precursor Protein induces Astrocytosis *J. Neurochem 2001 Jul;78(1):109-20*

JH Seo, SH Kim, HS Kim, CH Park, SJ Jeong, JH Lee, SH Choi, KA Chang, **Jong-Cheol Rah**, JW Koo, EM Kim and YH Suh. Effects of Nicotine on APP Secretion and Ab- or CT105-Induced Toxicity 2001 *Biol.Psychiatry 2001 Feb 1; 49(3):240-7*

HS Kim, CH Park, SH Cha, JH Lee, SW Lee, YM Kim, **Jong-Cheol Rah,** SJ Jeong and YH Suh, C-terminal fragment of Alzheimer's APP destabilize calcium homeostasis and renders neuronal cells vulnerable to excitotoxicity. *FASEB J. 2000 Aug;14(11):1508-17.*

SJ Jeong, HS Kim, CH Park, KA Chang, DH Geum, CH Pak, JH Seo, **Jong-Cheol Rah,** JH Lee, SH Choi, SG Lee and YH Suh, Subcellular localization of presenilins during mouse preimplantation development. *FASEB J. 2000 Nov; 14(14): 2171-2176.*

CH Park, SH Choi, Y Piao, SH Kim, YJ Lee, HS Kim, SJ Jeong, **Jong-Cheol Rah**, JH Seo, KA Chang, YJ Jung and YH Suh. Glutamate and aspartate impair memory retenion and damage hypothalamic neurons in adult mice. *Toxicol Lett. 2000 May 19; 115(2): 117-25*

YH Suh, HS Kim, JP Lee, CH Park, SJ Jeong, SS Kim, **Jong-Cheol Rah**, JH Seo, SS Kim. Roles of A beta and carboxyl terminal peptide fragments of amyloid precursor protein in Alzheimer Disease. *J Neural Transm Suppl 2000;(58): 65-82.*

(**Buchkapitel**)
YH Suh, HS Kim, CH Park, JH Seo, JP Lee, SJ Jeong, SS Kim, JH Lee, SH Choi, KA Chang, **Jong-Cheol Rah**, SS Kim. Etiological roles of Ab and carboxyl terminal peptide fragments of amyloid precursor protein in Alzheimer disease. *Neuroscientific Basis of Dementia.*

Goettingen, 17.09.2004